Title: A recombinant commensal bacteria elicits heterologous antigen-specific immune responses during pharyngeal carriage

Authors: Jay R Laver[1,2]*, Diane Gbesemete[1,2], Adam P Dale[1,2], Zoe C Pounce[1], Carl N Webb[1,2], Eleanor F Roche[1], Jonathan M Guy[1], Graham Berreen[1], Konstantinos Belogiannis[1], Alison R Hill[1,2], Muktar M Ibrahim[1], Muhammad Ahmed[1], David W Cleary[1,2], Anish K Pandey[1,2], Holly E Humphries[3], Lauren Allen[3], Hans de Graaf[1,2], Martin C Maiden[4], Saul N Faust[1,2], Andrew R Gorringe[3] and Robert C Read[1,2]

Affiliations:

1. **Faculty of Medicine and Institute for Life Sciences**, University of Southampton, Southampton, UK
2. **NIHR Southampton Biomedical Research Centre** and **NIHR Southampton Clinical Research Facility,** University Hospital Southampton NHS Foundation Trust, Southampton, UK
3. **Public Health England**, Porton Down, Salisbury, UK
4. **Department of Zoology**, University of Oxford, Oxford, UK

*To whom correspondence should be addressed: J.R.Laver@soton.ac.uk

One Sentence Summary: Engineered human-specific commensal bacteria with surface-expressed vaccine target provoke antigen-specific antibodies during prolonged pharyngeal carriage.

Abstract:

The human nasopharynx contains a stable microbial ecosystem of commensal and potentially pathogenic bacteria, which can elicit protective primary and secondary immune responses. Experimental intranasal infection of human adults with the commensal *Neisseria lactamica* produces safe, sustained pharyngeal colonization. This has potential utility as a vehicle for sustained release of antigen to the human mucosa, but commensals in general are thought to be immunologically tolerated. Here, we show that engineered *N. lactamica*, chromosomally transformed to express a heterologous vaccine antigen, safely induces systemic, antigen-specific immune responses during carriage. When *N. lactamica* expressing the meningococcal vaccine antigen Neisseria Adhesin A (NadA) was inoculated intranasally into human volunteers, all colonized participants carried the bacteria asymptomatically for at least 28 days, with the majority (86%) still carrying the bacteria at 90 days. Compared to an otherwise isogenic, but phenotypically wild type genetically modified strain, colonization with NadA-expressing *N. lactamica* generated NadA-specific IgG- or IgA-secreting plasma cells within 14 days of colonization and NadA-specific IgG memory B cells within 28 days of colonization. NadA-specific IgG memory B cells were detected in peripheral blood of colonized participants for at least 90 days. Over the same period there was seroconversion against NadA and also generation of serum bactericidal antibody activity against a NadA-expressing meningococcus. The controlled infection was safe, and there was no transmission to adult bedroom-sharers during the 90 day period. Genetically modified *N. lactamica* could therefore be used to generate beneficial immune responses to heterologous antigens during sustained pharyngeal carriage.

Introduction

Natural protective immunity to invasive disease caused by nasopharyngeal pathobionts including *Streptococcus pneumoniae*, *Haemophilus influenzae* and *Neisseria meningitidis* (Nmen) is a consequence of repetitive, transient, asymptomatic carriage commencing in infancy. In each case, carriage is associated with seroconversion against cognate antigen (*1-3*). This natural mechanism could be harnessed using safe, genetically modified, live bacterial vectors to provide innovative mucosal vaccines. The human commensal bacterium *Neisseria lactamica* (Nlac) is a harmless colonizer of babies and young children. The frequency of colonization wanes during early childhood with niche replacement by the closely related pathobiont Nmen (*4*). Controlled human intranasal infection of wild type (WT) Nlac results in safe colonization of human volunteers, which is sustained for at least 6 months, and is accompanied by both humoral and mucosal immune responses (*5*) and reduced natural acquisition of Nmen (*6*). During experimental human colonization the genome of Nlac remains stable (*7*). This, together with the inherent adjuvant properties of its outer membrane components (*8*) suggests the bacterium could be adapted as a microbial factory/delivery platform, producing molecules of biological or therapeutic relevance, such as vaccine antigens, *in situ* following colonization (*9-11*). However, commensal bacteria have long been considered to be immunologically tolerated in symbiotic mutualism with the host (*12*), which could defeat this objective.

The principal intervention reported here includes controlled infection and deliberate release of genetically modified Nlac (GM-Nlac), which required approval by the UK Government's Department for the Environment, Food and Rural Affairs (DEFRA). It is important to note that Nlac is relatively resistant to genetic manipulation (*13*) due to its repertoire of restriction

endonucleases (*14*). Therefore, a novel cloning system was used to integrate heterologous genes into the chromosome using hypermethylated nucleic acids (Figure S1). A full description of the genetic modifications made to produce the challenge organisms is published on the DEFRA website: (https://www.gov.uk/government/publications/genetically-modified-organisms-university-of-southampton-17r5001).

Transformation of Nlac confirmed it as a naturally competent bacterium (Figure S2), with horizontal gene transfer affected by similar factors to other members of the genus (Figure S3). As the GMO was manufactured for deliberate release to the environment, the use of antibiotic resistance markers was avoided by exploiting endogenous lactose fermentation by Nlac β-galactosidase (coded for by the *lacZ* gene) (Figure S4). This enabled blue/white colony screening on media containing 5-bromo-4-chloro-3-indolyl-β-D-galactopyranoside (X-gal) to detect mutants. High-level expression of heterologous genes is achieved using a novel, synthetic promoter that uses the transcription enhancement property of DNA preceding the meningococcal *porA* gene (Figure S5).

The genomically-defined Nlac strain Y92-1009 (*15*) was transformed with a construct containing the coding sequence for *Neisseria* adhesin A (NadA) (allele 1), a meningococcal-specific member of the type V autotransporter family of outer membrane proteins (*16*), to generate strain 4NB1. NadA is one of the strongly immunogenic, recombinant protein components of the 4CMenB vaccine (Bexsero), and the only component capable of generating sterilizing immunity following immunisation of a transgenic mouse model of meningococcal colonization (*17*). NadA expression in Nmen is associated with an increased level of adhesion to human epithelial

cell lines (*16*), but is expressed in a minority of Nmen lineages so is non-essential for virulence (*18*). A second (control) strain (4YB2) was transformed with a construct otherwise identical to the first, except for the replacement of the *nadA* coding sequence with a 14 bp, non-coding linker sequence (Figure S6).

Here we report the pre-clinical quality and safety evaluation, and deployment of these recombinant strains in a first-in-man, controlled human infection model experiment (CHIME) to determine whether an engineered commensal can elicit beneficial immune responses to heterologous antigen. Co-primary objectives of the CHIME were (i) establishing safety of genetically transformed Nlac, and (ii) measuring NadA-specific immunity in healthy volunteers following nasal inoculation with NadA-expressing Nlac, compared to the control GM strain.

Results

Constitutive surface expression of functional NadA in Nlac strain 4NB1

The expression of *nadA* in the meningococcus is phase variable (*19*) and regulated by the NadR repressor protein, which becomes de-repressed by salivary concentrations of the metabolite 4-hydroxyphenylacetic acid (4HPA) (*20*). Longitudinal analysis of serial Nmen isolates recovered from the human nasopharynx reveals that NadA expression decreases over time, likely a result of seroconversion against NadA and antibody-mediated selective pressure against NadA expression (*21*). To prevent the gene from becoming phase 'OFF' in strain 4NB1 during the CHIME, transcription of the *nadA* gene in the construct is driven by a hybrid, non-phase variable *porA/porB* promoter. The transcription activity of this hybrid promoter is enhanced by 200

nucleotides of 'upstream activation sequence' (UAS) of the WT *porA* promoter, which is optimal for increasing gene expression (Figure S5).

Flow cytometry using anti-NadA monoclonal antibody (mAb) 6e3 (*22*) demonstrates that Nlac strain 4NB1 expresses NadA on its surface, in contrast to both WT Y92-1009 and control strain 4YB2 (Figure 1A). Visualization of 4NB1 membrane proteins separated by SDS-PAGE reveals that NadA is expressed as a multimer, most likely a trimer given its apparent molecular weight of approximately 120 kDa (Figure 1A). Similarly, flow cytometry using an affinity-purified, anti-NadA polyclonal antibody mixture (pAb), [PE-JRL-3] (Figure 1B), demonstrates that the abundance of NadA expression on the surface of strain 4NB1 is similar to that of Nmen strain N54.1, a serogroup Y WT carriage isolate shown to strongly express NadA (allele 2/3) (*23*). Both strain 4NB1 and N54.1 express substantially more NadA than the widely-studied Nmen strain MC58 (allele 1), itself a serogroup B WT carriage isolate. These data, confirmed by western blot, suggest the heterologous expression of the *nadA* gene by Nlac results in presentation of trimeric NadA on the bacterial surface, at an abundance equivalent to that of naturally circulating, NadA-expressing meningococci (Figure 1B). Consistent with the role of NadA as an adhesin (*16*), and supportive of its functional expression in 4NB1, this strain exhibits increased association with confluent monolayers of HEp-2 epithelial cells as compared to wild type Nlac (Figure 1C).

Immunisation of mice with deoxycholate-extracted outer membrane vesicles (dOMV) derived from strain 4NB1 (4NB1-dOMV) generated potent serum bactericidal antibody (SBA) activity against Nmen strain 5/99, a NadA-overexpressing reference strain (*24*). In contrast, immunizing

mice with WT Y92-1009 dOMV generates no SBA (Figure 1D). This is consistent with previous observations in humans that antibody responses directed against the native outer membrane proteins of Nlac are not bactericidal (*25*), and suggests that the SBA activity is instead linked to the presence of antibody targeting NadA. This is supported by the SBA activity of control serum NA9136, which was extracted from whole blood taken from a human donor 28 days after immunization with Bexsero (Figure 1D).

Pathogenic potential of recombinant Nlac is equivalent to wild type Nlac

To gain approval for Deliberate Release of GM-Nlac in a CHIME, it was necessary to demonstrate no increase in the pathogenic potential of these strains over wild type. Nmen expresses polysaccharide capsule (*26*), which affords resistance to killing by human serum and constitutes the key determinant of the organism's ability to cause invasive disease. It is plausible that Nlac might become more pathogenic if it could deposit polysaccharide capsule on its surface. Given the propensity of Nlac to take up DNA containing *Neisseria* DNA uptake sequences (DUS) (see Supplementary Information), the most likely potential source of ectopic capsule synthesis genes during human colonization is Nmen, in the genome of which the *Neisseria* DUS is overrepresented (*27*), and which shares the nasopharyngeal niche with Nlac. The uptake and assimilation of an antibiotic resistance marker (gene *aphA3*, coding Kan^R) from three different genomic sources into the chromosome of WT Nlac strain Y92-1009, GM-Nlac strain 4NB1 and Nmen strain MC58 was therefore measured (Figure 2A). Genomic DNA (gDNA) derived from Y92-1009*ΔnlaIII:aphA3* efficiently transformed both WT Y92-1009 and strain 4NB1, consistent with donor and recipient strains having homologous patterns of DNA

methylation, which precludes degradation of the gDNA by restriction endonuclease activities and increases transformation efficiency (TE). The same gDNA also transformed Nmen strain MC58, although less efficiently. Conversely, whilst gDNA derived from mutants MC58*ΔsiaD:aphA3* (in which the Kan^R gene inactivates a capsule biosynthesis gene) and MC58*ΔnadA:aphA3* (in which the Kan^R gene inactivates the endogenous *nadA* gene) was able to transform MC58; neither gDNA was able to generate a single Nlac transformant (n = 5 experiments). The TE of 4NB1 with Nmen gDNA, under conditions ideal for transformation, is therefore < 1 transformant per 2 x 10^9 CFU, and is the same as the TE of the parental strain. We conclude that the likelihood of GM-Nlac assimilating capsule synthesis genes from Nmen remains as low as the WT parental strain and that the risk of this occurring is negligible.

Both GM-Nlac strains retained susceptibility to standard antibiotics for the treatment of meningococcal disease (Figure 2B). E-tests demonstrated that the minimal inhibitory concentrations (MICs) of ciprofloxacin and ceftriaxone for GM-Nlac were well below the European Committee on Antimicrobial Susceptibility Testing (EUCAST) breakpoints for Nmen and those previously established in 286 Nlac isolates (*28*).

Neither strain 4NB1 nor 4YB2 proved any more pathogenic than WT Y92-1009 in a mouse model of systemic infection at two different inoculum doses (Figure 2C), however, systemic infection with the larger dose of strain 4NB1 resulted in the generation of potent SBA responses against Nmen strain 5/99 (Figure 2C).

GM-Nlac safely colonizes the human upper respiratory tract in a CHIME

Amongst 42 volunteers screened, 26 were free from Nlac and Nmen carriage and eligible for participation (Figure 3A). Participants were assigned, initially in 1-person but subsequently in up-to-5-person blocks, to either the 'intervention' (strain 4NB1) or 'control' (strain 4YB2) study arm. Participants were admitted to a hospital clinical research facility (CRF) for the first 4.5 days after inoculation (i.e. the 'admission period'). Volunteers were deemed 'colonized' by GM-Nlac following recovery of one or more colonies of GM-Nlac from either nasal wash fluid or throat swabs at any point within 14 days of inoculation. Eligible volunteers were inoculated in each study block until at least 11 volunteers had been successfully colonized. The colonization status of Nlac and Nmen for each participant during the study period of 90 days is shown in Figure 3B. Note that neither the Nmen strain acquired by Participant 25 prior to challenge, nor the Nmen strain acquired after Day 28 by Participant 4 were shown to express NadA. The latter point is important because it meant that samples from this participant could be included in all analyses of sNadA-specific immunity.

In the event of withdrawal from the study (n = 2) or at day 90 post-inoculation (n = 24), a single dose of oral ciprofloxacin (500 mg) was administered, which eliminated carriage of both strains of GM-Nlac within 2 days (Figure 3B). During both the admission period (Figure S7) and the follow-up period (Figure S8), there were only a small number of solicited and/or unsolicited symptoms reported, and similarly few clinically observed (Figure S9) or laboratory test-identified (Figure S10) adverse events recorded. Upon clinical review, none of these events were deemed to be related or likely-related to carriage of either GM-Nlac strain and the number of adverse events in the intervention study arm was similar to the control study arm. There were no serious adverse events, no antibiotic eradication or treatment given due to adverse events, and no

study withdrawal due to adverse events. At no point throughout the study was GM-Nlac detected in exhaled breath samples or on surgical facemasks worn prior to each visit to the CRF. Additionally, there was no detectable transmission of GM-Nlac to 'bedroom-sharing contacts' of volunteers, as established by culture of oropharyngeal swab taken from these individuals at multiple time points (n = 8).

Colonization with NadA-expressing GM-Nlac expands circulating Nlac-specific and NadA-specific, antibody secreting cells

Two enzyme-linked immunospot (ELISpot) assays were employed to detect either IgG-secreting cells or IgA-secreting cells (collectively: antibody-secreting cells, ASC) in the peripheral blood of participants with specificity to one of the following: (i) dOMV derived from strain 4YB2 (4YB2-dOMV), (ii) 4NB1-dOMV, (iii) the soluble domain of NadA (sNadA). We compared the maximum ('peak') number of ASC spot-forming units (SFU) per 200,000 peripheral blood mononuclear cells (PBMC) developed against each antigen post-inoculation, assuming one SFU equated to one ASC. In view of the rapidity and transience of circulation of plasmablasts following infection or vaccination (*29*), 'peak' responses were measured in samples taken at either day 7 or day 14 post-inoculation (i.e. +7-14). Note that analysis of the number of IgG-secreting cells (Figure 4, A through F) was conducted separately to the analysis of IgA-secreting cells (Figure 4, G through L).

In 4YB2-colonized participants there was consensus between the pattern of changes in both the IgG-secreting and IgA-secreting cell datasets. Specifically, there was a significant increase in the number of cells with specificity to either 4YB2-dOMV (Figure 4A and Figure 4G) or 4NB1-

dOMV (Figure 4B and Figure 4H) at peak in comparison to baseline, but no significant change in the number of cells with specificity to sNadA (Figure 4C and Figure 4I).

In 4NB1-colonized participants however, the two datasets were discrepant. Whilst there was no difference between the baseline and peak measurements of 4YB2-dOMV-specific, IgG-secreting cells (Figure 4D), there was a significant increase between the baseline and peak measurements of 4YB2-dOMV-specific, IgA-secreting cells (Figure 4J). In contrast, the peak number of 4NB1-dOMV-specific cells was significantly increased in both datasets from these participants compared to baseline (Figure 4E and Figure 4K). Similarly, the peak number of sNadA-specific cells was significantly increased over baseline in these participants (Figure 4F and Figure 4L).

Colonization with NadA-expressing GM-Nlac elicits seroconversion against NadA and stimulates anti-meningococcal serum bactericidal antibody activity

Colonization with either strain of GM-Nlac led to a significant and sustained increase in the interpolated reciprocal titer of anti-WT Nlac dOMV-specific IgG (hereafter, anti-Nlac IgG) present in the sera of volunteers at Days 28, 56 and 90 compared to baseline (Figure 5). As expected, in 4YB2-colonized participants (Figure 5A), there was a significant and sustained increase in the titer of anti-Nlac IgG from baseline (Median = 72.3; Range = 16.7 – 474.6) to Day 90 (Median = 164.6; Range = 46.0 – 586.3). This includes a Median maximum fold change in anti-Nlac IgG of 2.9 (range: 1.5 – 16.9). Similarly in 4NB1-colonized participants (Figure 5B), there was a significant and sustained increase in the titer of anti-Nlac IgG from baseline (Median = 34.3; Range = 21.7 – 134.5) to Day 90 (Median = 104.5; Range = 34.2 – 223.6), including a Median maximum fold change of 2.8 (range:

1.4 – 12.8). Anti-Nlac IgG calculated for sera taken from 4YB2-colonized participants was not significantly different to that taken from 4NB1-colonized participants. These data indicate that both sets of participants were capable of generating immunological responses, specifically that there was no generalized defect in either: (i) the ability of the participants in one or other arm to respond immunologically to infection with GM-Nlac, or (ii) one or other of the GM-Nlac strains to elicit an immunological response from the participants. These data confirm that GM-Nlac-colonized participants are generally responsive to the presence of the colonizing bacteria and generate IgG against epitopes found on the surface of WT Nlac.

The titer of anti-sNadA IgG was also measured in each serum sample, using an endpoint enzyme-linked immunosorbent assay (ELISA) (endpoint = $OD_{490nm} \geq 1.4$, equivalent to an interpolated reciprocal titer of anti-sNadA IgG = 17.245 in reference serum NA9136, see Figure S11). Prior to inoculation, the majority of participants had undetectable levels of anti-sNadA IgG in their sera (reciprocal titer: ≤ 2), consistent with the absence of colonization by NadA-expressing Nmen at enrolment. Analysis of the maximum fold changes in anti-sNadA IgG shows that, whilst there is no increase in anti-sNadA IgG measurable in the sera of 4YB2-colonized participants (Figure 5C); we measured at least a 2-fold rise in the reciprocal endpoint titer of anti-sNadA IgG at one or more time points in 5 of the 10 4NB1-colonized participants (Figure 5C and D).

Additionally, each serum sample was assayed for serum bactericidal antibody activity versus the NadA-overexpressing Nmen strain 5/99 using human complement (Figure 5E). The SBA titers of participants at baseline varied in both arms of the study. In the Control arm, 9 of the 11 participants had a Day 0 interpolated SBA titer < 4 (i.e. non-protective against 5/99-induced

meningococcal disease) (*30*); while 7 of the 10 participants in the Intervention arm were similarly not protected at Day 0. Across the 90 day course of the study, colonization with GM-Nlac resulted in participants having an SBA titer >4 (i.e. protective). This occurred in 4/9 participants (44.4 %) in the Control arm, , and 5/7 in the Intervention arm (71.4 %). The numbers of initially `unprotected` participants at Day 0 who became and remained `protected` at Day 90 were 3 and 4 in the Control and Intervention arms, respectively (shown in grey, Figure 5E). Importantly, one of the 3 participants in the Control arm was the same individual that had lost carriage of GM-Nlac after Day 28 and acquired NadA-negative Nmen carriage at some point before their visit at Day 56 (italicized, Figure 5E).

Colonization with NadA-expressing GM-Nlac increases the circulating sNadA-specific memory B cell pool

IgG B cell memory to GM-Nlac and specifically to NadA was assessed by ELISpot assay (*31*), assuming that one SFU in this assay equated to one memory B cell (for representative outputs see Figure S12).

In 4YB2-colonized participants, there was a significant but temporary increase in the percentage of the total number of IgG-secreting memory B cells (hereafter, % of memory B cells) with specificity to either 4YB2-dOMV or 4NB1-dOMV at Day 28, as compared to baseline. These increases were no longer evident at 90 days post-inoculation (Figures 6A and 6B, respectively). Importantly, there were no significant differences between the % of memory B cells with specificity to sNadA

measured at any point in these participants (Figure 6C), and no change in IgG memory B cells with specificity to influenza hemagglutinin (FluHA) (i.e. the positive control antigen) (Figure 6D).

The same transient increase in the % of memory B cells specific for 4YB2-dOMV was evident in 4NB1-colonized participants (Figure 6E), but interestingly there was a significantly increased % of IgG memory B cells specific for 4NB1-dOMV at Day 90 (Figure 6F). In contrast to participants in the Control arm, there was a significant increase in the % of IgG memory B cells with specificity to sNadA measured at both Day 28 and Day 90, compared to baseline (Figure 6G). Again, the proportion of IgG memory B cells with specificity to influenza hemagglutinin remained consistent and unchanged (Figure 6H), indicating stability of the assay over time and that changes to the composition of the circulating memory B cell pool in response to Nlac-dOMV or sNadA were specific to the experimental intervention.

Importantly, in every participant that was colonized with strain 4NB1, there was a relative increase in the % of memory B cells with specificity to sNadA (Figure 6I).

Discussion

We have demonstrated the utility of genetically modified *N. lactamica* as a platform for the presentation of antigen to the upper respiratory tract (URT) of humans and shown its ability to elicit antigen-specific immunity during a 90-day period of asymptomatic colonization. This CHIME has shown that GM-Nlac can be deployed safely, survive and thrive in its biological niche and be effectively eradicated as necessary, without transmitting to other adults living in close proximity of the study participants. This technological advance may in future be translated

to generate novel vaccines that exploit the natural biological process of colonization, or delivery systems for therapeutics or experimental medicine investigation.

Remarkably, we find that a single, intranasal dose of a recombinant human commensal expressing a heterologous vaccine antigen (NadA), expands antigen-specific IgG memory B cells in all recipients by 90 days after inoculation (Figure 6I). In contrast, expansion of circulating memory B cell responses to non-NadA surface antigens was relatively transient. This discrepancy could plausibly represent the difference between an immunological priming event and recall of a memory response, given that natural carriage of Nlac during childhood does not result in immunological priming against Nlac surface antigens (*32*) and the observation that NadA-specific, IgG memory B cells were detected in PBMC harvested at baseline in a majority of participants (Figure 6). Although there is some evidence that antigen-specific plasma cells are found in peripheral blood 6 to 7 days after a booster immunization, in contrast to the appearance of such cells after day 10 in response to primary immunization (*33*), the dynamics of this may be influenced by the route of administration and effective dose of the antigen; both of which differ significantly from parenteral vaccination in our nasally-inoculated CHIME. Our analyses of plasma cell numbers therefore make no attempt to discriminate between putative 'priming' and 'recall' responses on the basis of the dynamics of plasma cell formation, instead comparing the dynamics-agnostic 'peak' value of plasma cells in each participant. The immune responses we observed could therefore represent either 'priming' or 'recall', but to discriminate between these responses will require further studies with strains expressing different, perhaps synthetic antigens, to which the majority of humans are more likely to be immunologically naïve. In this study, our data suggests at least a booster-like potential for this technology, especially as a means

to provoke anamnestic responses against established vaccine antigens with which recipients have already been immunized.

Although the presence of NadA-specific IgG memory B cells in the circulation beyond 90 days has not been established, this could be investigated in future work. Studies on the longevity of memory B cells have shown they have the potential to exist in a senescent state for years until reactivated by exposure to cognate antigen (*34*), although it is conceivable that the context of the immunization (i.e. colonization of a mucosal surface with a bacterial commensal versus intramuscular injection) could play a role in the dynamics of memory B cell availability and reactivation (*35, 36*). In this study, the eradication of carriage of each GM-Nlac strain with antibiotics at Day 90 could therefore be considered a limitation to the study design, however such a precaution was considered necessary, given the experimental nature of the challenge agent and the potential for the genetically modified commensal to be shed into the environment and to spread between humans. That no shedding of GM-Nlac nor its onward transmission to bedroom-sharing adults was observed in this study is reassuring, *vis a vis* (i) reducing the potential to inadvertently infect vulnerable (e.g. immunocompromised) members of the community and (ii) the ethics of obtaining informed consent for participation in future studies. However, the snapshots of these processes taken from a small number of participants and their close contacts may not reflect the transmissibility of the GM organism from all participants across the length of the study period.

Memory B cells do not have a primary antibody-secreting function, but promptly differentiate into plasma cells upon effective re-stimulation by cognate antigen (*37*). This confers the

potential to rapidly produce antibody following memory B cell activation by a pathogen or pathobiont, such as one establishing pharyngeal colonization, preventing further progression to clinical disease. Commensurate with this, presentation of NadA to the upper respiratory tract mucosa by strain 4NB1 elicits significant increases in the numbers of both IgG-secreting and IgA secreting, sNadA-specific plasma cells (Figure 4F and Figure 4L), which are largely absent when a participant is colonized by the control strain, 4YB2 (Figure 4C and Figure 4G). Interestingly, individuals with large sNadA-specific plasma cell responses also tended to have larger 4YB2- and 4NB1-dOMV-specific plasma cell responses, although we were unable to determine whether this correlation was significant due to the sample size. This might indicate that Nmen-specific memory B cells (and, by extension, plasma cells) are cross-reactive with the surface antigens of Nlac. Regarding the small number of 4YB2-colonised individuals in whom sNadA-specific plasma cells were detected, we speculate these events represent either displacement of long-lived plasma cells specific for sNadA from their niche in the bone marrow (*38*) or capture of plasma cells with cross reactive specificity to a closely related antigen, e.g. plasma cells targeting epitopes in the YadA domain of other type V autotransporters (*39*). The expansion of IgA-secreting plasma cells broadly reflects the patterns observed for IgG-secreting plasma cells (Figure 4), with the exception that the 'peak' number of IgA-secreting plasma cells recognizing 4YB2-dOMV antigens in 4NB1-colonized participants was significantly increased over baseline (Figure 4J), whereas no significant change was observed in the numbers of IgG-secreting, 4YB2-dOMV-specific plasma cells (Figure 4D). This difference could be attributed to compartmentalization of the mucosal immune response (*40*) and/or slightly different dynamics in plasma cell formation and circulation between the IgG and IgA memory B cell pools in certain individuals.

In five of the 4NB1-colonised participants, we observed an at least 2-fold increase in the reciprocal endpoint anti-sNadA IgG titer after inoculation, compared to baseline (Figure 5C). This indicates that, upon colonization with a genetically modified commensal bacterium that strongly expresses multimeric NadA, these individuals experienced immune responses specifically against the heterologous antigen. The ability of NadA to provoke systemic immune responses when administered intranasally has been investigated in mice, where recombinant NadA was shown to be poorly immunogenic, unless combined with heat-labile enterotoxin from *E. coli* as an adjuvant (*41*). Here, we show that prolonged nasopharyngeal colonization of human volunteers with NadA-expressing GM-Nlac leads to relatively modest increases in anti-sNadA IgG titers in a subset of participants, demonstrating the utility of the recombinant organism to act as both antigen presentation platform and adjuvant (*8*). These antibody titers, though modest, are less than a single $\log_{10}$ lower than titers we observed in serum after parenteral vaccination of an individual with the NadA-containing meningococcal vaccine Bexsero (Figure S11B). Some normal human adults, with no history of meningococcal disease have similar anti-NadA IgG titres to children convalescing from meningococcal infection with NadA-expressing strains (*42*), further evidence that repeated, asymptomatic colonisation with URT commensals throughout a lifetime can lead to seroconversion and, potentially, protection from disease.

To measure efficacy of meningococcal vaccines, serum bactericidal antibody (SBA) activity is the internationally-accepted correlate of protection. An SBA reciprocal titer greater than or equal to 4 is considered to be protective against meningococcal disease when using human complement (*30*). Parenterally-delivered vaccines such as the glycoconjugate vaccines and the

non-capsular (i.e. protein-based) vaccines (e.g. Bexsero), elicit high SBA titers (*43*). In contrast, natural nasopharyngeal colonisation by meningococci elicits very modest and variable SBA titers (*44*). In this study, we measured SBA activity in the serum of all colonized study participants against Nmen reference strain 5/99 (Figure 5E). Though the study was not powered to test the effect of NadA expression by GM Nlac on SBA titers *a priori*, our data suggest that colonisation with strain 4NB1 has potential efficacy in eliciting protection against meningococcal disease caused by NadA-expressing Nmen. In individuals presumed to be protected at baseline (i.e. with an SBA titer ≥ 4) in either study arm, colonization for 90 days with either GM Nlac strain resulted in a no more than 2.9-fold increase in SBA titer (Figure 5E), which is consistent with previous studies of intranasal re-challenge of immunized individuals with cognate antigen (*45*). However, in individuals with non-protective SBA titers against 5/99-induced meningococcal disease at baseline, a higher proportion of individuals colonized with strain 4NB1 became and then remained protected against meningococcal disease at Day 90 than was observed among individuals colonized with strain 4YB2. Although these now-protected individuals did not all have detectable anti-sNadA IgG titers (Figure 5C), it should be noted that not all anti-NadA antibody clones are bactericidal (*22, 46*) and that SBA responses to Bexsero are considered to be the result of the synergistic action of multiple antibody clones, targeting multiple bacterial antigens (*47*). Therefore, the ability of a given participant to mount an SBA response is likely conditioned by their history of prior exposure to various clones of meningococci. Although an appropriately-powered sample of participants is necessary to confirm the ability of this GM Nlac strain to elicit protective SBA titers, these data suggest that strain 4NB1 may have improved efficacy above that of wild type Nlac in protecting against meningococcal disease through

nasopharyngeal colonization and carriage (*6*), and that future transformants could be refined to generate more potent SBA responses.

IgA-secreting plasma cells specific for NadA were detected in the blood of 4NB1-colonised participants (Figure 4G to Figure 4L). From this we infer the likelihood of salivary IgA being generated in these individuals. We have previously demonstrated production of salivary IgA against outer membrane vesicles of wild type *N.lactamica* following a CHIME with wild-type *N.lactamica* (*5*). In the current study we used the ORACOL system for collection of saliva and in our hands the volumes of saliva recovered were small. Although we were able to detect sNadA IgA in 2 participants colonized with GM Nlac (Figure S13), in other participants, the criteria for confirmation of anti-sNadA IgA were not met (see Supplementary Information). Although this may be artefactual due to the methodological requirement for dilution (i.e. anti-sNadA IgA is present in saliva, but at a reciprocal titer less than 3), this result is also biologically plausible due to sequestration of antigen-specific IgA onto the surface of colonising bacteria, as has been suggested in relation to antibody against capsular polysaccharide in a *Streptococcus pneumoniae* CHIME (*48*). Future studies, focusing on the mucosal immune response to colonizing GMOs, will require larger volumes of saliva to enable adequate measurements of antigen-specific IgA to be made.

Although the findings of this study showcase one application for the use of a genetically modified commensal capable of colonizing the URT, specifically the ability to boost immunity developed against antigen from circulating pathobionts; the use of a safe GMO in a CHIME has potential utility in related areas of translational medicine. These include: (i) analysis of the role

of individual microbial gene products in the processes of colonization, carriage, and systemic and mucosal immunological responses, (ii) the impact of vaccination on the carriage of bacteria expressing cognate antigen, (iii) as an experimental platform to manipulate the composition of the upper respiratory tract microbiome and (iv) as a means of potentially inducing immunological tolerance to specific antigens/allergens.

Materials and Methods

Study Design

The clinical protocol for the CHIME has been published elsewhere (*49*), including the study rationale, objectives, inclusion and exclusion criteria, and stopping rules. This was a prospective controlled human infection model experiment (NCT03630250) with co-primary outcomes of establishing the safety of GM-Nlac for human inoculation and NadA-specific immunogenicity in colonized participants. The study was reviewed by the South Central Oxford A Research Ethics Committee (reference: 18/SC/0133). Informed consent for participation in the study was obtained from healthy volunteers aged 18-45 years. Key exclusion criteria included (i) colonization by *Neisseria spp*. in throat swabs at the screening (i.e. one week prior to inoculation) and challenge day visits, (ii) active cigarette or illicit drug smoking, (iii) previous vaccination with a NadA containing vaccine (i.e. Bexsero). The study was single blinded and block randomized. Consent by participants to undergo enhanced hygiene training and to limit social activities for the duration of the study were obtained *a priori*, as was informed consent of a single, nominated bedroom-sharing close contact of inoculated participants (where applicable). Microbiological and immunological data generation and analysis was done by a blinded laboratory study team. No outliers were excluded. Deliberate Release of these genetically

modified organisms in a CHIME was approved by the UK government Department for Environment, Food and Rural Affairs (reference: 17/R50/01). Animal experiments were approved by the Public Health England, Porton Down Ethical Review Committee and authorised under an appropriate UK Home Office project license.

Bacterial isolates and routine culture methods

All stocks of Nlac, Nmen, and their mutant derivatives (Table S1) were maintained as frozen glycerol stocks at -80 ^{o}C. Upon recovery from cryostorage Nlac was cultured on tryptone soya agar (TSA) supplemented with X-Gal (40 μg ml^{-1}) where appropriate. Nmen was cultured on Columbia agar supplemented with horse blood (5 % v/v) (CBA), supplemented with kanamycin (50 μg ml^{-1}) where appropriate. Routine liquid culture of Nlac was performed in TSB, at 37 ^{o}C, 5 % CO_2.

Nmen serogroup B strain MC58 and its mutant derivatives (MC58*ΔnadA* & MC58*ΔsiaD*) were cultured in Mueller-Hinton broth (MHB), supplemented with kanamycin (50 μg ml^{-1}). Nmen serogroup Y strain N54.1 and its mutant derivative (N54.1*ΔnadA*) were cultured in MHB supplemented with 5 mM 4-hydroxyphenylacetic acid (4HPA) (Sigma-Aldrich, cat no. H50004-5G). Nmen NadA-overexpressing strain 5/99 was cultured in modified Frantz medium (*50*)

For determination of clinically relevant antibiotic MICs, Nlac was cultured as a lawn on Mueller-Hinton agar supplemented with horse blood (5 % v/v) in the presence of the appropriate e-test strips: ciprofloxacin and ceftriaxone (Biomerieux). Note that as no interpretative criteria exist for determining antibiotic susceptibility of Nlac (WT or GM), two reference criteria were used. The first was the European Committee on Antimicrobial Susceptibility Testing (EUCAST)

breakpoints for *N. meningitidis* and the effective treatment of meningococcal disease and the second was the antibiotic susceptibility profile of 286 isolates of WT *N. lactamica* (*28*).

Detection and identification of *Neisseria* species in clinical samples

Neisseria species were isolated from clinical samples using GC selective agar plates, supplemented with 10 % (v/v) lysed horse blood, VCAT selective supplement (Oxoid, cat no. SR0104) (1 % v/v), Vitox supplement (Oxoid, cat no. SR0090) (2 % v/v), glucose (0.4 % w/v), Amphotericin B (10 μg ml^{-1}) and X-gal (40 μg ml^{-1}) (GC+Xgal) (Southern Group Laboratories). Pre-clinical tests demonstrated that only Nlac grew as blue coloured colonies. For each participant at each time point, up to 10 colonies of blue, putative GM-Nlac were subcultured onto fresh GC+X-gal plates for the preparation of stocks and lysates for diagnostic PCR. White-coloured, putative Nmen colonies were tested for oxidase activity using oxidase detection strips (Oxoid, cat no. MB0266). All oxidase positive, Gram-negative diplococci were subcultured onto fresh Columbia agar plates supplemented with chocolated horse blood (5 % v/v) (CHOC), incubated overnight at 37 ^{o}C, 5 % CO_2 and then identified using API NH kits (Biomerieux, cat no. 10400), performed according to the manufacturer's instructions. Bacterial stocks were created of all carriage Nmen isolates identified during the study.

Culture methods for preparation of human challenge inocula

To prepare the inocula, seed cultures of the appropriate GM-Nlac strain were grown overnight at 37 ^{o}C, 5 % CO_2 on TSA plates supplemented with X-gal. Blue-colored GM-Nlac colonies were

subcultured in TSB (Vegitone) at 37 ^{o}C, 5 % CO_2 to an OD_{600nm} of 1.5 arbitrary units. Bacteria were washed and then resuspended in Frantz medium:glycerol (70 % : 30 % v/v). Aliquots were stored in numbered 'Master Stock' cryovials at -80 ^{o}C. Master stock viability and purity was determined by culture on TSA, CBA and CHOC plates overnight at 37 ^{o}C, 5 % CO_2. Subsequently, contaminant-free 'Master Stock' vials were diluted into ice-cold Frantz medium:glycerol (70% : 30% v/v) to a final concentration of 5 x 10^6 CFU ml^{-1}. One-millilitre aliquots were then stored in numbered 'Inoculum' cryovials at -80 ^{o}C. The average viability of the 'Inoculum' vials was calculated as 4.8 x 10^6 CFU ml^{-1} for strain 4YB2 (n = 7) and 4.8 x 10^6 CFU ml^{-1} (n = 8) for strain 4NB1.

Preparation of inoculum for intranasal administration

A 1 ml 'Inoculum' vial containing the appropriate GM-Nlac strain was thawed at RT, vortexed, and 500 µl was diluted into 4.5 ml sterile PBS pH 7.4 (Severn Biotech). Intranasal inoculation of participants occurred within 30 min of defrosting the vial and was performed with sterile Pasteur pipettes (1 per nostril). The purity and viability of the inoculation dose was determined by culture on CHOC agar.

Preparation of gDNA

Bacterial gDNA was harvested from mid log phase cultures of each bacterial strain using a GeneJET Genomic DNA Purification kit (Thermofisher, cat no. K0722) according to Protocol D

(Gram-negative bacteria) in the manufacturer's instructions. The concentration of gDNA was measured using a Nanodrop spectrophotometer (Shimadzu).

Transformation of Neisseria species

Mid-log phase cultures of WT Nlac strains Y92-1009, 4NB1 and WT Nmen strain MC58 were pelleted, washed in PBS and resuspended in TSB supplemented with 10 mM $MgSO_4$ at an OD_{600nm} = 0.3. One milliliter aliquots of each bacterial suspension were incubated at 37 ^oC, 5 % CO_2 for 3 h with 1 x 10^4 pmoles of gDNA harvested from one of the following Nlac or Nmen mutant strains: (i) Nlac strain Y92-1009*ΔnlaIII:aphA3*, (ii) Nmen strain MC58*ΔnadA:aphA3*, (iii) Nmen strain MC58*ΔsiaD:aphA3*. Aliquots of each suspension were spread on CBA plates supplemented with kanamycin (50 μg ml^{-1}). The total viability (in CFU ml^{-1}) of each suspension was determined through serial dilution and plating on CBA. The number of kan^R colonies (in CFU ml^{-1}) was divided by the total number of bacteria (in CFU ml^{-1}) and normalized to 1 pmol gDNA to give transformation efficiency.

Diagnostic Polymerase Chain Reaction (PCR)

Bacterial isolates from clinical samples were identified as GM-Nlac using multiplex PCR. Briefly, lysates from putative GM-Nlac colonies were used as template DNA to amplify a GM signature sequence (Band3d, 284 bp) and/or the 16S rRNA gene (Band1, 469 bp). Genomic DNA from GM-Nlac strain 4NB1 (50 ng ml^{-1}) was used as a Band3d positive control, gDNA from WT Nmen strain H44/76 (50 ng ml^{-1}) was used as a Band1 positive control, and RNAse-

free H_2O was used as a negative control. Each PCR reaction volume (20 µl) comprised one of: control gDNA, test lysate or RNAse-free H_2O (1 µl), plus Platinum II Taq Hot-Start DNA polymerase Master mix (2x) (Thermofisher, cat no. 14966025) (10 µl), Band1FOR (10 µM) (0.8 µl), Band1REV (10 µM) (0.8 µl), Band3dFOR (5 µM) (0.4 µl), Band3dREV (5 µM) (0.4 µl) and RNAse-free H_2O (6.6 µl). PCR amplification used the following, 2-step thermal cycling parameters: [1 x 2 min @ 95 ^oC] followed by [35 x (5 sec @ 98 ^oC, 15 sec @ 60 ^oC and 15 sec @ 68 ^oC)]. Amplicons were analysed by 2% agarose gel electrophoresis and visualized under UV transillumination using a Gel Doc XR+ (Bio Rad). GM-Nlac was positively identified if two amplicons of 284 bp and 469 bp were present. A single amplicon of 469 bp was determined to be something other than GM-Nlac. PCR yielding zero amplicons was considered to have failed, and was repeated until definitively identified as being, or not being, GM-Nlac.

Flow cytometry

Surface expression of NadA on Neisseria spp. was assessed by flow cytometry of fixed cells. Briefly, bacteria (2 x 10^7 CFU) were labeled with either anti-NadA mAb 6e3 (*22*) or anti-NadA pAb (GSK) in wash buffer (PBS + 5 % FCS) for 30 min at 4 ^oC. Cells were labelled with goat anti-mouse IgG-Alexafluor488 antibody in wash buffer for 30 min at 4 ^oC, and then fixed in formalin for 15 min. Bacteria were gated based upon forward and side scatter profiles and a total of 10,000 events were acquired on FacsCalibur (BD Biosciences). Relative NadA expression levels were measured as the Mean Fluorescence Intensity (MFI) of Alexafluor488, recorded in the FL-1 channel for the gated events.

Adherence assay

HEP-2 cells (2 x 10^5 cells $well^{-1}$) were seeded into 24-well plates and cultured for 2 days in Dulbecco's Modified Eagle's medium (DMEM) supplemented with 10 % Foetal Calf Serum (FCS) at 37 ^oC, 5 % CO_2. HEP-2 cells were then washed twice in sterile PBS, then infected at MOI = 100 with the relevant bacterial strain. Plates were incubated at 37 ^oC, 5 % CO_2 and at 2 h, 4 h and 6 h, supernatants were aspirated and wells washed five times with PBS. Two percent saponin in PBS (250 µl $well^{-1}$) was added and plates were incubated for 15 min at 37 ^oC, 5 % CO_2. Wells were supplemented with PBS to a final volume of 1 ml and cells were mechanically agitated through pipetting. The number of viable bacteria was determined by plating serially diluted saponized cell lysate onto CBA plates. The viability of each lysate was normalized to the number of HEP-2 cells per well, which was estimated from the cell count of duplicate wells.

Isolation of Outer Membrane Vesicles

OMV were deoxycholate-extracted from bacterial cell pellets grown in modified Caitlin (MC7) medium (*50*). Briefly, *Neisseria* were cultured overnight at 37 ^oC, 5 % CO_2 to OD_{600nm} > 2.0 and pelleted by centrifugation at 4500 *g* for 1 h. Cell pellets were resuspended using a glass homogeniser into 0.1 M Tris-HCl (pH 8.6) with 10 mM EDTA and 0.5 % (w/v) deoxycholic acid sodium salt. These suspensions were centrifuged at 20,000 *g* for 30 min at 4 ^oC, and the supernatant was retained. The homogenization procedure was performed twice. dOMV were harvested from the combined supernatants by ultracentrifugation at 100,000 *g* for 2 h at 4 ^oC. Pelleted dOMV were gently resuspended into 50 mM Tris-HCl (pH 8.6) with 2 mM EDTA,

20 % (w/v) sucrose and 1.2 % deoxycholic acid sodium salt. dOMV were again pelleted by ultracentrifugation at 100,000 *g* for 2 h at 4 ºC, before resuspension into 50 mM Tris-HCl with 3 % sucrose, which formed the final formulation. The protein content of the dOMV formulation was measured by the DC Protein assay (Biorad), with reference to a BSA standard curve.

Murine Immunisations with dOMV

Groups of ten 6-8-week-old BALB/c mice were immunized by subcutaneous injection with three doses of 10 µg Nlac dOMV containing 0.33% Alhydrogel (*51*) at day 0, 21 and 28. Sera were collected on day 35.

Murine intraperitoneal (i/p) challenge model

Bacteria were pelleted from mid-log phase cultures of WT Nlac strain Y92-1009 and the GM-Nlac strains 4YB2 and 4NB1 and resuspended at different concentrations into 50 µl PBS supplemented with 10 mg of human holo-Transferrin (Sigma-Aldrich, cat no. T4132). Six groups of NIH/OLA mice (6-8 weeks), comprised of 5 male and 5 female mice per group, were challenged with 'high' or 'low' i/p doses of the Nlac/GM-Nlac strains. Viability of each dose was determined by colony count on CBA plate cultures. Twenty-four hours after challenge, the mice were given an additional i/p dose of 10 mg human holo-Transferrin. The health of the mice was assessed based on their outward appearance and behaviour and was recorded every 4 h in the first 2 days and then every 6-8 h up to 5 days post-challenge. Behaviourally 'normal' mice were considered 'healthy' (recorded as 'H'), whilst those experiencing mild discomfort presented as

'arched' (recorded as 'A') and/or 'ruffled' (recorded as 'R').

Serum bactericidal assays

All SBA assays were performed against Nmen strain 5/99, resuspended in bactericidal buffer (BB; Hanks buffered saline solution (Invitrogen) and 1% BSA) at 6 x 10^4 CFU ml^{-1}. Twofold dilutions of heat-inactivated sera were prepared in microtiter plates (20 µl), to which Nmen (10 µl) was added followed by IgG-depleted pooled human plasma as an exogenous human complement source (10 µl) (i.e. 25% final concentration). Plates were incubated at 37°C for 1 h with shaking at 900 rpm. Each sample and control well was then plated onto CBA using the tilt method and incubated overnight at 37 ºC, 5% CO_2. The following day colonies were counted and % survival was determined in comparison to colony numbers in the t = zero control. Dilutions of sera were deemed bactericidal if bacterial survival rates were ≤ 50 %. SBA reciprocal titres were determined as the reciprocal of the most diluted serum sample that was bactericidal.

Recombinant expression of the soluble domain of NadA

Recombinant expression of sNadA was carried out commercially by BioServUK (Sheffield, UK), broadly consistent with the methodology described by Cecchini and colleagues (*52*). Briefly, the coding sequence for *nadA* allele 1, minus the sequence coding for the C-terminal YadA domain (*nadAΔ285-364*), was cloned from pJL0017 into pRSETα to include a C-terminal 6His-tag. Protein secreted into growth medium by the transformed *E. coli* strain BL21 (DE3)

was purified using HiFliQ column chromatography and buffer exchanged into PBS (pH7.5). Analysis of purified sNadA by SDS-PAGE showed a single band by silver staining under reducing and denaturing conditions, and three bands, consistent with homotrimer formation, under denaturing but non-reducing conditions. Purified sNadA was cross-reactive with anti-NadA mAb 6e3 (GSK) in western blotting analysis. Purified sNadA was stored at -80 ^{o}C and diluted in PBS to make working stocks (1 mg ml^{-1}), which were stored at -20 ^{o}C.

ELISA for measurement of human anti-Nlac IgG

Nunc Maxisorb 96-well plates were coated overnight at 5 ^{o}C with WT Nlac Y92-1009 dOMV (10 µg ml^{-1}) in carbonate coating buffer (pH 9.6). Coated plates were washed five times with PBS containing 1 % Tween 20 (PBST) (Skatron SkanWasher 400) and blocked with PBST containing 5 % (v/v) FCS for 90 min at RT. Plates were washed five times with PBST and then loaded in duplicate with serially diluted test samples and reference serum (NA9136). Dilutions were prepared in Sterilin Serowell (low binding) plates with a starting dilution of 1/25 followed by three-fold serial dilution across the plate. Loaded plates were incubated with shaking at RT for 90 min. Plates were then washed five times with PBST prior to incubation at RT for 90 min with goat anti-human IgG Fcγ-fragment-specific alkaline phosphatase conjugate (Jackson Immunoresearch Laboratories cat no. 109-055-098) diluted 1/1750 in PBST + 5 % (v/v) FCS. This was followed by a wash step as above, and addition of AP yellow (p-nitrophenyl phosphate) substrate (BioFX Laboratories, Cat. No. PNPP-0100) for 55 min at RT. The reaction was stopped with 3M NaOH. Optical density was read using a VersaMax plate reader at 405nm with a reference wavelength of 690nm. SoftMax® PRO Enterprise software (Molecular Devices) was

used to fit an un-weighted five parameter logistic (5PL) log curve to titrations of the reference serum for each plate. Test sample titres were calculated by interpolation from the reference serum dose response curve (interpolated titre multiplied by dilution factor). A mean of the acceptable values from all dilutions was then taken as the final value for each test serum.

ELISA for measurement of human anti-sNadA IgG endpoint titers

Corning Costar EIA/RIA 96 well plates were coated at 4 ºC with sNadA (10 μg ml^{-1}) in carbonate coating buffer (pH 9.6). Coated plates were washed three times with PBS and blocked with 5 % FCS-PBS at 37 ºC for 2 h. Plates were washed four times with PBS and then loaded (in duplicate) with twofold dilutions of test sera (50 μl). Control serum (NA9136) was diluted 1/16 in 5 % FCS-PBS, as this dilution was shown to generate a positive signal under the conditions used in this ELISA (Supplementary Figure 11). Loaded plates were incubated at 37 ºC, 5 % CO_2 for 1 h, then washed five times with PBS supplemented with 0.05 % Tween 20 (PBS-T). Biotinylated, rat-derived anti-human IgG mAb (M1310G05) (Biolegend, cat no. 410718) was diluted 1/1000 in 5 % FCS-PBS and 50 μl was added to each well. Plates were incubated at 37 ºC, 5 % CO_2 for 1 h, then washed five times with PBS-T. A streptavidin-horse radish peroxidase (HRP) conjugate (Biolegend, cat no. 405210) was also diluted 1/1000 in 5 % FCS-PBS and added to each well (50 μl). Plates were incubated at 37 ºC, 5 % CO_2 for 1 h, then washed five times with PBS-T and a single wash with PBS. Chromogenic substrate, o-phenylenediamine dihydrochloride (OPD) (Thermofisher, cat no. 34006), was prepared by dissolving 1 OPD tablet into 9 ml of dH_2O supplemented with 1 ml stable peroxide substrate buffer (Thermofisher, cat no. 34062). The plate was incubated with OPD substrate (100 μl $well^{-1}$) at 32 ºC for exactly 20 min. Signal development was stopped with 2 N

H_2SO_4 (50 µl $well^{-1}$), and the color-change quantified on a Versamax plate reader (Molecular Devices) measuring at optical density 490nm (OD_{490nm}). The reciprocal endpoint titre of each test serum was considered to be the reciprocal titre of the least diluted serum sample tested that generated an OD_{490nm} in excess of 1.4 arbitrary units in this assay (equivalent to an interpolated reciprocal titer of 17.245 of control serum NA9136, see Supplementary Figure S11B).

ELISA for detection of human anti-sNadA sIgA

Corning Costar EIA/RIA 96 well plates were coated at 4 °C with one of: sNadA (20 µg ml^{-1}) in carbonate coating buffer (pH 9.6) (50 µl), bovine serum albumin (BSA) (20 µg ml^{-1}) in carbonate coating buffer (pH 9.6) (50 µl), or carbonate coating buffer (pH 9.6) alone. Each saliva sample was centrifuged to clear particulate matter and then diluted threefold into ChonBlock Sample Diluent/Blocking buffer (SD/B buffer) (Chondrex Inc., cat. no. 9068). Plates were washed three times with PBS and blocked with 5 % FCS-PBS at 37 °C for 2 h. Plates were washed four times with PBS before pairs of wells, one sNadA-coated and the other uncoated, were loaded with 50 µl of each diluted saliva sample. The remaining diluted saliva sample was retained for measurement of total IgA. Saliva NP12803, found to contain anti-BSA IgA, was diluted fourfold into SD/B buffer and used as a protocol control to determine the efficacy of downstream ELISA reagents. Saliva-loaded plates were incubated at 37 °C, 5 % CO_2 for 1 h, then washed five times with PBS-T. Murine anti-human IgA mAb [3B7] (abcam, cat. no. ab7400) was diluted 1/1000 in SD/B buffer and 50 µl was added to each well. Plates were incubated at 37 °C, 5 % CO_2 for 1 h, then washed five times with PBS-T. Rat anti-mouse IgG mAb [SB77e], conjugated to HRP (abcam, cat. no. ab99603) was diluted 1/1000 in Chonblock detection antibody dilution buffer (Chondrex Inc., cat. no. 90681) and

added to each well (50 µl). Plates were incubated at 37 ºC, 5 % CO_2 for 1 h, then washed five times with PBS-T and a single wash with PBS. Chromogenic substrate OPD was prepared by dissolving 1 OPD tablet into 9 ml of dH_2O supplemented with 1 ml stable peroxide substrate buffer. The plate was incubated with OPD substrate (100 µl $well^{-1}$) at 32 ºC for exactly 20 min. Signal development was stopped with 2 N H_2SO_4 (50 µl $well^{-1}$), and the color-change quantified on a Versamax plate reader (Molecular Devices) measuring at optical density 490nm (OD_{490nm}). The threshold for a 'positive' signal in a sNadA-coated well was an OD_{490nm} reading equal to or in excess of 0.07, and in an uncoated well the threshold for a 'positive' signal was an OD_{490nm} reading equal to or in excess of 0.068 (see Supplementary Information). For a saliva sample to be considered 'anti-sNadA IgA positive' in this ELISA (i.e. to be considered as containing anti-sNadA IgA at a reciprocal titer equal to or in excess of 3), we required a positive signal in the sNadA-coated well and a negative signal in the uncoated well. Positive signals in uncoated wells were considered to result from non-specific interactions of the sample with another component of the ELISA.

ELISA for measurement of total human sIgA

Corning Costar EIA/RIA 96 well plates were coated at 4 ºC with murine anti-human IgA mAb [3B7] (20 µg ml^{-1}) in carbonate coating buffer (pH 9.6) (50 µl). Saliva samples were diluted x30, x300 and x3000-fold in SD/B buffer. Solutions of human IgA (isolated from colostrum, Sigma-Aldrich, cat. no. I2636) were prepared at 1 mg ml^{-1}, 0.1 mg ml^{-1} and 0.01 mg ml^{-1}. Following plate washing (3 x PBS) and well blocking with 5 % FCS-PBS for 2h at 37 ºC, 50 µl aliquots of each standard and sample dilution were loaded into duplicate wells and incubated for 1h at 37 ºC. Plates were washed five times with PBS-T. Murine anti-human IgA mAb [1H9],

conjugated to HRP, was diluted 1/1000 times in Chonblock detection antibody dilution buffer and added to each well (50 µl). Plates were incubated at 37 °C, 5 % CO_2 for 1 h, then washed five times with PBS-T and a single wash with PBS. The plate was incubated with OPD substrate (100 µl $well^{-1}$) at 32 °C for exactly 20 min. Signal development was stopped with 2 N H_2SO_4 (50 µl $well^{-1}$), and the color-change quantified on a Versamax plate reader (Molecular Devices) measuring at optical density 490nm (OD_{490nm}). The average of duplicate OD_{490nm} readings was used to interpolate the concentration of IgA present in each saliva sample with reference to the IgA standards. Where more than one interpolation was possible, the IgA concentration was calculated as the average value of the interpolations.

Isolation of peripheral blood mononuclear cells

PBMC were isolated from whole blood of CHIME participants by density gradient centrifugation and used immediately in the plasma cell ELISpot assay. The remainders were stored in LN_2 for later use in the memory B cell ELISpot assay.

Polyclonal stimulation of peripheral blood mononuclear cells

PBMC were cultured and polyclonally stimulated as outlined previously (*53*). Briefly, PBMC isolated from the whole blood of participants taken at Day 0, Day 28 and Day 90 visits were cultured separately in 96-well tissue culture plates (ThermoFisher) at 2 x 10^5 cells per well in 200 µl AIM/V + albumax medium (Gibco, Invitrogen) supplemented with 10 % FCS and 50 µM β-mercaptoethanol (hereafter, AIM/V+). Cultures were supplemented with 3 µg ml^{-1} human

phosphorothioate-modified oligodeoxynucleotide containing CpG motifs (ODN2006: 5'-TCG TCG TTT TGT CGT TTT GTC GTT-3') (InvivoGen), 10 ng ml^{-1} IL-2 (R&D Systems), and 10 ng ml^{-1} IL-10 (Pharmingen, BD), and incubated for 5 days at 37 ^{o}C, 5 % CO_2.

ELISPOT Assay

Ninety-six-well ELISpot plates (Multiscreen HTS plate, Merck Millipore, cat no. MSIPS4510) were activated with 70 % (v/v) ethanol, washed three times with PBS and coated with 100 µl PBS containing one of the following antigens: keyhole limpet hemocyanin (KLH) (Sigma-Aldrich) (10 µg ml^{-1}), tetanus toxoid (TT) (2.5 level of flocculation (LOF) units /ml), influenza hemagglutinin (FluHA) (influenza antigen reagent 09/174, H1N1, NIBSC, UK) (0.5 µg ml^{-1}), dOMV derived from GM-Nlac strain 4YB2 (4YB2-dOMV) (10 µg ml^{-1}), dOMV derived from GM-Nlac strain 4NB1 (4NB1-dOMV) (10 µg ml^{-1}), sNadA (10 µg ml^{-1}) or rat-anti-human IgG mAb (clone M1310G05, IgG2a, k, Biolegend) (anti-IgG mAb) (10 µg ml^{-1}). All plates were stored at 4 ^{o}C overnight. Prior to use, plates were washed four times with PBS and blocked by incubation at 37 ^{o}C for 2 h with AIM-V medium supplemented with 10 % FCS. Blocked plates were washed four times with PBS, before adding PBMC to each well and incubating for 18 h at 37 ^{o}C, 5 % CO_2. For the plasma cell ELISPOT, PBMC were freshly isolated and plated in duplicate at 2 x 10^5 cells $well^{-1}$ in AIM-V medium + 10 % FCS. For the memory B cell assay, polyclonally-stimulated PBMC (see above) were harvested and washed in AIM/V+ media by centrifugation at 300 *g*. Cells were resuspended in AIM/V+ medium at a concentration of 5 x 10^6 cells ml^{-1}, serially diluted, and seeded into ELISpot plate wells (200 µl volume) in

duplicate or triplicate at concentrations of 5 x 10^6 cells ml^{-1}, 2 x 10^6 cells ml^{-1}, 1 x 10^6 cells ml^{-1} and 2.5 x 10^5 cells ml^{-1}.

Following incubation, plates were washed four times with PBS-T and cells were lysed by washing three times with dH_2O, followed by 5 min incubation at RT in dH_2O. Plates were washed as before and incubated for 1 h at 37 ºC, 5 % CO_2, with alkaline phosphatase-conjugated anti-human IgG pAb (Sigma-Aldrich), prepared in PBS supplemented with 0.01 % Tween 20 and 1 % goat serum (Binding Buffer). Unbound pAb was removed by washing with PBS-T, rinsing the backs of the PVDF membranes gently with tap water and a final three washes with PBS. Plates were then incubated at RT with 50 µl $well^{-1}$ BCIP substrate solution (prepared from SigmaFAST BCIP tablets in dH_2O, Sigma cat no. B5655) for 13 min, before washing with tap water. ELISpot plates were dried and imaged using an AID ELISpot reader. IgG spot-forming units (SFU) were counted using the AID ELISpot software package, version 3.5. For the memory B cell assay, antigen-specific IgG SFU frequencies were derived for NadA, 4NB1-dOMV, and 4YB2-dOMV-coated wells from the lowest input cell concentration where a mean of 1-20 IgG SFU were counted following subtraction of KLH background. These antigen- specific SFU were expressed as a percentage of total IgG SFUs, as described previously (*54*).

Statistical Analysis

Standard deviations (SDs) associated with serological responses to WT Nlac derived from our first Nlac CHIME were utilised to inform the sample size calculation (*5*). This gave SDs on a log-10 scale of 0.26 for serum IgG. Using the SD of 0.26, it was calculated that a 4-fold rise in

Nlac-specific IgG titer would be confirmed with 10 carriers of (GM-)Nlac with 90% power using analysis of variance.

All statistical analyses were performed using GraphPad Prism software (version 8.0). Parametrically- and non-parametrically-distributed continuous variables were summarised with mean ± standard deviation (SD) or median, respectively, and analysed using an appropriate parametric or non-parametric test, as indicated in each figure legend. The proportion of participants with ≥ 2-fold rise in anti-NadA IgG titer in control vs. intervention groups was compared using Fisher's exact test. All p values were two-tailed and p values ≤ 0.05 were considered statistically significant.

Supplementary Materials:

Supplementary Information

Figure S1. The impact of endogenous restriction endonuclease activity on transformation efficiency in *N. lactamica* Y92-1009 and the use of DNA hypermethylation to abrogate its effect.

Figure S2. WT *N. lactamica* Y92-1009 is a piliated, naturally competent organism and requires expression of the type IV pilus for the horizontal acquisition of DNA.

Figure S3. Factors effecting transformation efficiency of *N. lactamica* Y92-1009 with hypermethylated DNA.

Figure S4. Ablation and complementation of β-galactosidase activity through targeted mutagenesis of *N. lactamica* Y92-1009.

Figure S5. The nucleotide sequence upstream of the meningococcal *porA* gene is an upstream activation sequence (UAS) that enhances gene expression.

Figure S6. Plasmids for the chromosomal transformation of *N. lactamica* Y92-1009 with a highly active, constitutive, heterologous gene expression cassette and the endogenous β-galactosidase gene for antibiotic-free screening of successful transformants.

Figure S7. Adverse events reported during the admission period of the controlled human infection model experiment.

Figure S8. Adverse events reported during the follow-up period of the controlled human infection model experiment.

Figure S9. Clinically observed adverse events during the admission and follow-up periods of the controlled human infection model experiment.

Figure S10. Laboratory parameter adverse events during the admission and follow-up periods of the controlled human infection model experiment.

Figure S11. Determination of endpoint titre for anti-sNadA IgG in human serum samples.

Figure S12. Representative outputs from IgG-secreting memory B cell ELISpot assay on participants colonized with GM-Nlac.

Figure S13. Results of salivary IgA ELISAs.

Table S1. Bacterial strains used in this study.

Table S2. Plasmids used in this study.

Table S3. Primers used in this study.

References:

1. D. Goldblatt, M. Hussain, N. Andrews, L. Ashton, C. Virta, A. Melegaro, R. Pebody, R. George, A. Soininen, J. Edmunds, N. Gay, H. Kayhty, E. Miller, Antibody responses to nasopharyngeal carriage of Streptococcus pneumoniae in adults: a longitudinal household study. *J Infect Dis* **192**, 387-393 (2005).
2. D. B. Hall, M. K. Lum, L. R. Knutson, W. L. Heyward, J. I. Ward, Pharyngeal carriage and acquisition of anticapsular antibody to Haemophilus influenzae type b in a high-risk population in southwestern Alaska. *Am J Epidemiol* **126**, 1190-1197 (1987).
3. G. R. Jones, M. Christodoulides, J. L. Brooks, A. R. Miller, K. A. Cartwright, J. E. Heckels, Dynamics of carriage of Neisseria meningitidis in a group of military recruits:

subtype stability and specificity of the immune response following colonization. *J Infect Dis* **178**, 451-459 (1998).

4. R. Gold, I. Goldschneider, M. L. Lepow, T. F. Draper, M. Randolph, Carriage of Neisseria meningitidis and Neisseria lactamica in infants and children. *J Infect Dis* **137**, 112-121 (1978).
5. C. M. Evans, C. B. Pratt, M. Matheson, T. E. Vaughan, J. Findlow, R. Borrow, A. R. Gorringe, R. C. Read, Nasopharyngeal colonization by Neisseria lactamica and induction of protective immunity against Neisseria meningitidis. *Clin Infect Dis* **52**, 70-77 (2011).
6. A. M. Deasy, E. Guccione, A. P. Dale, N. Andrews, C. M. Evans, J. S. Bennett, H. B. Bratcher, M. C. Maiden, A. R. Gorringe, R. C. Read, Nasal Inoculation of the Commensal Neisseria lactamica Inhibits Carriage of Neisseria meningitidis by Young Adults: A Controlled Human Infection Study. *Clin Infect Dis* **60**, 1512-1520 (2015).
7. A. Pandey, D. W. Cleary, J. R. Laver, A. Gorringe, A. M. Deasy, A. P. Dale, P. D. Morris, X. Didelot, M. C. J. Maiden, R. C. Read, Microevolution of Neisseria lactamica during nasopharyngeal colonisation induced by controlled human infection. *Nat Commun* **9**, 4753 (2018).
8. G. Sardinas, K. Reddin, R. Pajon, A. Gorringe, Outer membrane vesicles of Neisseria lactamica as a potential mucosal adjuvant. *Vaccine* **24**, 206-214 (2006).
9. H. Chi, X. Wang, Y. Shao, Y. Qin, Z. Deng, L. Wang, S. Chen, Engineering and modification of microbial chassis for systems and synthetic biology. *Synth Syst Biotechnol* **4**, 25-33 (2019).

10. C. Michon, P. Langella, V. G. Eijsink, G. Mathiesen, J. M. Chatel, Display of recombinant proteins at the surface of lactic acid bacteria: strategies and applications. *Microb Cell Fact* **15**, 70 (2016).

11. Z. Zhou, X. Chen, H. Sheng, X. Shen, X. Sun, Y. Yan, J. Wang, Q. Yuan, Engineering probiotics as living diagnostics and therapeutics for improving human health. *Microb Cell Fact* **19**, 56 (2020).

12. L. V. Hooper, J. I. Gordon, Commensal host-bacterial relationships in the gut. *Science* **292**, 1115-1118 (2001).

13. A. O'Dwyer C, K. Reddin, D. Martin, S. C. Taylor, A. R. Gorringe, M. J. Hudson, B. R. Brodeur, P. R. Langford, J. S. Kroll, Expression of heterologous antigens in commensal Neisseria spp.: preservation of conformational epitopes with vaccine potential. *Infect Immun* **72**, 6511-6518 (2004).

14. B. Q. Qiang, I. Schildkraut, Two unique restriction endonucleases from Neisseria lactamica. *Nucleic Acids Res* **14**, 1991-1999 (1986).

15. A. K. Pandey, D. W. Cleary, J. R. Laver, M. C. J. Maiden, X. Didelot, A. Gorringe, R. C. Read, Correction to: Neisseria lactamica Y92-1009 complete genome sequence. *Stand Genomic Sci* **13**, 4 (2018).

16. B. Capecchi, J. Adu-Bobie, F. Di Marcello, L. Ciucchi, V. Masignani, A. Taddei, R. Rappuoli, M. Pizza, B. Arico, Neisseria meningitidis NadA is a new invasin which promotes bacterial adhesion to and penetration into human epithelial cells. *Mol Microbiol* **55**, 687-698 (2005).

17. C. M. Buckwalter, E. G. Currie, R. S. W. Tsang, S. D. Gray-Owen, Discordant Effects of Licensed Meningococcal Serogroup B Vaccination on Invasive Disease and Nasal Colonization in a Humanized Mouse Model. *J Infect Dis* **215**, 1590-1598 (2017).

18. M. Comanducci, S. Bambini, D. A. Caugant, M. Mora, B. Brunelli, B. Capecchi, L. Ciucchi, R. Rappuoli, M. Pizza, NadA diversity and carriage in Neisseria meningitidis. *Infect Immun* **72**, 4217-4223 (2004).

19. A. van der Ende, C. T. Hopman, J. Dankert, Multiple mechanisms of phase variation of PorA in Neisseria meningitidis. *Infect Immun* **68**, 6685-6690 (2000).

20. L. Fagnocchi, E. Pigozzi, V. Scarlato, I. Delany, In the NadR regulon, adhesins and diverse meningococcal functions are regulated in response to signals in human saliva. *J Bacteriol* **194**, 460-474 (2012).

21. M. Alamro, F. A. Bidmos, H. Chan, N. J. Oldfield, E. Newton, X. Bai, J. Aidley, R. Care, C. Mattick, D. P. Turner, K. R. Neal, D. A. Ala'aldeen, I. Feavers, R. Borrow, C. D. Bayliss, Phase variation mediates reductions in expression of surface proteins during persistent meningococcal carriage. *Infect Immun* **82**, 2472-2484 (2014).

22. I. Bertoldi, A. Faleri, B. Galli, P. Lo Surdo, A. Liguori, N. Norais, L. Santini, V. Masignani, M. Pizza, M. M. Giuliani, Exploiting chimeric human antibodies to characterize a protective epitope of Neisseria adhesin A, one of the Bexsero vaccine components. *FASEB J* **30**, 93-101 (2016).

23. F. A. Bidmos, K. R. Neal, N. J. Oldfield, D. P. Turner, D. A. Ala'Aldeen, C. D. Bayliss, Persistence, replacement, and rapid clonal expansion of meningococcal carriage isolates in a 2008 university student cohort. *J Clin Microbiol* **49**, 506-512 (2011).

24. V. Masignani, M. Pizza, E. R. Moxon, The Development of a Vaccine Against Meningococcus B Using Reverse Vaccinology. *Front Immunol* **10**, 751 (2019).

25. A. R. Gorringe, S. Taylor, C. Brookes, M. Matheson, M. Finney, M. Kerr, M. Hudson, J. Findlow, R. Borrow, N. Andrews, G. Kafatos, C. M. Evans, R. C. Read, Phase I safety and immunogenicity study of a candidate meningococcal disease vaccine based on Neisseria lactamica outer membrane vesicles. *Clin Vaccine Immunol* **16**, 1113-1120 (2009).

26. O. B. Harrison, H. Claus, Y. Jiang, J. S. Bennett, H. B. Bratcher, K. A. Jolley, C. Corton, R. Care, J. T. Poolman, W. D. Zollinger, C. E. Frasch, D. S. Stephens, I. Feavers, M. Frosch, J. Parkhill, U. Vogel, M. A. Quail, S. D. Bentley, M. C. Maiden, Description and nomenclature of Neisseria meningitidis capsule locus. *Emerg Infect Dis* **19**, 566-573 (2013).

27. S. A. Frye, M. Nilsen, T. Tonjum, O. H. Ambur, Dialects of the DNA uptake sequence in Neisseriaceae. *PLoS Genet* **9**, e1003458 (2013).

28. L. Arreaza, C. Salcedo, B. Alcala, J. A. Vazquez, What about antibiotic resistance in Neisseria lactamica? *J Antimicrob Chemother* **49**, 545-547 (2002).

29. K. Fink, Origin and Function of Circulating Plasmablasts during Acute Viral Infections. *Front Immunol* **3**, 78 (2012).

30. R. Borrow, G. M. Carlone, N. Rosenstein, M. Blake, I. Feavers, D. Martin, W. Zollinger, J. Robbins, I. Aaberge, D. M. Granoff, E. Miller, B. Plikaytis, L. van Alphen, J. Poolman, R. Rappuoli, L. Danzig, J. Hackell, B. Danve, M. Caulfield, S. Lambert, D. Stephens, Neisseria meningitidis group B correlates of protection and assay standardization--

international meeting report Emory University, Atlanta, Georgia, United States, 16-17 March 2005. *Vaccine* **24**, 5093-5107 (2006).

31. S. Crotty, R. D. Aubert, J. Glidewell, R. Ahmed, Tracking human antigen-specific memory B cells: a sensitive and generalized ELISPOT system. *J Immunol Methods* **286**, 111-122 (2004).

32. A. T. Vaughan, A. Gorringe, V. Davenport, N. A. Williams, R. S. Heyderman, Absence of mucosal immunity in the human upper respiratory tract to the commensal bacteria Neisseria lactamica but not pathogenic Neisseria meningitidis during the peak age of nasopharyngeal carriage. *J Immunol* **182**, 2231-2240 (2009).

33. G. Blanchard-Rohner, A. S. Pulickal, C. M. Jol-van der Zijde, M. D. Snape, A. J. Pollard, Appearance of peripheral blood plasma cells and memory B cells in a primary and secondary immune response in humans. *Blood* **114**, 4998-5002 (2009).

34. S. Crotty, P. Felgner, H. Davies, J. Glidewell, L. Villarreal, R. Ahmed, Cutting edge: long-term B cell memory in humans after smallpox vaccination. *J Immunol* **171**, 4969-4973 (2003).

35. S. Hapfelmeier, M. A. Lawson, E. Slack, J. K. Kirundi, M. Stoel, M. Heikenwalder, J. Cahenzli, Y. Velykoredko, M. L. Balmer, K. Endt, M. B. Geuking, R. Curtiss, 3rd, K. D. McCoy, A. J. Macpherson, Reversible microbial colonization of germ-free mice reveals the dynamics of IgA immune responses. *Science* **328**, 1705-1709 (2010).

36. K. A. Pape, J. J. Taylor, R. W. Maul, P. J. Gearhart, M. K. Jenkins, Different B cell populations mediate early and late memory during an endogenous immune response. *Science* **331**, 1203-1207 (2011).

37. F. Weisel, M. Shlomchik, Memory B Cells of Mice and Humans. *Annu Rev Immunol* **35**, 255-284 (2017).

38. M. Odendahl, H. Mei, B. F. Hoyer, A. M. Jacobi, A. Hansen, G. Muehlinghaus, C. Berek, F. Hiepe, R. Manz, A. Radbruch, T. Dorner, Generation of migratory antigen-specific plasma blasts and mobilization of resident plasma cells in a secondary immune response. *Blood* **105**, 1614-1621 (2005).

39. M. Domina, V. Lanza Cariccio, S. Benfatto, D. D'Aliberti, M. Venza, E. Borgogni, F. Castellino, C. Biondo, D. D'Andrea, L. Grassi, A. Tramontano, G. Teti, F. Felici, C. Beninati, Rapid profiling of the antigen regions recognized by serum antibodies using massively parallel sequencing of antigen-specific libraries. *PLoS One* **9**, e114159 (2014).

40. M. Shimoda, T. Nakamura, Y. Takahashi, H. Asanuma, S. Tamura, T. Kurata, T. Mizuochi, N. Azuma, C. Kanno, T. Takemori, Isotype-specific selection of high affinity memory B cells in nasal-associated lymphoid tissue. *J Exp Med* **194**, 1597-1607 (2001).

41. F. Bowe, E. C. Lavelle, E. A. McNeela, C. Hale, S. Clare, B. Arico, M. M. Giuliani, A. Rae, A. Huett, R. Rappuoli, G. Dougan, K. H. Mills, Mucosal vaccination against serogroup B meningococci: induction of bactericidal antibodies and cellular immunity following intranasal immunization with NadA of Neisseria meningitidis and mutants of Escherichia coli heat-labile enterotoxin. *Infect Immun* **72**, 4052-4060 (2004).

42. D. J. Litt, S. Savino, A. Beddek, M. Comanducci, C. Sandiford, J. Stevens, M. Levin, C. Ison, M. Pizza, R. Rappuoli, J. S. Kroll, Putative vaccine antigens from Neisseria meningitidis recognized by serum antibodies of young children convalescing after meningococcal disease. *J Infect Dis* **190**, 1488-1497 (2004).

43. R. C. Read, Neisseria meningitidis and meningococcal disease: recent discoveries and innovations. *Curr Opin Infect Dis* **32**, 601-608 (2019).

44. C. Trotter, J. Findlow, P. Balmer, A. Holland, R. Barchha, N. Hamer, N. Andrews, E. Miller, R. Borrow, Seroprevalence of bactericidal and anti-outer membrane vesicle antibodies to Neisseria meningitidis group B in England. *Clin Vaccine Immunol* **14**, 863-868 (2007).

45. J. B. Wing, L. Smart, R. Borrow, J. Findlow, H. Findlow, A. W. Heath, R. C. Read, Kinetics of immune responses to nasal challenge with meningococcal polysaccharide one year after serogroup-C glycoconjugate vaccination. *Clin Infect Dis* **52**, 1317-1323 (2011).

46. E. Malito, M. Biancucci, A. Faleri, I. Ferlenghi, M. Scarselli, G. Maruggi, P. Lo Surdo, D. Veggi, A. Liguori, L. Santini, I. Bertoldi, R. Petracca, S. Marchi, G. Romagnoli, E. Cartocci, I. Vercellino, S. Savino, G. Spraggon, N. Norais, M. Pizza, R. Rappuoli, V. Masignani, M. J. Bottomley, Structure of the meningococcal vaccine antigen NadA and epitope mapping of a bactericidal antibody. *Proc Natl Acad Sci U S A* **111**, 17128-17133 (2014).

47. M. Giuliani, E. Bartolini, B. Galli, L. Santini, P. Lo Surdo, F. Buricchi, M. Bruttini, B. Benucci, N. Pacchiani, L. Alleri, D. Donnarumma, W. Pansegrau, I. Peschiera, I. Ferlenghi, R. Cozzi, N. Norais, M. M. Giuliani, D. Maione, M. Pizza, R. Rappuoli, O. Finco, V. Masignani, Human protective response induced by meningococcus B vaccine is mediated by the synergy of multiple bactericidal epitopes. *Sci Rep* **8**, 3700 (2018).

48. E. Mitsi, A. M. Roche, J. Reine, T. Zangari, J. T. Owugha, S. H. Pennington, J. F. Gritzfeld, A. D. Wright, A. M. Collins, S. van Selm, M. I. de Jonge, S. B. Gordon, J. N. Weiser, D. M. Ferreira, Agglutination by anti-capsular polysaccharide antibody is

associated with protection against experimental human pneumococcal carriage. *Mucosal Immunol* **10**, 385-394 (2017).

49. D. Gbesemete, J. R. Laver, H. de Graaf, M. Ibrahim, A. Vaughan, S. Faust, A. Gorringe, R. C. Read, Protocol for a controlled human infection with genetically modified Neisseria lactamica expressing the meningococcal vaccine antigen NadA: a potent new technique for experimental medicine. *BMJ Open* **9**, e026544 (2019).

50. T. K. Mukhopadhyay, D. Halliwell, C. O'Dwyer, P. A. Shamlou, M. S. Levy, N. Allison, A. Gorringe, K. M. Reddin, Rapid characterization of outer-membrane proteins in Neisseria lactamica by SELDI-TOF-MS (surface-enhanced laser desorption ionization-time-of-flight MS) for use in a meningococcal vaccine. *Biotechnol Appl Biochem* **41**, 175-182 (2005).

51. A. R. Gorringe, K. M. Reddin, S. G. Funnell, L. Johansson, A. Rytkonen, A. B. Jonsson, Experimental disease models for the assessment of meningococcal vaccines. *Vaccine* **23**, 2214-2217 (2005).

52. P. Cecchini, R. Tavano, P. Polverino de Laureto, S. Franzoso, C. Mazzon, P. Montanari, E. Papini, The soluble recombinant Neisseria meningitidis adhesin NadA(Delta351-405) stimulates human monocytes by binding to extracellular Hsp90. *PLoS One* **6**, e25089 (2011).

53. A. M. Buisman, C. G. de Rond, K. Ozturk, H. I. Ten Hulscher, R. S. van Binnendijk, Long-term presence of memory B-cells specific for different vaccine components. *Vaccine* **28**, 179-186 (2009).

54. S. Crotty, T follicular helper cell differentiation, function, and roles in disease. *Immunity* **41**, 529-542 (2014).

55. O. H. Ambur, S. A. Frye, M. Nilsen, E. Hovland, T. Tonjum, Restriction and sequence alterations affect DNA uptake sequence-dependent transformation in Neisseria meningitidis. *PLoS One* **7**, e39742 (2012).

56. M. W. van Passel, A. Bart, A. C. Luyf, A. H. van Kampen, A. van der Ende, Identification of acquired DNA in Neisseria lactamica. *FEMS Microbiol Lett* **262**, 77-84 (2006).

57. J. Perez-Ortega, A. Rodriguez, E. Ribes, J. Tommassen, J. Arenas, Interstrain Cooperation in Meningococcal Biofilms: Role of Autotransporters NalP and AutA. *Front Microbiol* **8**, 434 (2017).

58. S. Budroni, E. Siena, J. C. Dunning Hotopp, K. L. Seib, D. Serruto, C. Nofroni, M. Comanducci, D. R. Riley, S. C. Daugherty, S. V. Angiuoli, A. Covacci, M. Pizza, R. Rappuoli, E. R. Moxon, H. Tettelin, D. Medini, Neisseria meningitidis is structured in clades associated with restriction modification systems that modulate homologous recombination. *Proc Natl Acad Sci U S A* **108**, 4494-4499 (2011).

59. K. D. Lunnen, J. M. Barsomian, R. R. Camp, C. O. Card, S. Z. Chen, R. Croft, M. C. Looney, M. M. Meda, L. S. Moran, D. O. Nwankwo, et al., Cloning type-II restriction and modification genes. *Gene* **74**, 25-32 (1988).

60. A. van der Ende, C. T. Hopman, S. Zaat, B. B. Essink, B. Berkhout, J. Dankert, Variable expression of class 1 outer membrane protein in Neisseria meningitidis is caused by variation in the spacing between the -10 and -35 regions of the promoter. *J Bacteriol* **177**, 2475-2480 (1995).

61. H. S. Koo, H. M. Wu, D. M. Crothers, DNA bending at adenine . thymine tracts. *Nature* **320**, 501-506 (1986).

62. R. R. Plaskon, R. M. Wartell, Sequence distributions associated with DNA curvature are found upstream of strong E. coli promoters. *Nucleic Acids Res* **15**, 785-796 (1987).

63. H. Tettelin, N. J. Saunders, J. Heidelberg, A. C. Jeffries, K. E. Nelson, J. A. Eisen, K. A. Ketchum, D. W. Hood, J. F. Peden, R. J. Dodson, W. C. Nelson, M. L. Gwinn, R. DeBoy, J. D. Peterson, E. K. Hickey, D. H. Haft, S. L. Salzberg, O. White, R. D. Fleischmann, B. A. Dougherty, T. Mason, A. Ciecko, D. S. Parksey, E. Blair, H. Cittone, E. B. Clark, M. D. Cotton, T. R. Utterback, H. Khouri, H. Qin, J. Vamathevan, J. Gill, V. Scarlato, V. Masignani, M. Pizza, G. Grandi, L. Sun, H. O. Smith, C. M. Fraser, E. R. Moxon, R. Rappuoli, J. C. Venter, Complete genome sequence of Neisseria meningitidis serogroup B strain MC58. *Science* **287**, 1809-1815 (2000).

64. C. Yanisch-Perron, J. Vieira, J. Messing, Improved M13 phage cloning vectors and host strains: nucleotide sequences of the M13mp18 and pUC19 vectors. *Gene* **33**, 103-119 (1985).

Acknowledgments:

We thank all of our study participants and the staff at the NIHR Clinical Research Facility at Southampton General Hospital for delivery of the clinical component of this study, notably Nursing Lead Sarah Horswill, Human Challenge Coordinator Sara Hughes and the CRF laboratory support staff. We thank Caroline Barker and the members of the Southampton Public and Patient Involvement group for their assistance in shaping the national press release that preceded our application to DEFRA. We thank Martin Cannell and Ivy Wellman from DEFRA and Richard Lockey from University of Southampton for guiding us through the Deliberate Release application process. We also thank Mariagrazia Pizza and colleagues at GSK for antibody reagents, and Chris Bayliss for kindly providing meningococcal strain N54.1.

Funding: This work was funded by the UK Medical Research Council (MR/N013204/1: 'A genetically modified nasopharyngeal commensal as a platform for bacterial therapy', and MR/N026993/1: 'Pathfinder: Experimental Human Challenge with Genetically Modified Commensals to Investigate Respiratory Tract Mucosal Immunity and Colonization') with additional funding from the MRC Confidence in Concept Award and the Wessex Institute for Vaccines and Infectious Disease. Robert Read is an NIHR Senior Investigator (NF-SI-0617-10010), Adam Dale is supported by the Wellcome Trust Research Training Fellowship (203581/Z/16/Z) and the work is supported by the National Institute for Health Research Southampton Biomedical Research Centre (IS-BRC-1215-20004).

Author contributions: J.R.L., D.G., A.P.D., M.C.M., S.N.F., A.R.G. and R.C.R. designed the study. D.G., H.D.G., S.N.F. and R.C.R. wrote the clinical protocol. J.R.L. developed the Nlac transformation technology. J.R.L., Z.C.P., G.B., K.B., D.W.C., A.K.P. and H.E.H. performed the pre-clinical laboratory experiments. J.R.L., C.N.W. and E.F.R. manufactured the challenge

inocula. D.G., J.R.L., C.N.W., E.F.R., M.M.I. and A.R.H conducted or supported the clinical study. H.E.H., L.A., M.A., J.M.G., J.R.L and A.R.G. performed serological analyses and analysed the serological data. A.P.D., E.F.R., A.R.H. and J.R.L. performed cellular experiments and analysed the cellular data. J.R.L, A.P.D., A.R.H., D.G. and R.C.R. wrote the paper.

Competing interests: J.R.L. and R.C.R. declare competing interests in the form of being 'Inventors' on University of Southampton Patent: WO2017103593A1. All other authors declare no competing interests.

Figure 1.

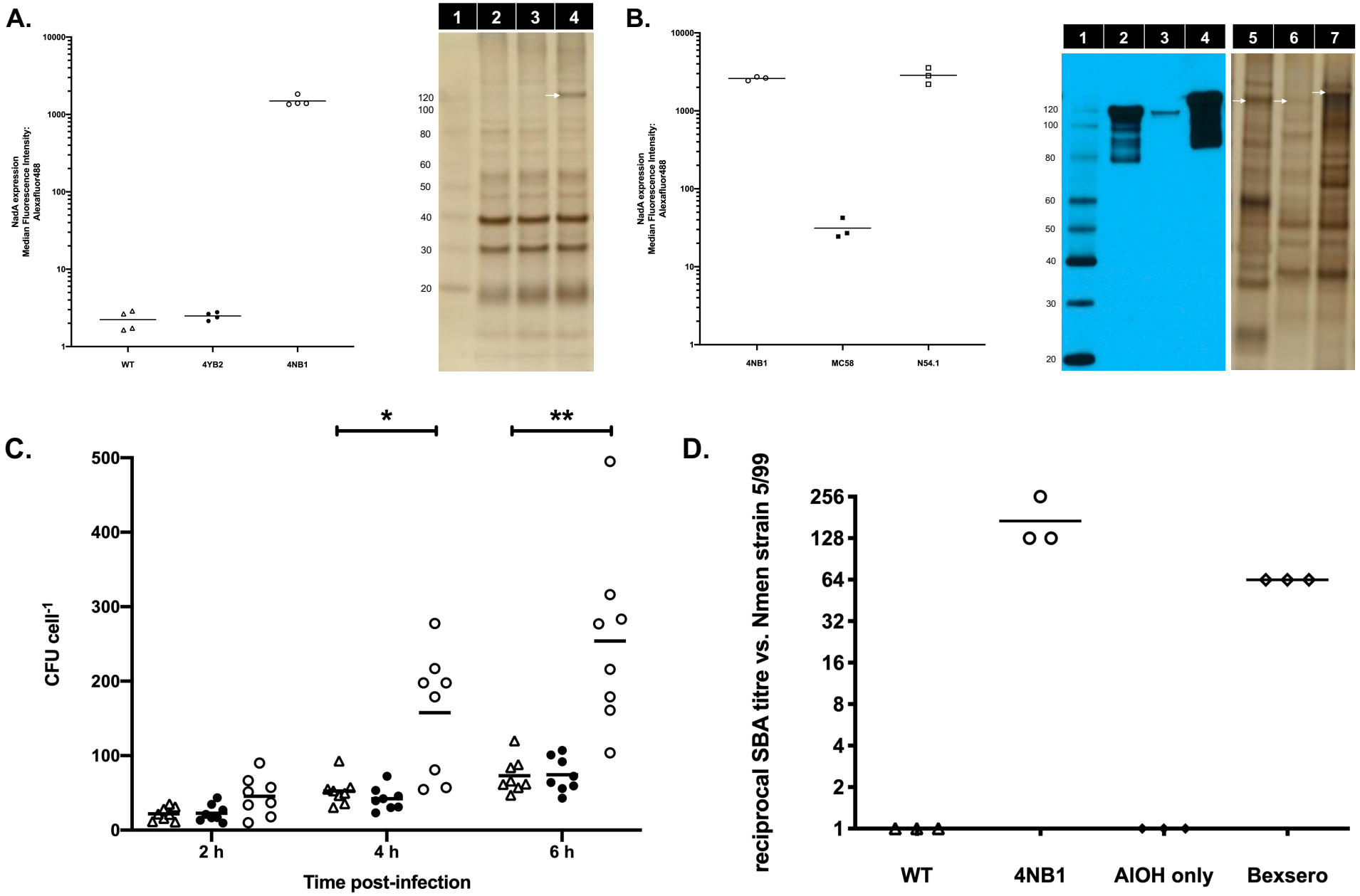
A.
NadA expression
Median Fluorescence Intensity:
Alexafluor488
10000
1000
100
10
1
WT
4YB2
4NB1
1 2 3 4
120
100
80
60
50
40
30
20
B.
NadA expression
Median Fluorescence Intensity:
Alexafluor488
10000
1000
100
10
1
4NB1
MC58
N54.1
1 2 3 4 5 6 7
120
100
80
60
50
40
30
20
C.
*
**
CFU cell-1
500
400
300
200
100
0
2 h
4 h
6 h
Time post-infection
D.
reciprocal SBA titre vs. Nmen strain 5/99
256
128
64
32
16
8
4
2
1
WT
4NB1
AlOH only
Bexsero

Figure 1: *N. lactamica*-expressed NadA functions as an adhesin and is immunogenic in mice.

(**A**) (*Left)* Graph showing Median Fluorescence Intensity (MFI) of cultures of WT Nlac strain Y92-1009 (△) and the GM derivatives 4YB2 (●) and 4NB1 (○), labeled with murine anti-NadA monoclonal antibody 6e3 and goat-derived, anti-mouse IgG conjugated to Alexafluor488. Bars represent Mean ± SD, n = 4. (*Right*) Membrane preparations derived from WT Nlac strain Y92-1009 (Lane 2) and the GM derivatives 4YB2 (Lane 3) and 4NB1 (Lane 4), were separated by SDS-PAGE and visualized by silver staining (total protein = 2 μg per lane). Band representing NadA multimer is indicated with a white arrow. Molecular weight (in kDa) of protein standards (Lane 1) are shown. (**B**) (*Left*) Graph showing MFI of cultures of GM Nlac strain 4NB1 (○) and Nmen strains MC58 (■) and N54.1 (□), labeled with rabbit anti-NadA polyclonal antibody [PE-JRL-3] and goat-derived, anti-rabbit IgG conjugated to Alexafluor488. Bars represent Mean ± SD, n = 3. (*Right*) Membrane preparations derived from GM Nlac strain 4NB1 (Lanes 2 & 5) and Nmen strains MC58 (Lanes 3 & 6) and N54.1 (Lanes 4 & 7) (total protein = 5 μg per lane), were separated by SDS-PAGE and either visualized by silver staining (Lanes 5 through 7), or transferred to PVDF membrane and probed in a western blot using rabbit anti-NadA polyclonal antibody [PE-JRL-3] (Lanes 1 through 4). Bands representing NadA multimers on silver stained gel are indicated with white arrows. Molecular weight (in kDa) of protein standards (Lane 1) are shown. (**C**) Association of WT Nlac Y92-1009 (△) and the GM derivatives 4YB2 (●) and 4NB1 (○) with monolayers of HEP-2 epithelial cells over time, presented as colony forming units (CFU) per cell. Bars indicate Mean. $*p \leq 0.05$, $**p \leq 0.01$ 2-way ANOVA with Dunnett's multiple comparisons test vs. Mean of 'WT' at each time point (n = 8). (**D**) Reciprocal endpoint serum bactericidal antibody titer measured in triplicate assays of pooled mouse sera vs. the

NadA-overexpressing Nmen strain 5/99. Mice (n = 10 per group) were immunized intraperitoneally with either: (i) dOMV derived from either WT Nlac Y92-1009 (△), or the GM derivative 4NB1 (○) supplemented with aluminium hydroxide (AlOH) as adjuvant, or (ii) AlOH alone (◆). Serum NA9136, derived from whole blood extracted from a human male 28 days after vaccination with Bexsero (◊), was included as a positive control with each assay replicate. Bars represent Mean ± SD.

Figure 2.

A.

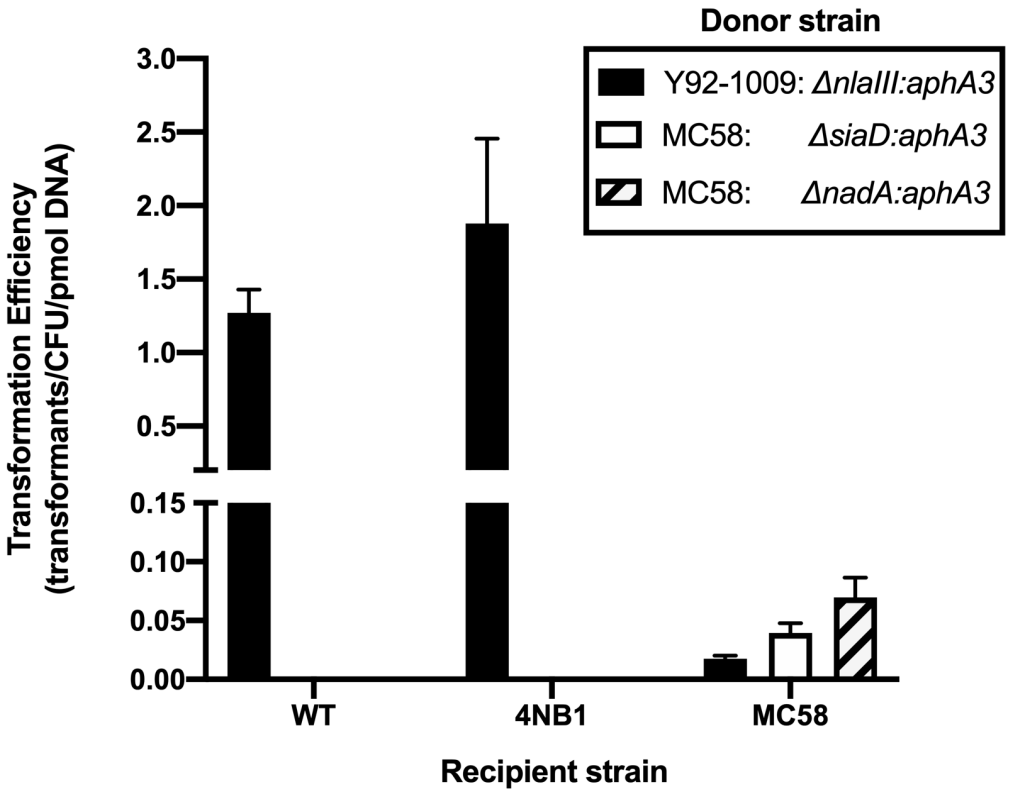

B.

Minimal Inhibitory Concentrations (mg/L)

		WT	4YB2	4NB1
ciprofloxacin	A	0.003	0.008	0.003
ceftriaxone	B	< 0.002	< 0.002	0.003

A susceptibility: ≤ 0.03 mg/L (EUCAST), ≤ 0.06 mg/L (Arreaza *et al.*)

B susceptibility: ≤ 0.125 mg/L (EUCAST), ≤ 0.25 mg/L (Arreaza *et al.*)

Figure 2.

C.

Strain	Dose	Actual CFU/dose	6 h	8 h	12 h	16 h	21 h	24 h	2 days	3 days	4 days	5 days
WT	Low	1.7×10^5	10H	10H	10H	10H	10H	10H	10H	10H	10H	10H
	High	2.5×10^7	10H	10H	10H	10H	10H	10H	10H	10H	10H	10H
4YB2	Low	1.2×10^5	10H	10H	10H	10H	10H	10H	10H	10H	10H	10H
	High	2.2×10^7	10H	10H	10H	10H	10H	10H	10H	10H	10H	10H
4NB1	Low	1.7×10^5	10H	10H	10H	10H	10H	10H	10H	10H	10H	10H
	High	2.9×10^7	2A 8H	10H	1A,R 9H	10H	10H	10H	10H	10H	10H	10H

Strain	Sex	Dose	Pre-Bleed Titre	Post-Challenge Titre
WT	Female	Low	<1:2	<1:2
	Female	High	<1:2	<1:2
	Male	Low	<1:2	<1:2
	Male	High	<1:2	1:2
4YB2	Female	Low	<1:2	<1:2
	Female	High	<1:2	<1:2
	Male	Low	<1:2	<1:2
	Male	High	<1:2	<1:2
4NB1	Female	Low	<1:2	1:4
	Female	High	<1:2	1:256
	Male	Low	-	1:2
	Male	High	<1:2	1:256

Figure 2: Genetically modified *N. lactamica* is no more likely to become transformed than its wild type parental strain, remains susceptible to clinically relevant antibiotics and is both non-pathogenic and immunogenic in a murine model of systemic infection.

(**A**) Transformation efficiency (TE) of WT Nlac Y92-1009, the NadA-expressing GM-Nlac strain 4NB1 and WT Nmen strain MC58 with 0.0001 pmol of gDNA from one of three *Neisseria* strains: (i) Nlac Y92-1009*ΔnlaIII:aphA3* (*black bars*), (ii) Nmen MC58*ΔsiaD:aphA3* (*white bars*) and (iii) Nmen MC58*ΔnadA:aphA3* (*hatched bars*). Bars represent Mean ± SD (n = 5). (**B**) MICs (mg L^{-1}) of antibiotics used clinically to treat meningococcal disease versus GM-Nlac strain 4NB1, as determined by e-test. Tests carried out according to European Committee on Antimicrobial Susceptibility Testing (EUCAST) methodology. (**C**) (*Top*) Qualitative health scores for groups of mice inoculated intraperitoneally (i/p) with 'high' and 'low' doses of one of WT Nlac Y92-1009, or the GM-Nlac strains 4YB2 and 4NB1. Bacteria were injected, along with 10 mg human holo-transferrin on Day 0. A second injection of 10 mg human holo-transferrin was made after 24 h. Mice were regularly monitored over 5 days. The number of mice assessed as exhibiting normal or 'healthy' (H) behaviour, and the number of mice exhibiting classic signs of mild discomfort such as having an 'arched' (A) or 'ruffled' (R) appearance were recorded. After the first day no mice exhibited any signs of discomfort. (*Bottom*) Reciprocal endpoint serum bactericidal antibody titers vs. Nmen strain 5/99 in sera from individual mice challenged i/p as described above.

Figure 3.

A.

	Number of challenge participants	Number of contact participants	%age Male	Age (mean)	BMI (mean)
Control	14	2	50	26.3	26.3
Intervention	12	6	58.3	32.2	27.3

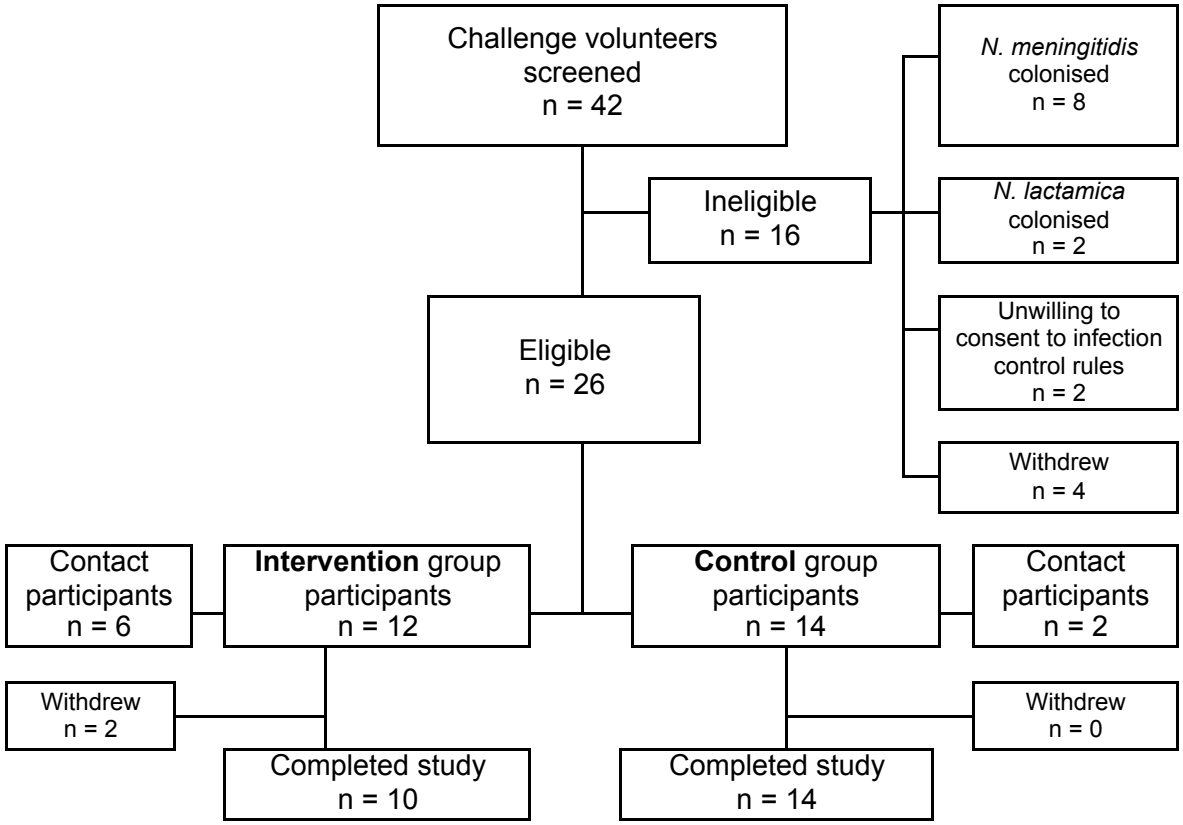

B.

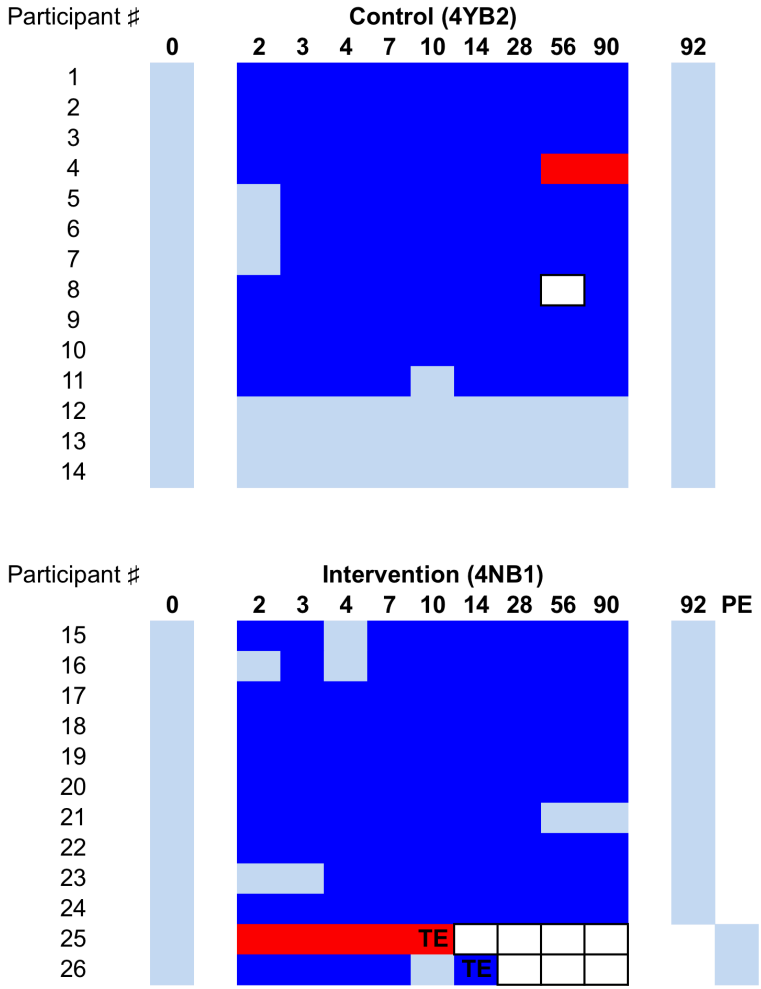

Figure 3: Controlled human infection model experiment using genetically modified *N. lactamica*.

(**A**) (*Top*) Demographic data of participants challenged with the control, WT-equivalent strain of GM-Nlac (4YB2, **Control**) or the NadA-expressing strain of GM-Nlac (4NB1, **Intervention**). The size of the inocula in each arm (Mean ± SD) was ($3.26 \pm 0.84 \times 10^5$) CFU of strain 4YB2 (**Control**) and ($3.74 \pm 1.22 \times 10^5$) CFU of strain 4NB1 (**Intervention**) ($p = 0.2595$, unpaired, two-tailed *t* test). (*Bottom*) Study flow diagram showing allocation to groups and study completion. (**B**) Pattern of *Neisseria* species carriage for all volunteers throughout the course of the study, showing **Control** and **Intervention** groups. Participant numbers are assigned arbitrarily. Days post-inoculation at time of sampling are shown in bold. Color blocks represent: nonattendance (*white, bordered*), no *Neisseria* species cultured (*light blue*), 1+ colonies of PCR-verified GM-Nlac cultured (*dark blue*), Nmen cultured in the absence of Nlac/GM-Nlac (*red*). Abbreviations: **TE** – triggered eradication following withdrawal from study, **PE** – post-eradication visit to certify clearance of GM-Nlac (= **TE** + 2 days).

Figure 4.

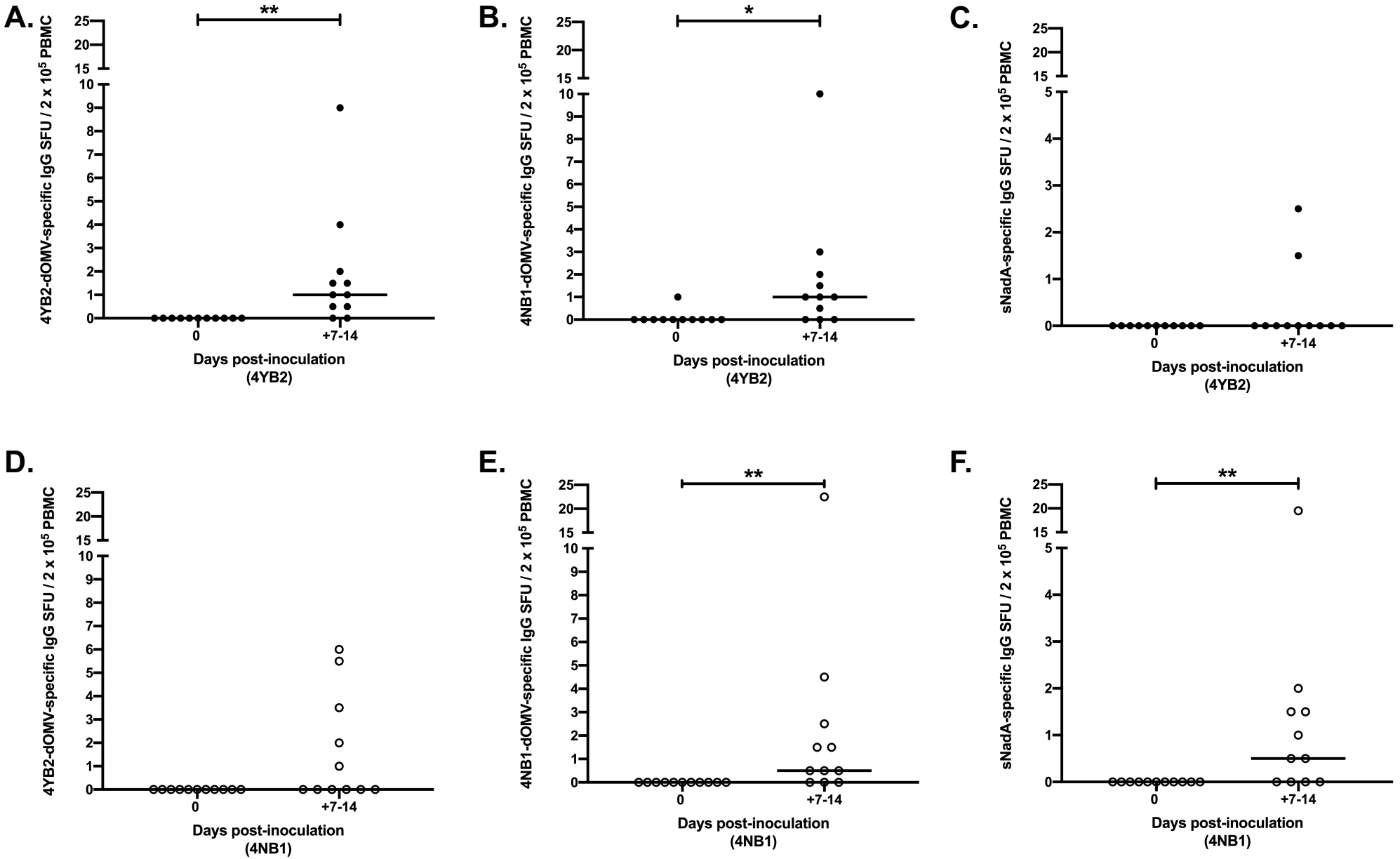
A.
B.
C.
D.
E.
F.
4YB2-dOMV-specific IgG SFU / 2 x 10^5 PBMC
4NB1-dOMV-specific IgG SFU / 2 x 10^5 PBMC
sNadA-specific IgG SFU / 2 x 10^5 PBMC
**
*
0
+7-14
Days post-inoculation
(4YB2)
(4NB1)

Figure 4.

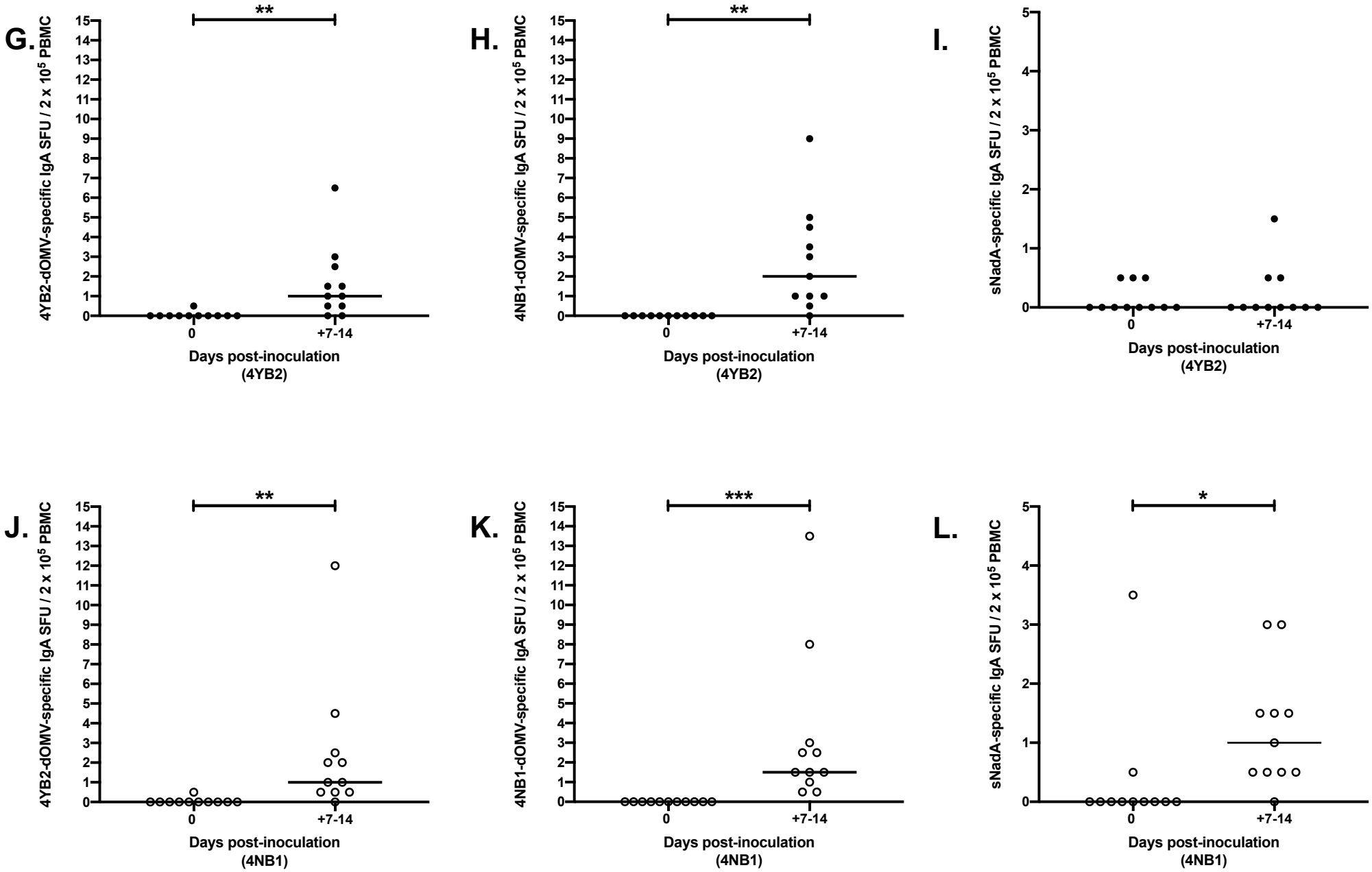
G.
H.
I.
J.
K.
L.
4YB2-dOMV-specific IgA SFU / 2 x 10^5 PBMC
4NB1-dOMV-specific IgA SFU / 2 x 10^5 PBMC
sNadA-specific IgA SFU / 2 x 10^5 PBMC
**
***
*
0
+7-14
Days post-inoculation
(4YB2)
(4NB1)

Figure 4: Colonization with NadA-expressing genetically modified *N. lactamica* results in the circulation of IgG-secreting plasma cells and IgA-secreting plasma cells specific for NadA.

PBMC isolated from whole blood at baseline and on Days 7 & 14 post-challenge with either control, WT-equivalent GM-Nlac (4YB2, ●) or NadA-expressing GM-Nlac (4NB1, ○) were assessed by ELISpot for the presence of antibody secreting cells specific for: 4YB2-dOMV (**A, D, G** and **J**), 4NB1-dOMV (**B**, **E, H** and **K**) or sNadA (**C**, **F, I** and **L**). Either IgG-secreting plasma cells (**A** through **F**) or IgA-secreting plasma cells (**G** through **L**) were visualized as spot forming units (SFU) and adjusted for non-specific SFU by deducting the appropriate average number of SFU from KLH-coated membranes. Data are presented as the number of antigen-specific IgG or IgA SFU per 2 x 10^5 PBMC. For each participant, the largest number of antigen-specific IgG or IgA SFU per 2 x 10^5 PBMC (universally measured at either Day 7 or Day 14, i.e. the 'peak') is shown (+7-14). Bars indicate Median. *$p \leq 0.05$, ** $p \leq 0.01$ Wilcoxon matched-pairs signed rank test (n = 11).

Figure 5.

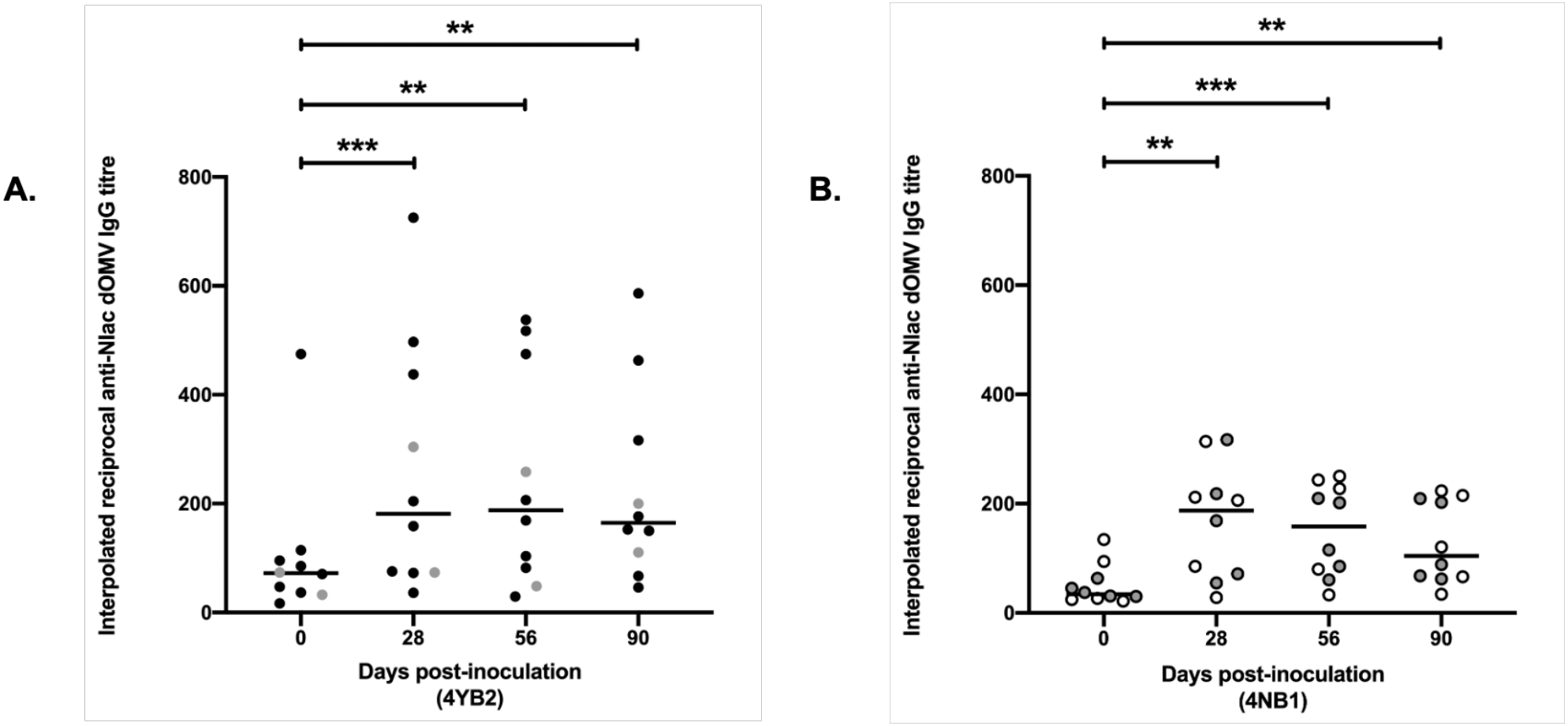
A.
**
**
***
800
600
400
200
0
Interpolated reciprocal anti-Nlac dOMV IgG titre
0
28
56
90
Days post-inoculation
(4YB2)
B.
**
***
**
800
600
400
200
0
Interpolated reciprocal anti-Nlac dOMV IgG titre
0
28
56
90
Days post-inoculation
(4NB1)

Figure 5.

C.

Participant ♯	Control (4YB2)				
	0	28	56	90	Max fold change
1	16	16	16	16	**1**
2	<2	<2	<2	<2	**1**
3	<2	<2	<2	<2	**1**
4	8	8	8	8	**1**
5	<2	<2	<2	<2	**1**
6	<2	<2	<2	<2	**1**
7	<2	<2	<2	<2	**1**
8	<2	<2	<2	<2	**1**
9	<2	<2	<2	<2	**1**
10	<2	<2	<2	<2	**1**
11	<2	<2	<2	<2	**1**

Participant ♯	Intervention (4NB1)				
	0	28	56	90	Max fold change
15	<2	8	8	8	**8**
16	<2	<2	<2	<2	**1**
17	<2	<2	4	4	**4**
18	<2	<2	<2	<2	**1**
19	<2	8	8	8	**8**
20	<2	<2	<2	<2	**1**
21	4	8	4	4	**2**
22	<2	<2	<2	<2	**1**
23	<2	4	<2	<2	**4**
24	<2	<2	<2	<2	**1**

D.

Arm	≥ 2-fold increase reciprocal endpoint anti-NadA IgG titre	< 2-fold increase reciprocal endpoint anti-NadA IgG titre
Control	0	10
Intervention	5	5

Figure 5.

E.

Participant #	Control (4YB2)			
	0	**28**	**56**	**90**
1	10.7	14.8	15.2	21.9
2	<2	<2	<2	<2
3	5.1	7.4	8.2	7.4
4	*<2*	*<2*	*<2*	*9.7*
5	<2	2.7	2.5	2.6
6	2.8	6.8	5.1	2.6
7	2.6	<2	<2	<2
8	3.5	10.6		5.8
9	<2	<2	2.5	<2
10	<2	<2	3.4	<2
11	3.7	7.3	4.7	5

Participant #	Intervention (4NB1)			
	0	**28**	**56**	**90**
15	10.1	24.2	29.2	25.9
16	<2	<2	2.9	<2
17	9.2	10.2	11.7	9.3
18	10.1	8.9	11.6	10.4
19	<2	6.5	13.8	15.6
20	<2	<2	4.7	<2
21	<2	<2	6.5	7
22	3.2	5.3	6.9	7.2
23	<2	<2	<2	<2
24	2.6	8.4	32	31.1

Figure 5: Colonization with genetically modified *N. lactamica* results in increased serological concentrations of IgG directed against *N. lactamica* surface epitopes, including NadA when present and stimulates vaccine-like serum bactericidal antibody responses versus meningococcal strain 5/99 in a subset of participants

Sera from volunteers colonized with (**A**) 4YB2 (Control, ●) or (**B**) 4NB1 (Intervention, ○) were assayed for IgG with specificity to epitopes present on WT Nlac dOMV (anti-Nlac dOMV IgG). Titers of anti-Nlac dOMV IgG in serum samples were interpolated with reference to serum NA9136. Bars denote Median. $^{**}p \leq 0.01$, $^{***}p \leq 0.001$ Friedman's 2-way Analysis of Variance by Ranks with Dunn's multiple comparisons test vs. '0' as control column. Only complete data sets at all time points were analysed (4YB2: n = 10, 4NB1: n = 10). Participants (numbered as in Figure 3B) in whose serum there was a detectable reciprocal endpoint titre of anti-sNadA IgG (i.e. ≥ 2) at one or more time points are depicted/filled in grey (**A, B, C** and **D**). (**C**) Sera were assayed for anti-sNadA IgG, using an endpoint ELISA. The reciprocal endpoint titer of each serum was considered to be the reciprocal titer of the least dilute serum sample tested that generated an $OD_{490nm} \geq 1.4$. A reciprocal endpoint titer of anti-sNadA IgG < 2 was considered to have a value of 1 for the purposes of calculating fold change, which was always in comparison to sera from Day 0. (**D**) Contingency table showing the numbers of participants from both arms of the study with either a ≥ 2-fold increase in the reciprocal endpoint anti-sNadA IgG titer, or a < 2-fold increase (i.e. no detectable change) in the reciprocal endpoint anti-sNadA IgG titer. Participants were considered to have a 2-fold increase if we measured a 2-fold increase in anti-sNadA IgG in at least one post-baseline serum sample. $p = 0.0325$, Fisher's exact test. (**E**) Sera were assayed for serum bactericidal antibody activity versus Nmen strain

5/99 using human complement. Interpolated reciprocal SBA titers, representing the dilution factor of each serum sample at which meningococcal cells were killed by 50 % as compared to controls, for each participant at each time point are shown. Participants (numbered as in Figure 3B) whose serum contained a non-protective SBA titer (i.e. < 4) at Day 0 but in whom there was a protective SBA titer (i.e. ≥ 4) at Day 90 are filed in grey. SBA titers in serum derived from participants that acquired meningococcal carriage are italicized. In concomitant assays, reference serum NA9136 was calculated to have a Mean reciprocal SBA titer of 82.09 ± 29.14 against Nmen strain 5/99 (n = 46).

Figure 6.

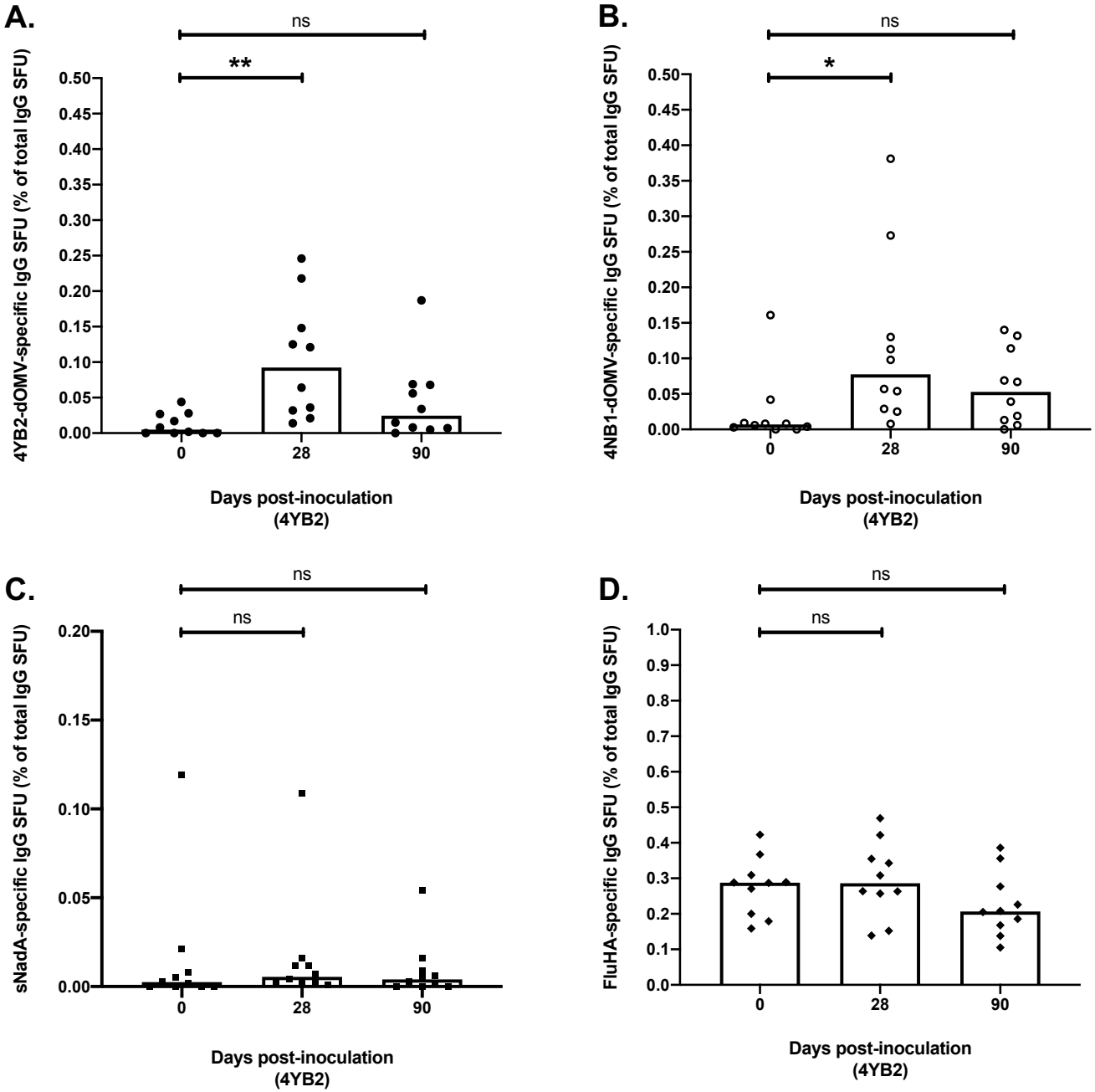
A.
ns
**
4YB2-dOMV-specific IgG SFU (% of total IgG SFU)
0.50
0.45
0.40
0.35
0.30
0.25
0.20
0.15
0.10
0.05
0.00
0
28
90
Days post-inoculation
(4YB2)
B.
ns
*
4NB1-dOMV-specific IgG SFU (% of total IgG SFU)
0.50
0.45
0.40
0.35
0.30
0.25
0.20
0.15
0.10
0.05
0.00
0
28
90
Days post-inoculation
(4YB2)
C.
ns
ns
sNadA-specific IgG SFU (% of total IgG SFU)
0.20
0.15
0.10
0.05
0.00
0
28
90
Days post-inoculation
(4YB2)
D.
ns
ns
FluHA-specific IgG SFU (% of total IgG SFU)
1.0
0.9
0.8
0.7
0.6
0.5
0.4
0.3
0.2
0.1
0.0
0
28
90
Days post-inoculation
(4YB2)

Figure 6.

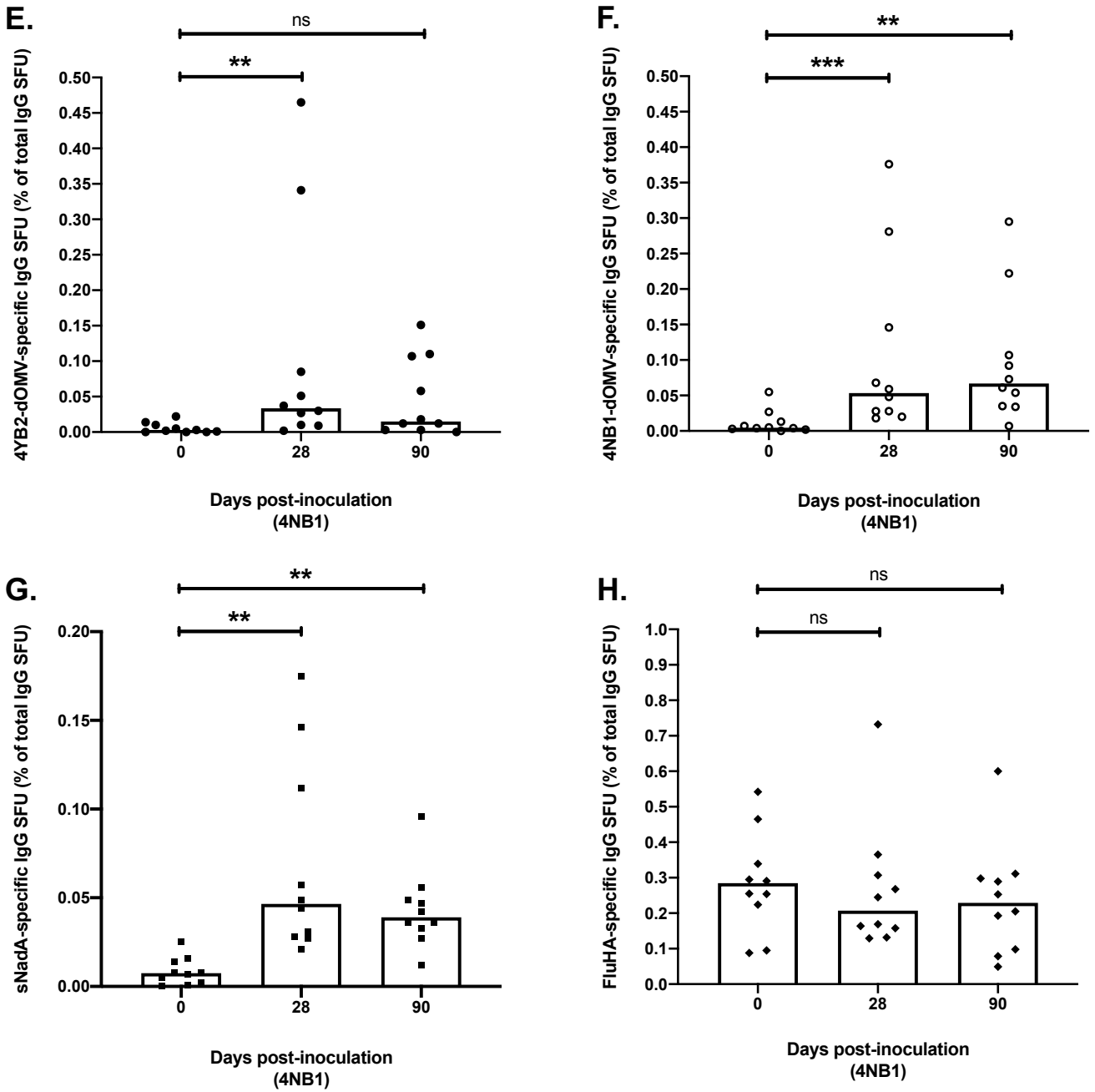
E.
ns
**
4YB2-dOMV-specific IgG SFU (% of total IgG SFU)
0.50
0.45
0.40
0.35
0.30
0.25
0.20
0.15
0.10
0.05
0.00
0
28
90
Days post-inoculation
(4NB1)
F.
**
***
4NB1-dOMV-specific IgG SFU (% of total IgG SFU)
0.50
0.45
0.40
0.35
0.30
0.25
0.20
0.15
0.10
0.05
0.00
0
28
90
Days post-inoculation
(4NB1)
G.
**
**
sNadA-specific IgG SFU (% of total IgG SFU)
0.20
0.15
0.10
0.05
0.00
0
28
90
Days post-inoculation
(4NB1)
H.
ns
ns
FluHA-specific IgG SFU (% of total IgG SFU)
1.0
0.9
0.8
0.7
0.6
0.5
0.4
0.3
0.2
0.1
0.0
0
28
90
Days post-inoculation
(4NB1)

Figure 6.

I.

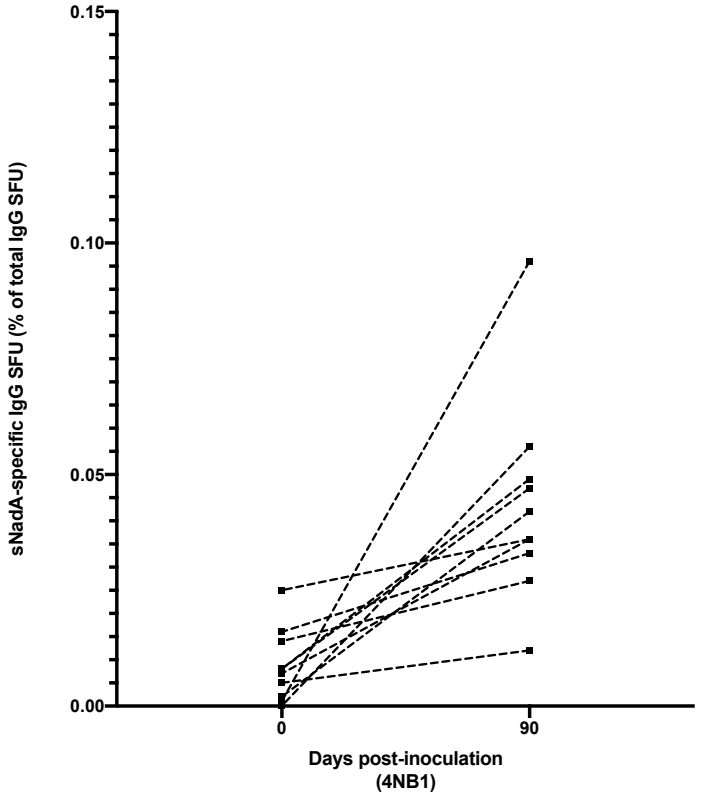
0.15
0.10
0.05
0.00
sNadA-specific IgG SFU (% of total IgG SFU)
0
90
Days post-inoculation
(4NB1)

Figure 6: Colonization with genetically modified *N. lactamica* expressing NadA results in increased numbers of circulating, NadA-specific IgG memory B cells.

PBMC isolated from whole blood at baseline and on Days 28 & 90 post-challenge with either control, WT-equivalent GM-Nlac (4YB2) or NadA-expressing GM-Nlac (4NB1) were polyclonally stimulated and assessed by ELISpot for the presence of IgG-secreting cells specific for: 4YB2-dOMV (●, **A** and **E**), 4NB1-dOMV (○, **B** and **F**), sNadA (■, **C, G** and **I**) and FluHA (control antigen) (◆, **D** and **H**). IgG-secreting cells were visualized as spot forming units (SFU) and averages were adjusted for non-specific SFU by deducting the appropriate average number of SFU from KLH-coated membranes. Antigen-specific IgG-secreting SFU are shown as a percentage of the total number of IgG-secreting SFU. Top bar of columns represents Median. ns: $p > 0.05$, *$p \leq 0.05$, **$p \leq 0.01$, ***$p \leq 0.001$, Friedman's 2-way Analysis of Variance by Ranks with Dunn's multiple comparisons test vs. '0' as control column. (**I**) Percentages of NadA-specific SFU as proportions of the total number of IgG-secreting SFU at baseline and Day 90. Points derived from the same participant are linked by dashed lines.

Supplementary Materials:

Supplementary Information

The development of *Neisseria lactamica* Transformation Technology (NTT)

1. The role of restriction endonuclease activity in transformation of Nlac

As in other *Neisseria* species, the Nlac genome contains multiple repeat elements, the most abundant of these being the Neisserial DNA Uptake Sequence (DUS) (*27*). The DUS is a non-palindromic sequence of twelve nucleotides (5' – ATGCCGTCTGAA – 3') that increases the efficiency of DNA uptake by both Nmen and *Neisseria gonorrhoeae* (*55*). The presence of this repeat element in Nlac, along with evidence of horizontal gene transfer (*56*) indicates that this commensal is genetically competent; though to date there has only been a single report of targeted mutagenesis in Nlac at a single locus (*57*), despite extensive efforts (*13*). We posited that the most significant barrier to Nlac transformation is its unique combination of restriction/modification systems, which includes two type II restriction endonucleases, NlaIII and NlaIV (*14*). These enzymes bind to and cut 4-nucleotide target sequences in DNA. The role of restriction enzymes in shaping Neisserial populations has been identified in the meningococcus, where horizontal acquisition of restriction enzymes by Nmen results in the phylogenetic clustering of isolates into distinct clades (*58*).

We investigated the restriction activity of NlaIII, creating a construct designed to introduce the *aphA3* gene, conferring kanamycin resistance, into the *nlaIII* chromosomal locus of the Nlac strain, Y92-1009. This locus was chosen because the *nlaIII* coding sequence is devoid of NlaIII sites (5'-CATG-3'). We synthesised Nlac-codon optimised versions of *aphA3* and *CLOVER*, a

derivative of the eukaryotic green fluorescent protein, placing both under transcriptional control of the promoter for the α-2,3-sialyltransferase gene (*lst*) of Nlac. 'CATG' sequences were excluded from the *aphA3* gene and the promoter sequence, whereas 2 'CATG' sites (called 'a' and 'b' with respect to their position after the *CLOVER* start codon) were deliberately introduced into the coding sequence of *CLOVER*. These genes were cloned into the *nlaIII* locus in plasmid pJL0001. Site-directed mutagenesis was then used to produce plasmids containing either one (1a and 1b) or neither (0) of the 'CATG' sites. Along with the original *CLOVER*-containing plasmid (2), these plasmids were used as templates in high-fidelity PCR, where a variety of *ΔnlaIII*::*CLOVER-aphA3* constructs, each containing a different number of 'CATG' sequences, were amplified. These were used as donor material for transformation of WT Nlac, whereby 0.5 pmol of PCR product was overlaid onto fledgling Nlac colonies and incubated at 30 ^{o}C, 5 % CO_2 overnight. Putative transformants were subsequently selected for by growth on kanamycin-containing TSA plates. Where the transformation efficiency (TE) of Nlac was below the limits of detection (i.e. zero bacterial colonies were recovered on any selective agar plates), the appropriate data points were calculated as if the transformation had derived a single transformant. Thus, the TE calculated for constructs containing at least 1 'CATG' sites are overestimates. As anticipated, the presence of one or more NlaIII restriction sites in the donor material significantly impaired the efficiency of transformation. Figure S1A shows that the transformation efficiency of WT Nlac is significantly affected by the presence of 'CATG' sequences, wherein the introduction of a single 'CATG' sequence into an otherwise CATG-free construct reduces the transformation efficiency by an average of 33 fold.

The restriction activity of many endonucleases is blocked by methylation of nucleosides in the enzyme's target nucleotide sequence, a function performed by cognate methylase enzymes (*59*). We hypothesised that a hypermethylated DNA molecule, i.e. a DNA molecule in which all the dCTP nucleotides were replaced with methylated dCTP (5-methyl-dCTP or 5mdCTP), would prove more resistant to restriction endonuclease activity than an identical, non-methylated PCR product. This would extend the intracellular life of the molecule and therefore increase the likelihood of homologous recombination. In support of this hypothesis, we showed that the *in vitro* DNA cleavage activities of NlaIII and NlaIV were inhibited by hypermethylation of the DNA substrate (Figure S1B).

Hypermethylated versions of the *ΔnlaIII*::*CLOVER-aphA3* constructs from Supplementary Figure 1A were used as donor material to transform WT Nlac. This resulted in significant increases in the frequency of Nlac transformation, with each construct now able to transform Nlac at comparable levels of efficiency (Figure S1C). Where two 'CATG' sequences are present in the transformation construct, use of hypermethylated PCR product is approximately 4000 times more efficient at transforming WT *Neisseria lactamica* than using an equivalent, non-methylated PCR product.

2. Characterization of natural competence in Nlac

Following the discovery that Nlac strain Y92-1009 can be efficiently transformed using hypermethylated PCR products, the influence of a number of factors on this process was investigated.

(A). *Transformation is Type IV pilus dependent*

Plasmid pZP0001 was designed such that the coding sequence of the Nlac *pilE* gene (NLY28420) was interrupted by an Nlac codon-optimised version of the *aadA1* (spec^R) gene. Using pZP0001 as a template, a hypermethylated PCR product of the *ΔpilE::aadA1* construct was amplified and used to transform WT Y92-1009. Putative transformants were selected for on spectinomycin-containing TSA. The presence of the *aadA1* gene in the *pilE* locus was confirmed by PCR, generating strain *ΔpilE*. Pili are noticeably absent from electron photomicrographs of mutant strain *ΔpilE*, as compared to the WT strain, an example of which is shown in Figure S2A.

To assess whether transformation of Nlac is pilus dependent, a new construct was designed in which the *nlaIII* coding sequence is disrupted by the *aphA3* (kan^R) gene. This construct was maintained in *E. coli* DH5α as pJL0005. Using pJL0005 as a template, a hypermethylated PCR product of the *ΔnlaIII::aphA3* construct was amplified and 0.5 pmol of hypermethylated DNA was used to attempt transformation of WT Nlac and the *ΔpilE* mutant derivative. Putative transformants were selected for on kanamycin-containing TSA. The number of putative transformants was considered to be equal to the number of kanamycin-resistant colonies evident after overnight growth at 37 ºC, 5 % CO_2 and adjusted for dilution factor and plating volume. The total number of bacteria present in the attempted transformation was enumerated by tenfold serial dilution of the bacterial suspension, followed by viable counting on CBA. The efficiency of Nlac transformation was normalized to the amount of DNA (pmol). Unlike the WT strain, which was readily transformed by the *ΔnlaIII::aphA3* construct, the *ΔpilE* strain was refractory to further transformation (Figure S2B). This suggests the uptake of DNA is dependent on the type IV pilus as in other species of *Neisseria*.

(B). *Transformation efficiency increases along with the length of sequence in a construct homologous to the bacterial chromosome*

The *aphA3* gene in the *ΔnlaIII::aphA3* construct is flanked on either side by DNA sequences homologous to the Nlac chromosome. These flanking regions were amplified from the *nlaIII* locus of the WT Nlac chromosome and are each 1.2 kbp in length. To investigate whether the efficiency of transformation is influenced by the length of these sequences, a number of PCR primer pairs were designed to amplify hypermethylated *ΔnlaIII::aphA3* constructs of different sizes. Due to the presence of an endogenous DUS in one of the flanking regions (the 5' flanking region, relative to the orientation of the *aphA3* gene), and the fact that DUS have been shown to influence transformation efficiency in other *Neisseria* species (*55*); those primers that would produce shorter constructs (≤ 300 bp) and therefore lack the endogenous DUS were designed to incorporate a terminal DUS.

Hypermethylated *ΔnlaIII::aphA3* constructs with different lengths of homology to the *nlaIII* locus were amplified from pJL0005. Equimolar amounts of hypermethylated DNA (0.5 pmol) were used to transform WT Nlac. Putative transformants were selected for on kanamycin-containing TSA. The number of putative transformants was considered to be equal to the number of kanamycin-resistant colonies evident after overnight growth at 37 ^{o}C, 5 % CO_2 and adjusted for dilution factor and plating volume. The total number of bacteria present in each attempted transformation was enumerated by tenfold serial dilution of the bacterial suspension, followed by viable counting on CBA. The efficiency of Nlac transformation was normalized to

the amount of DNA (pmol). As the length of DNA sequence homologous to the *nlaIII* locus increased, so did the efficiency of Nlac transformation (Figure S3A).

(C). *Transformation frequency is proportional to the concentration of transforming DNA*

Hypermethylated PCR was used to amplify the *ΔnlaIII::aphA3* construct from pJL0005, such that the regions flanking the *aphA3* gene were 600 bp in length. Different amounts of hypermethylated DNA were used to transform WT Nlac. Putative transformants were selected for on kanamycin-containing TSA. The number of putative transformants was considered to be equal to the number of kanamycin-resistant colonies evident after overnight growth at 37 ^{o}C, 5 % CO_2 and adjusted for dilution factor and plating volume. The total number of bacteria present in each transformation was enumerated by tenfold serial dilution of the bacterial suspension, followed by viable counting on CBA. WT Nlac is naturally competent, with transformants evident across the range of DNA used (5 x 10^{-6} pmol – 0.5 pmol) (Figure S3B). Although the range tested was limited by the availability of hypermethylated PCR product, the shape of the curve suggests our transformation system begins to saturate at DNA concentrations in excess of 0.5 pmol.

(D). *Transformation is more efficient in the presence of more than one DNA Uptake Sequence*

Hypermethylated PCR was used to amplify *ΔnlaIII::aphA3* constructs from pJL0005, such that the regions flanking the *aphA3* gene varied in length from 75 bp to 300 bp. Unless coded for in the PCR primers, these shorter length constructs did not contain the endogenous DUS present in the 5' flanking region of the *nlaIII* locus; but contained only the 1 DUS immediately downstream of the *aphA3* coding sequence (NB: this DUS was included as part of the original gene synthesis,

as a precautionary measure to maximize the chances of observing transformation in our initial experiments). Each construct was amplified in two forms, one of which contained a terminal DUS at the 5' end, whilst the other contained a scrambled DUS (S-DUS) in the same position (i.e. 5' – CAGTCGATATCG – 3'). Equimolar amounts of each construct (0.5 pmol) were used to transform WT Nlac. Putative transformants were selected for on kanamycin-containing TSA. The number of putative transformants was considered to be equal to the number of kanamycin-resistant colonies evident after overnight growth at 37 ºC, 5 % CO_2 and adjusted for dilution factor and plating volume. The total number of bacteria present in each transformation was enumerated by tenfold serial dilution of the bacterial suspension, followed by viable counting on CBA. The efficiency of Nlac transformation was normalized to the amount of DNA (pmol). There is a tendency towards a higher transformation efficiency when using constructs that contain more than a single DUS, although this was only significant for constructs containing flanking regions of 300 bp in length (Figure S3C).

3. Genetic modification without antibiotic resistance markers

With a view to developing strains of GM-Nlac suitable for human bacterial therapy, we sought to design a transformation system free from the use of antibiotic-resistance genes, to preclude dissemination of antimicrobial resistance. Nlac is unique among the *Neisseria* in its ability to metabolize lactose, due to its constitutive expression of β-galactosidase (β-gal), coded for by the *lacZ* gene. Colonies of β –gal-expressing bacteria appear blue on 5-bromo-4-chloro-3-indolyl-β-D-galactopyranoside (X-Gal)-containing medium, whilst bacteria that do not produce β-gal are white.

To utilise β-gal activity in a *lacZ*-driven screening system we first deleted the entire endogenous *lacZ* gene from Nlac, using the construct *ΔlacZ*:DUS. This construct was designed to effectively bring together the nucleotide sequences flanking the *lacZ* gene, excising the *lacZ* coding sequence following homologous recombination. Successful transformation with hypermethylated *ΔlacZ*:DUS was identified on X-Gal containing medium. White colonies, i.e. those lacking β-gal activity, were evident at low frequency. Removal of the *lacZ* coding sequence from the chromosome was confirmed by PCR (Figure S4A), yielding recombinant Nlac strain, Y92-1009 *ΔlacZ* (JRL0001). Although β-gal Specific Activity was ablated in this strain (Figure S4B), the growth of *ΔlacZ* (JRL0001) was not significantly impaired in rich medium (Figure S4C).

To complement the β-gal deficiency of JRL0001 and to demonstrate the feasibility of screening based on the activity of this gene product, we identified an approximately 2 kbp intergenic region in the Nlac chromosome, which we cloned into the HincII restriction site of pUC19. For ease of reference, we termed this intergenic locus *Neisseria* Heterologous Construct Insertion Site ♯1 (NHCIS1). Into NHCIS1 we cloned a copy of the *lacZ* gene, which we placed under transcriptional control of the Nlac Porin B (*porB*) gene promoter. Successful transformation of this hypermethylated construct into JRL0001 was screened for as the growth of blue colonies on X-Gal-containing medium. Chromosomal integration of the construct was confirmed by PCR of the NHCIS1 locus (Figure S4A) and the new strain was designated *ΔlacZ* NHCIS1:*lacZ* (JRL0002). β-gal Specific Activity was restored in this strain (Figure S4B). *In vitro* growth in rich medium was similar to WT (Figure S4C).

4. High level heterologous gene expression

In previous work conducted on the phase variable expression of the *porA* gene in Nmen, it was remarked upon that the sequence immediately 5' of the -35 box of the *porA* promoter bore resemblance to *upstream activator regions* (*60*). These sequences are characterized by multiple poly-'A' and/or poly-'T' nucleotide tracts, each of which causes a small bend in the DNA helix axis. When they occur in phase with the helix screw, the cumulative effect is to generate a nucleic acid with significant curvature (*61*). It has been shown that promoters with high transcription rates tend to have high curvature scores in their upstream sequences (*62*).

To investigate the role of a putative *porA* 'upstream activation sequence' (UAS) on gene expression, a series of plasmids were developed in which the Nlac *lacZ* gene was placed under the transcriptional control of the *lst* promoter and targeted to NHCIS1 (pJL0009). Other plasmids in this series were otherwise identical, but also included incrementally longer sequences derived from immediately upstream of the -35 box from the *porA* promoter in Nmen strain MC58 (pJL0010 to pJL0015). The length of the putative UAS preceding (i.e. 5' of) and abutted to the *lst* promoter ranged from 50 bp to 400 bp. These plasmids were used as templates to produce hypermethylated PCR constructs, which were each then transformed into JRL0001. Successful transformants were screened for as the growth of blue colonies on X-Gal-containing medium. Subsequent to PCR verification of the *lst*(X):*lacZ* construct into the NHCIS1 chromosomal locus (where X represents 0 to 400 bp), each strain (JRL1007 through JRL1001, respectively) was cultured to mid-log phase (OD_{600nm} = 0.3) and then used to make bacterial lysates, in which the Specific Activity of β-galactosidase was assayed (Figure S5).

These data show that the sequence immediately upstream of the RNA Polymerase binding site of the meningococcal *porA* gene acts as a UAS, with the function of enhancing gene transcription. The native *lst* promoter provides a baseline level of β-galactosidase activity when *lacZ* is expressed from this promoter at the NHCIS1 locus, but the Specific Activity of β-galactosidase is significantly increased when the upstream sequence of nucleotides is at least 150 bp long and is optimal at 200 bp. Further increases to the length of the enhancer sequence disrupt its function in the NHCIS1 context and leads to a reduced Specific Activity in these samples (i.e. at 250 and 400 bp).

5. Gene expression constructs for *N. lactamica*

Expression of heterologous genes to a high level is possible in Nlac using a chromosomally integrated gene expression cassette, amplified by high-fidelity, hypermethylated PCR from plasmids maintained in *E. coli* DH5α. The appropriate hypermethylated PCR product must be used to transform the *lacZ*-deficient mutant derivative of Nlac strain Y92-1009 (JRL0001), with screening for successful transformants to take place on medium containing X-gal. Successfully transformed bacteria will occur at low frequency and grow as blue colonies on X-gal medium, whereas non-transformed bacteria will instead grow as white colonies.

Figure S6A shows the plasmid map for pUC19NHCIS1::(X)-*lacZ* (pJL0016), a pUC19 derivative which contains sequence homologous to the Nlac Y92-1009 intergenic chromosomal locus NHCIS1, but which is bifurcated by a nucleotide sequence containing: (i) two gene expression promoters, (ii) a copy of the endogenous *lacZ* gene from Nlac strain Y92-1009 and (iii) a non-coding, 14 bp linker sequence. The (X) in the plasmid description denotes that the

plasmid itself does not code for heterologous genes, but can be adapted to express any coding sequence.

The promoters present in this construct are: (i) a synthetic hybrid of the meningococcal *porA* and *porB* promoters, wherein the homopolymeric guanosine tract that separates the -10 and -35 boxes of the WT *porA* promoter has been replaced by the equivalent, non-phase variable 17 bp sequence from the WT *porB* promoter. The hybrid promoter is placed downstream of the 200 bp *porA*-associated UAS in order to maximally enhance gene transcription (see Figure S5). (ii) a copy of the endogenous *lst* promoter from WT Nlac strain Y92-1009. The *lst* promoter drives expression of the *lacZ* gene in this construct.

The SalI and NotI restriction sites allow for directional cloning of heterologous nucleotide sequences into the plasmid, replacing both the *porA/porB* hybrid promoter and the14 bp non-coding linker sequence following a double digest. Note it is therefore important to include a suitable promoter sequence upstream of any heterologous nucleotide sequences to be cloned into this plasmid using restriction cloning.

Also note that the primers used to amplify the constructs for subsequent transformation into Nlac Y92-1009 (5PRIMEENDNHCIS1FOR and 3PRIMEENDNHCIS1REV) anneal to the termini of the NHCIS1 nucleotide sequence and do not amplify the pUC19-derived β-lactamase gene. Digestion of residual plasmid templates with restriction enzyme DpnI after amplification of hypermethylated constructs should be performed routinely after PCR, to ensure that Nlac is given no opportunity to assimilate antibiotic resistance genes.

This plasmid was used as the template DNA for hypermethylated PCR, which was subsequently transformed into JRL0001 to produce strain 4YB2.

Figure S6B shows the plasmid map for pUC19NHCIS1::*nadA-lacZ* (pJL0017), a derivative of pJL0016 into which an Nlac codon-optimised version of the *nadA* coding sequence has been cloned via Gibson Assembly (NEB). Briefly, we synthesised an Nlac codon-optimised version of *nadA* allele 1, the same as that found in WT meningococcal strain MC58, as a gBLOCK (Integrated DNA Technologies). As part of the synthesis, we placed the gene under transcriptional control of the *porA/porB* hybrid promoter, optimally enhanced with the 200 bp *porA*-associated UAS. The synthesised sequence was extended at either terminus by 30 bp, with sequence homologous to the appropriate restriction site (either SalI or NotI) plus sequences homologous to the nucleic acid sequences that flank these sites (i.e. NHCIS1 at the SalI (5') end, and the *lst* promoter at the NotI (3') end). SalI and NotI double-digested pJL0016 was supplemented with the *nadA* gBLOCK at a stoichiometric ratio of 3:1 (insert:vector) and the plasmid circularised using Gibson Assembly Master mix, according to the manufacturer's instructions. Following transformation into *E. coli* DH5α and verification of *nadA* sequence fidelity by Sanger sequencing (Source Bioscience), this plasmid was used as the template DNA for hypermethylated PCR, which was subsequently transformed into JRL0001 to produce strain 4NB1.

6. <u>Detection of anti-sNadA IgG: endpoint enzyme-linked immunosorbent assay</u>

To establish a threshold value for OD_{490nm} that constitutes a positive signal in our ELISA to detect serological anti-sNadA IgG, we obtained serum samples from the same human male both prior to and 28 days after vaccination with the Bexsero® and Menveo® anti-meningococcal disease vaccines (NA8746 and NA9136, respectively).

Figure S11A shows that vaccination with Bexsero, which contains NadA, results in a marked increase in the signal developed using our anti-sNadA IgG ELISA. Doubling dilutions of NA8746 (●) and NA9136 (○) were assayed for anti-sNadA IgG using the standard ELISA protocol (see Methods). An endpoint of $OD_{490nm} = 1.4$, representing a strong positive signal in the linear portion of the reference curve, was shown to be equivalent to an interpolated reciprocal anti-sNadA IgG titer of 17.245 in serum NA9136 (Figure S11B).

Figure S11 also shows representative examples of anti-sNadA IgG endpoint ELISA measurements in serum samples collected from the same participants over time. Serum was obtained from GM-Nlac-colonized participants at Day 00 (○), Day 28 (□), Day 56 (△) and Day 90 (●). All sera were triaged in an initial ELISA across a narrow range of concentrated dilutions (2-fold to 8-fold dilutions only) for generation of either a positive signal (i.e. $OD_{490nm} \geq 1.4$) (Figure S11C) or a negative signal (i.e. $OD_{490nm} < 1.4$) (Figure S11D). Where a positive signal was identified in one or more serum samples from a participant, the ELISA was repeated across a broader range of dilutions (2-fold to 256-fold dilutions) in order to determine a reciprocal endpoint titre (Figure S11E).

Figure S12 shows representative examples of the output from the IgG-secreting memory B cell ELISpot assay, conducted on PBMC that were isolated longitudinally from participants colonized with strain 4YB2 (Figure S12A) or 4NB1(Figure S12B), respectively.

7. Detection of anti-sNadA IgA: salivary enzyme-linked immunosorbent assay

Due to the fact that only a small volume of saliva had been collected for each participant at each time point, precluding a comprehensive analysis, we focussed on measuring antigen-specific (i.e. anti-sNadA) IgA. Our previous CHIMEs have shown that participants produce anti-Nlac IgA (*5*), but the ELISA signal in those measurements is composed from antibodies binding to multiple dOMV proteins, whereas we sought to identify only those binding to sNadA. To maximise the likelihood of generating a signal in the ELISA, saliva samples were diluted by the smallest amount possible to provide sufficient volume (i.e. x3), irregardless of total IgA content. In addition, the absence of a suitable positive control (i.e. a human saliva sample containing anti-sNadA IgA), meant it was necessary to measure salivary anti-sNadA IgA on the basis of exceeding a threshold signal intensity, which would be based on measurements taken using anti-sNadA IgA-free (i.e. negative) samples.

The first step in determining these thresholds was to determine what OD_{490nm} reading was measured in ELISA wells that had been exposed to all the components of the ELISA except for saliva itself, so as to establish a Mean and Standard Deviation (SD) of the OD_{490nm} measured in *empty*, sNadA-coated wells (= 0.04208 ± 0.008426) (n = 12). Next, a subset of saliva samples collected during a previous Nlac CHIME (n = 46) were diluted x3 in Chonblock SD/B buffer and assayed against sNadA-coated and uncoated ELISA wells. Any saliva sample that generated an

OD_{490nm} signal equal to or in excess of the appropriate Mean + 3SD (i.e. 0.068) was considered to have yielded an OD_{490nm} significantly larger than *empty* wells based on the 'empirical law', and to have an anti-sNadA IgA reciprocal titer of 3 or more (n = 1). These wells were excluded from downstream calculations. Following analysis of all remaining OD_{490nm} readings, the Mean ± SD for OD_{490nm} in the presence of human saliva was determined: sNadA-coated wells = 0.04518 ± 0.008153 (n = 45); uncoated wells = 0.04511 ± 0.007796 (n = 45).

Lab staff were blinded to the identity of saliva samples collected at either Day 00 or Day 28 as part of this study, which were organized so that saliva samples from the same participant were analyzed on the same ELISA plate. All saliva samples were diluted x3 in Chonblock SD/B buffer and assayed for anti-NadA IgA using the standard ELISA protocol (see Methods). The remainder of each diluted saliva sample was retained, further diluted and assayed for total IgA content (see Methods). Note that, in regard to the anti-sNadA IgA ELISA, where a saliva sample generated an OD_{490nm} equal to or in excess of the Mean + 3SD in uncoated wells (i.e. 0.068), it was classified as a 'false positive', insofar as the signal generated in the assay was due to either interactions with non-NadA assay components or because of non-specific interactions. The assumption was that such interactions would be common to both sNadA-coated and uncoated wells, therefore reducing confidence in the assay measurement of the sNadA-coated well. By definition therefore, only saliva samples yielding OD_{490nm} signals ≥ 0.07 in sNadA-coated wells and ≤ 0.068 in uncoated wells were considered to have an anti-sNadA IgA reciprocal titer greater than 3 and could be considered as 'anti-sNadA IgA-positive'.

Figure S13 shows the results of the two ELISAs.

Figure S1.

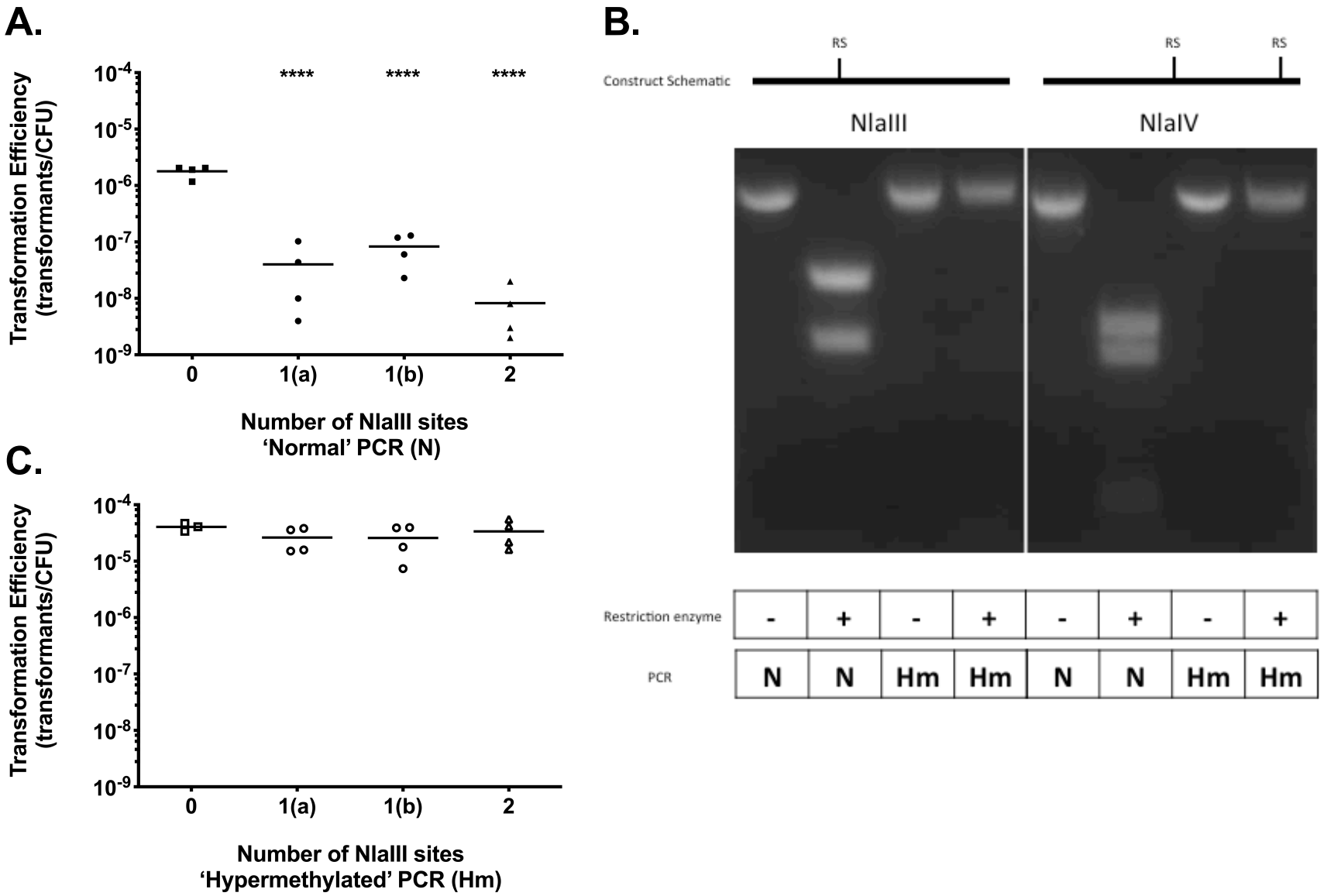
A.
Transformation Efficiency (transformants/CFU)
10-4
10-5
10-6
10-7
10-8
10-9
****
****
****
0
1(a)
1(b)
2
Number of NlaIII sites 'Normal' PCR (N)
C.
Transformation Efficiency (transformants/CFU)
10-4
10-5
10-6
10-7
10-8
10-9
0
1(a)
1(b)
2
Number of NlaIII sites 'Hypermethylated' PCR (Hm)
B.
Construct Schematic
RS
RS
RS
NlaIII
NlaIV
Restriction enzyme
- + - + - + - +
PCR
N N Hm Hm N N Hm Hm

Figure S1: The impact of endogenous restriction endonuclease activity on transformation efficiency in *N. lactamica* Y92-1009 and the use of DNA hypermethylation to abrogate its effect.

(**A**) Transformation efficiency (TE) of WT Nlac with *nlaIII*–targeted PCR constructs containing zero (■), one (●) or two (▲) NlaIII restriction sites (i.e. 5'-CATG-3'), presented as number of transformants per colony-forming unit (CFU) in the bacterial suspension. Constructs containing only 1 of the two possible restriction sites are discriminated by letter: 1(a) and 1(b). Where TE was below the limits of detection, the appropriate data points were calculated as if the transformation had derived a single transformant. ****$p \leq 0.0001$ 1-way ANOVA with Tukey's multiple comparisons test, differences from '0' shown. Bars indicate Mean (n = 4). (**B**) Two DNA amplicons, one containing a single NlaIII restriction site (RS) (see LHS) and the other containing 2 NlaIV RS (see RHS) were generated using both normal (i.e. non-hypermethylated) (N) and hypermethylated (Hm) PCR. One microgram (1 μg) of each product was digested *in vitro* overnight, using recombinant NlaIII or NlaIV as appropriate (NEB UK). Digested DNA fragments were separated by agarose gel electrophoresis. (**C**) Transformation efficiency (TE) of WT Nlac with *nlaIII*–targeted, hypermethylated PCR constructs containing zero (□), one (○) or two (△) NlaIII restriction sites (i.e. 5'-CATG-3'), identical in sequence to those in (a). TE is presented as the number of transformants per colony-forming unit (CFU) in the bacterial suspension. Constructs containing only 1 of the two possible restriction sites are discriminated by letter: 1(a) and 1(b). Bars indicate Mean ($n \geq 3$).

Figure S2.

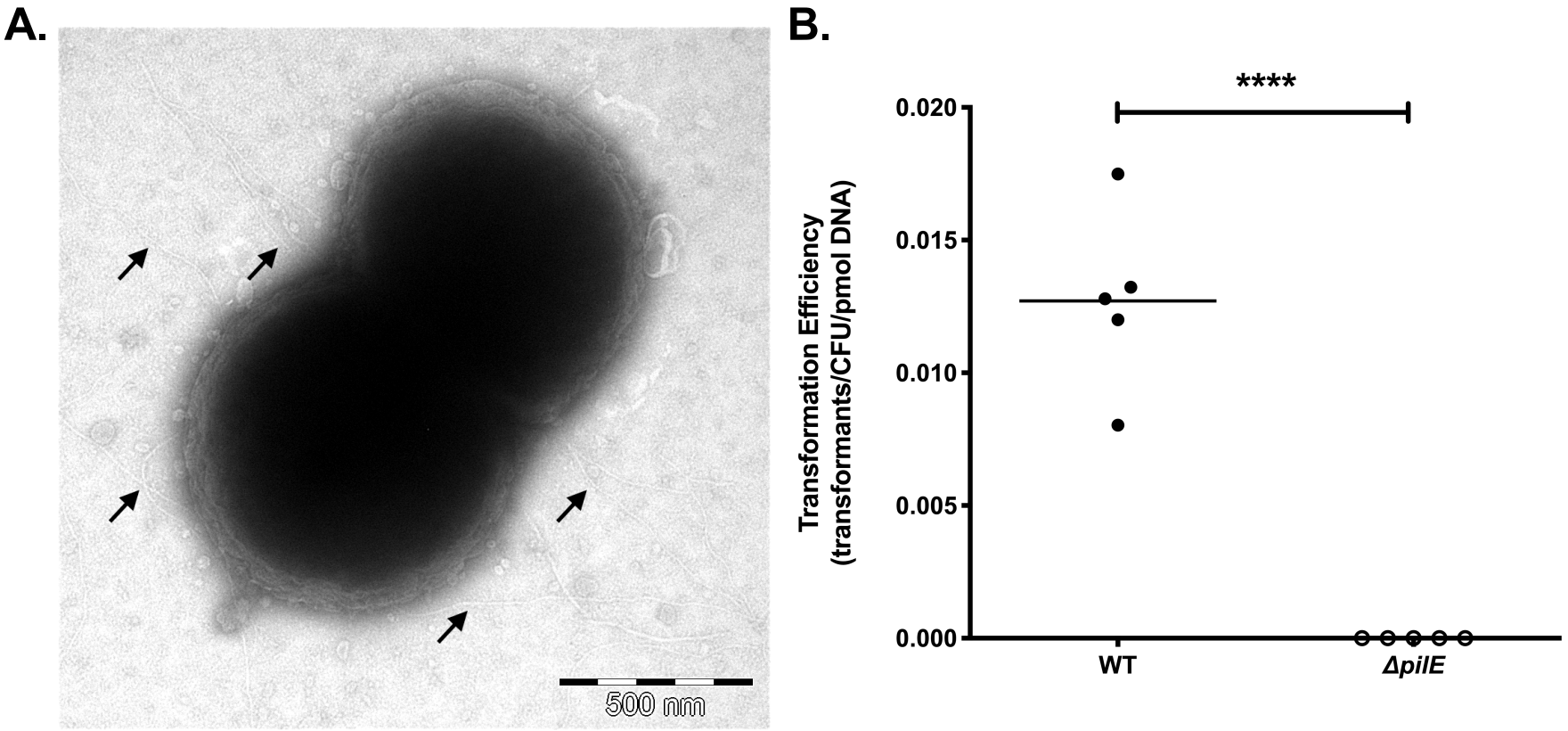
A.
500 nm
B.
****
Transformation Efficiency
(transformants/CFU/pmol DNA)
0.020
0.015
0.010
0.005
0.000
WT
ΔpilE

Figure S2: WT *N. lactamica* Y92-1009 is a piliated, naturally competent organism and requires expression of the type IV pilus for the horizontal acquisition of DNA.

(**A**) Negative-staining transmission electron microscopy of a WT *N. lactamica* diplococcus. Multiple filaments consistent with the Type IV pilus are evident (arrows). Scale bar shown.

(**B**) Transformation efficiency of WT *N. lactamica* strain Y92-1009 (●) and the non-piliated *ΔpilE* mutant derivative (○) using a hypermethylated *ΔnlaIII:aphA3* PCR product. TE is presented as the number of transformants per colony-forming unit (CFU) in the bacterial suspension, normalised to 1 pmol of the PCR product. Bar indicates Mean. ****$p \leq 0.0001$, n = 5, unpaired *t*-test.

Figure S3.

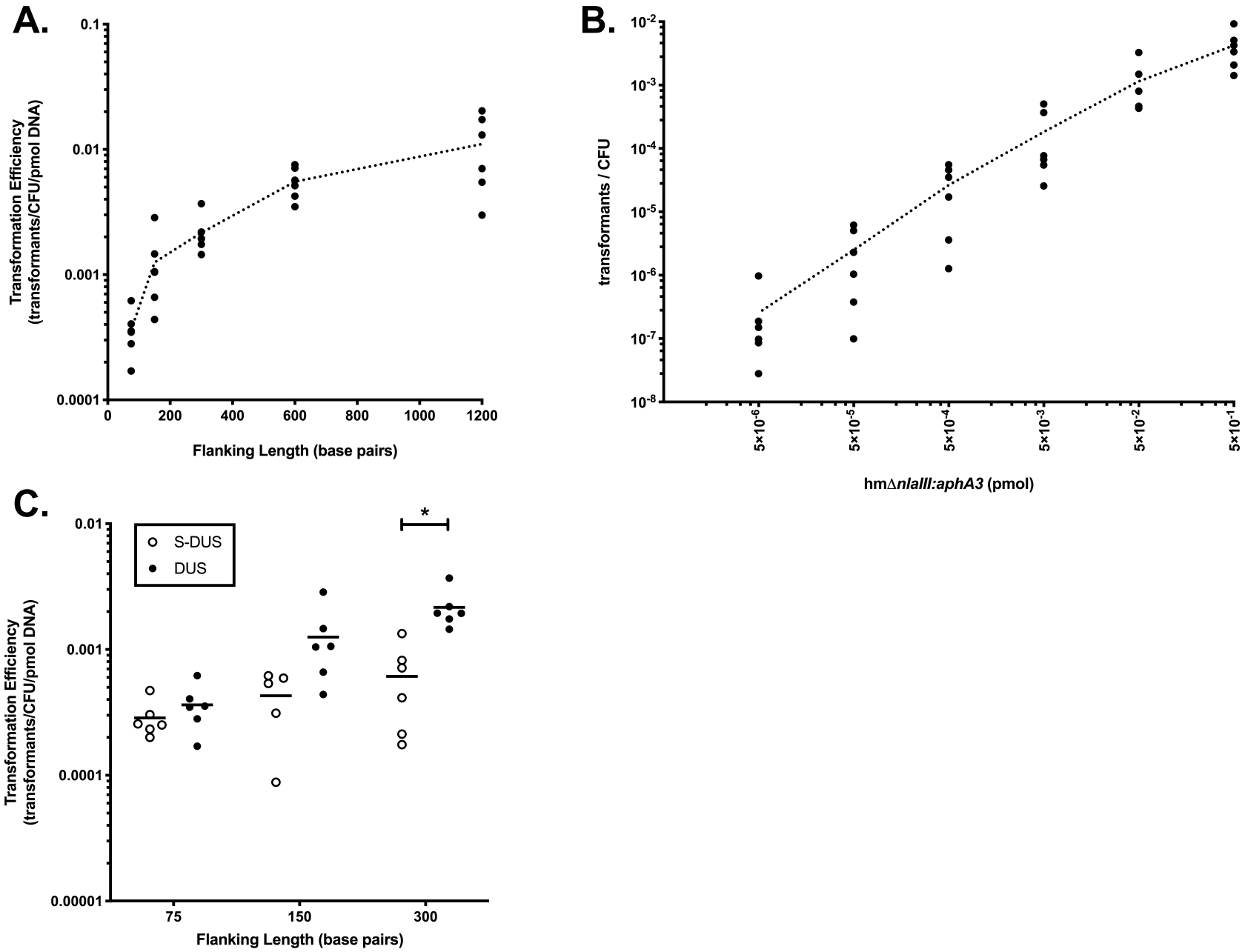
A.
Transformation Efficiency
(transformants/CFU/pmol DNA)
0.1
0.01
0.001
0.0001
0
200
400
600
800
1000
1200
Flanking Length (base pairs)
B.
transformants / CFU
10-2
10-3
10-4
10-5
10-6
10-7
10-8
5×10-6
5×10-5
5×10-4
5×10-3
5×10-2
5×10-1
hmΔnlaIII:aphA3 (pmol)
C.
Transformation Efficiency
(transformants/CFU/pmol DNA)
0.01
0.001
0.0001
0.00001
S-DUS
DUS
*
75
150
300
Flanking Length (base pairs)

Figure S3: Factors effecting transformation efficiency of *N. lactamica* Y92-1009 with hypermethylated DNA.

(**A**) Transformation efficiency increases with increased length of sequence homologous to bacterial chromosome. A panel of hypermethylated PCR constructs was amplified from pJL0005, such that the kanamycin resistance gene was flanked on either side by different lengths of sequence homologous to the *nlaIII* locus of Y92-1009 (75 base pairs (bp), 150 bp, 300 bp, 600 bp and 1200 bp). Primers that were designed to amplify constructs ≤ 300 bp incorporated a terminal DUS at the 5' end of the construct, to ensure parity with the two larger constructs, which contained an extra, endogenous DUS. Equimolar amounts (0.5 pmol) of each PCR product was used to transform WT *N. lactamica*, with transformants selected for on kanamycin-containing medium. Transformation efficiency is presented as the number of transformants per colony-forming unit (CFU) in the bacterial suspension, normalized to 1 pmol of each PCR product. Dotted line connects Mean values (n = 6). (**B**) Transformation frequency increases with the amount of DNA used for the transformation. A hypermethylated PCR construct was amplified from pJL0005, such that the kanamycin resistance gene was flanked on either side by 600 bp of sequence homologous to the *nlaIII* locus of Y92-1009. Nascent colonies of WT Y92-1009 were transformed with different amounts of PCR product and transformants were selected for on kanamycin-containing medium. Transformation frequency is presented as the number of transformants per colony-forming unit (CFU) in the bacterial suspension. Dotted line connects Mean values (n = 6). (**C**) Transformation efficiency is enhanced in the presence of multiple DNA Uptake Sequences. Pairs of constructs of different lengths were amplified from pJL0005, such that one pair contained 2 DUS per construct (DUS, hollow circles) and the other contained

one DUS and a scrambled DUS (S-DUS, filled circles). Equimolar amounts of each PCR product (0.5 pmol) were used to transform WT *N. lactamica*, with transformants selected for on kanamycin-containing medium. Transformation efficiency is presented as the number of transformants per colony-forming unit (CFU) in the bacterial suspension, normalised to 1 pmol of each PCR product. Bars represent Mean, $*p \leq 0.05$, paired samples *t* test, (n = 6).

Figure S4.

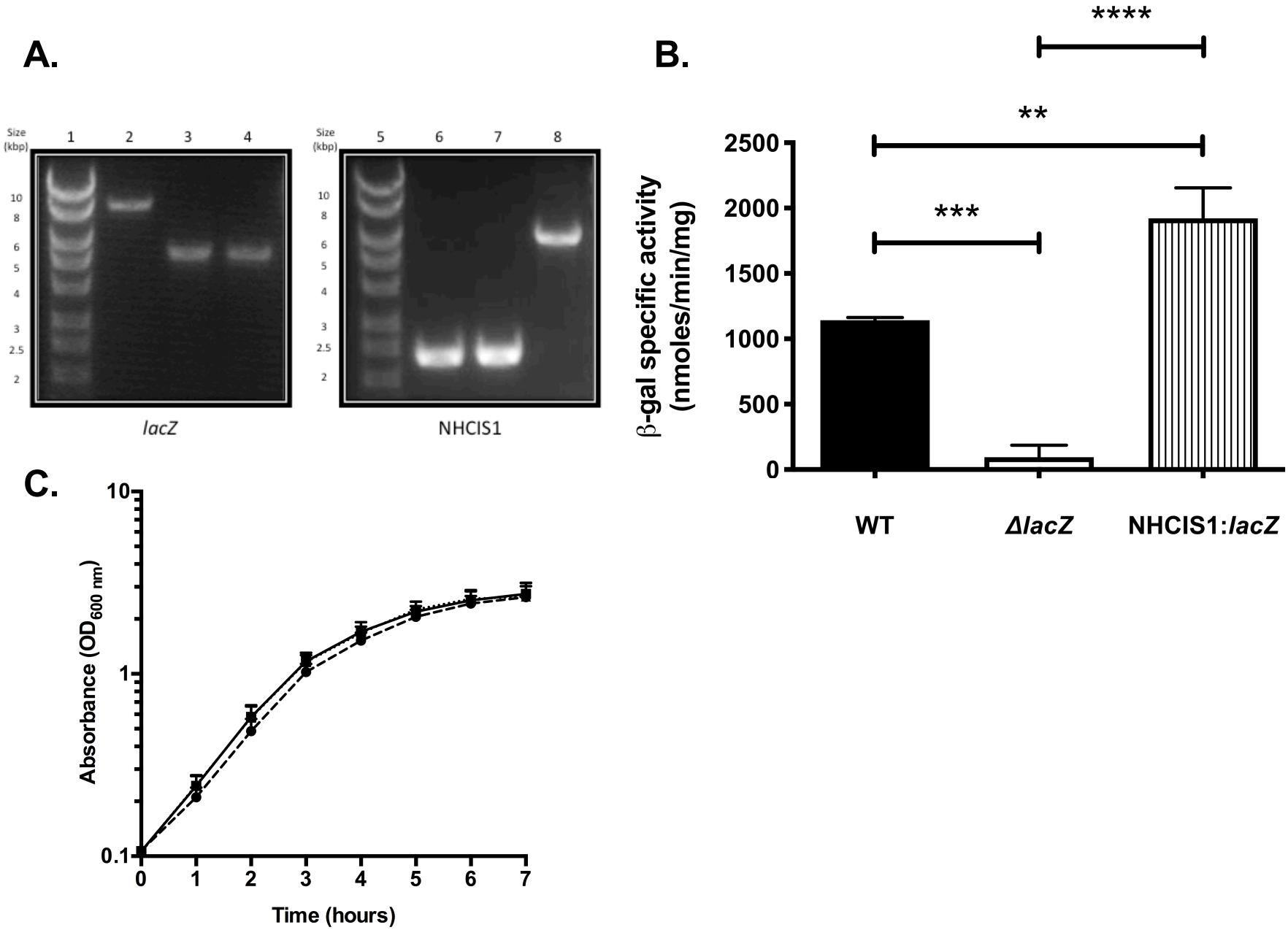
A.
Size (kbp)
1
2
3
4
10
8
6
5
4
3
2.5
2
lacZ
Size (kbp)
5
6
7
8
10
8
6
5
4
3
2.5
2
NHCIS1
B.
****
**
***
β-gal specific activity (nmoles/min/mg)
2500
2000
1500
1000
500
0
WT
ΔlacZ
NHCIS1:lacZ
C.
Absorbance (OD600 nm)
10
1
0.1
0
1
2
3
4
5
6
7
Time (hours)

Figure S4: Ablation and complementation of β-galactosidase activity through targeted mutagenesis of *N. lactamica* Y92-1009.

(**A**) PCR products obtained by amplification of the *lacZ* chromosomal locus (LHS) and an intergenic chromosomal locus designated the *Neisseria* Heterologous Construct Insertion Site number 1 (NHCIS1) (RHS) from genomic DNA purified from: WT Nlac Y92-1009 (Lanes 2 & 6), and mutant strains JRL0001 (*ΔlacZ*) (Lanes 3 & 7) and JRL0002 (*ΔlacZ* NHCIS1:*lacZ*) (Lanes 4 & 8). The expression of the *lacZ* gene in the NHCIS1:*lacZ* construct is driven by the promoter of the endogenous *porB* gene from *N. lactamica*. (**B**) β-galactosidase Specific Activity measured in lysates of log phase cultures of WT Nlac Y92-1009 and mutant strains JRL0001 (*ΔlacZ*) and JRL0002 (*ΔlacZ* NHCIS1:*lacZ*). Columns represent Mean ± SD. $^{**}p \leq 0.01$, $^{***}p \leq 0.001$, $^{****}p \leq 0.0001$, 1-way ANOVA with Tukey's Multiple Comparisons test (n = 6). (**C**) Growth curves of WT (■, solid line), JRL0001 (*ΔlacZ*) (●, dashed line) and JRL0002 (*ΔlacZ* NHCIS1:*lacZ*) (▲, dotted line) in TSB medium, shown as culture OD_{600nm} over time. Points represent the Mean ± SD (n = 6).

Figure S5.

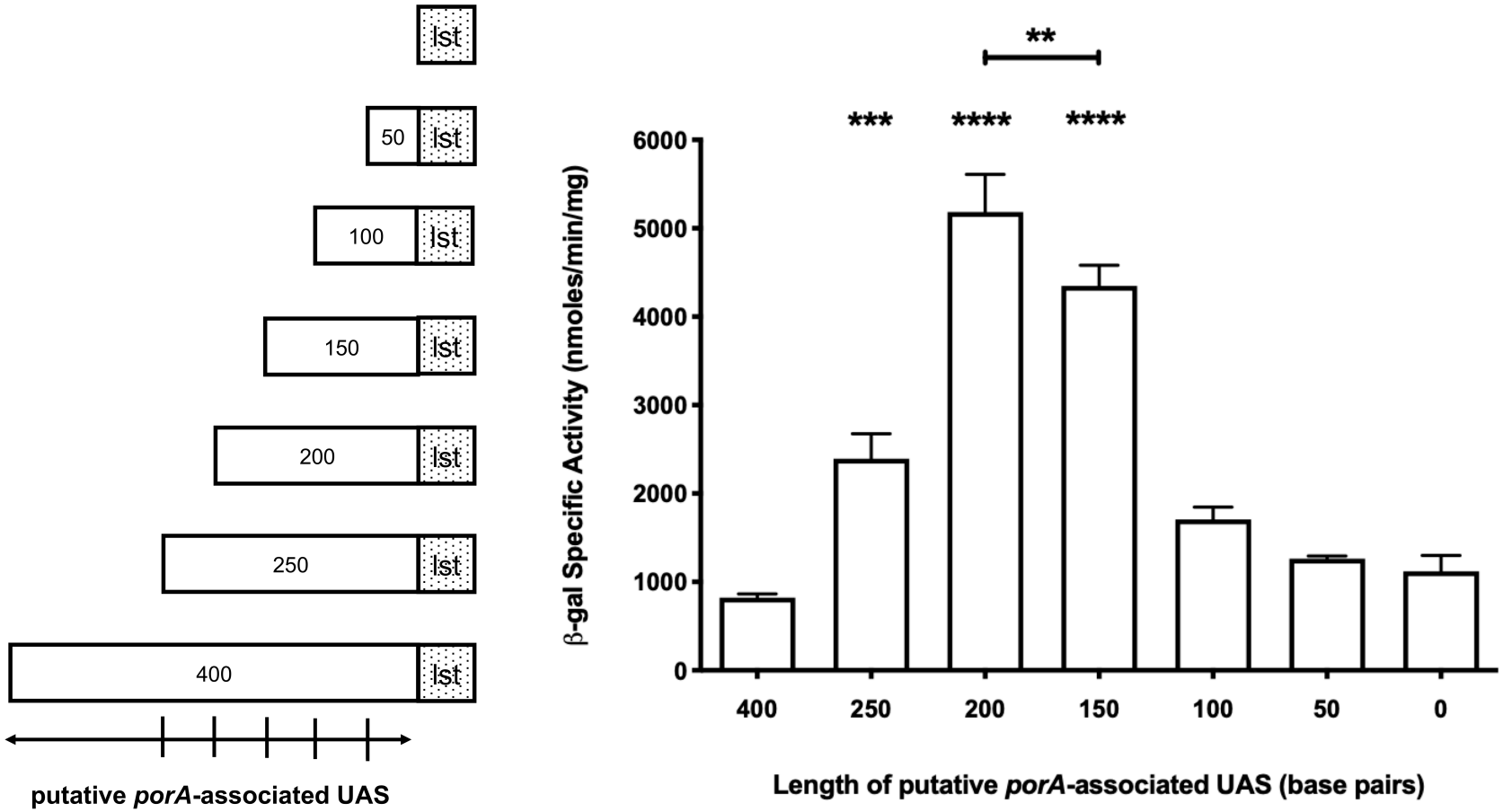
lst
50
100
150
200
250
400
putative porA-associated UAS
**
***
****
****
β-gal Specific Activity (nmoles/min/mg)
0
1000
2000
3000
4000
5000
6000
400
250
200
150
100
50
0
Length of putative porA-associated UAS (base pairs)

Figure S5: The nucleotide sequence upstream of the meningococcal *porA* gene is an upstream activation sequence (UAS) that enhances gene expression.

Specific Activity of β-galactosidase measured in lysates of recombinant Nlac strains: JRL1001 through JRL1007 (RHS). Each strain contains a chromosomally-integrated construct in the NHCIS1 locus, wherein *lacZ* expression is driven by either the endogenous *lst* gene promoter alone (0 bp, strain JRL1001), or the endogenous *lst* promoter preceded (5') by increasing lengths of the putative *porA*-associated UAS (50 bp to 400 bp, JRL1007 to JRL1002, respectively) (see schematic representations, LHS). $^{**}p \leq 0.01$, $^{***}p \leq 0.001$ $^{****}p \leq 0.0001$ 1-way ANOVA with Tukey's multiple comparisons test, differences from '0' shown, except where indicated. Bars represent Mean ± SD (n = 3).

Figure S6.

A.

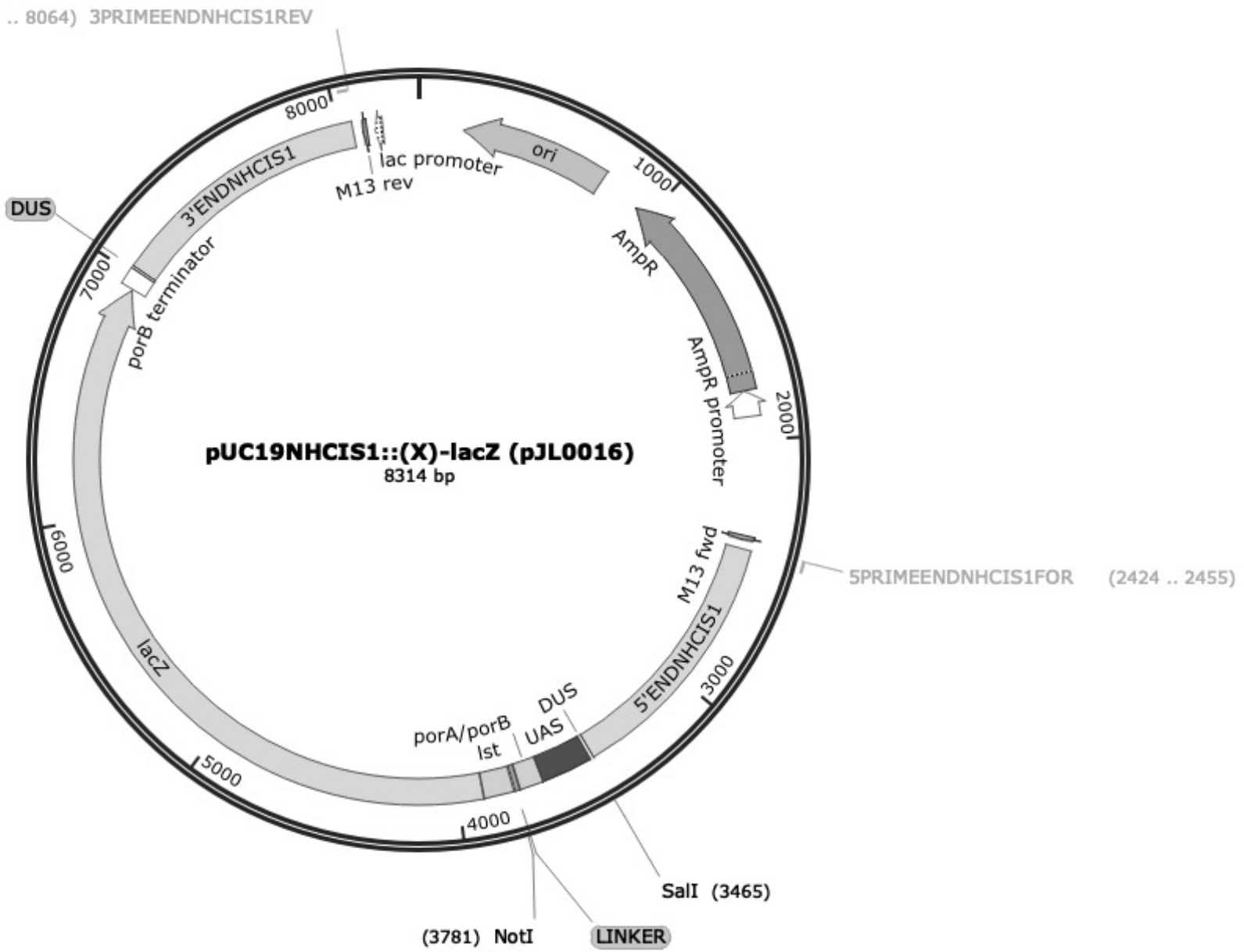
(8026 .. 8064) 3PRIMEENDNHCIS1REV
8000
3'ENDNHCIS1
lac promoter
M13 rev
ori
1000
DUS
7000
porB terminator
AmpR
AmpR promoter
2000
pUC19NHCIS1::(X)-lacZ (pJL0016)
8314 bp
6000
M13 fwd
5PRIMEENDNHCIS1FOR (2424 .. 2455)
lacZ
5'ENDNHCIS1
3000
porA/porB
lst
UAS
DUS
5000
4000
SalI (3465)
(3781) NotI
LINKER

Figure S6.

B.

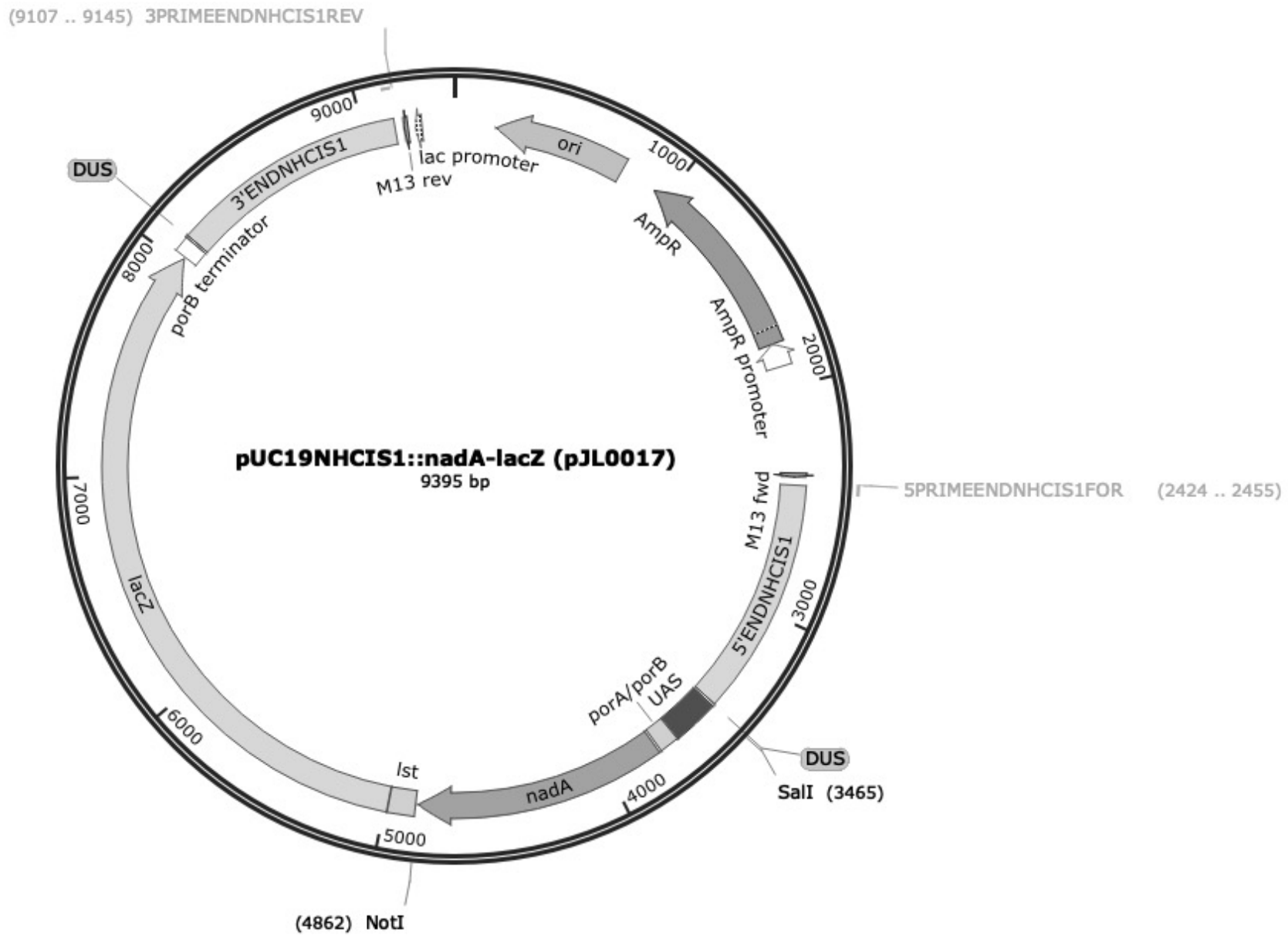
(9107 .. 9145) 3PRIMEENDNHCIS1REV
9000
3'ENDNHCIS1
lac promoter
M13 rev
ori
1000
DUS
AmpR
8000
porB terminator
AmpR promoter
2000
pUC19NHCIS1::nadA-lacZ (pJL0017)
9395 bp
7000
M13 fwd
5PRIMEENDNHCIS1FOR (2424 .. 2455)
lacZ
5'ENDNHCIS1
3000
porA/porB UAS
6000
lst
nadA
DUS
SalI (3465)
4000
5000
(4862) NotI

Figure S6: Plasmids for the chromosomal transformation of *N. lactamica* Y92-1009 with a highly active, constitutive, heterologous gene expression cassette and the endogenous β-galactosidase gene for antibiotic-free screening of successful transformants.

The size and features of each plasmid are shown. In both plasmids, the origin of replication (ori), the ampicillin resistance gene (AmpR) and its promoter (AmpR promoter), the lac promoter, and the sequences homologous to the M13 forward and reverse sequencing primers (M13 fwd/M13 rev) are derived from pUC19, allowing the plasmids to be maintained in *E. coli*. The positions of the SalI and NotI restriction sites to facilitate directional cloning are shown, as are the positions of the annealing sites of the primer pair used to amplify the construct (5PRIMEENDNHCIS1FOR and 3PRIMEENDNHCIS1REV). (**A**) pUC19NHCIS:(X)-*lacZ* was used as template DNA for hypermethylated amplification of the NHCIS:(X)-*lacZ* gene expression cassette that was used to create strain 4YB2. (**B**) pUC19NHCIS:*nadA*-*lacZ* was used as template DNA for hypermethylated amplification of the NHCIS:*nadA*-*lacZ* gene expression cassette that was used to create strain 4NB1. Plasmid maps drawn using Snapgene.

Figure S7.

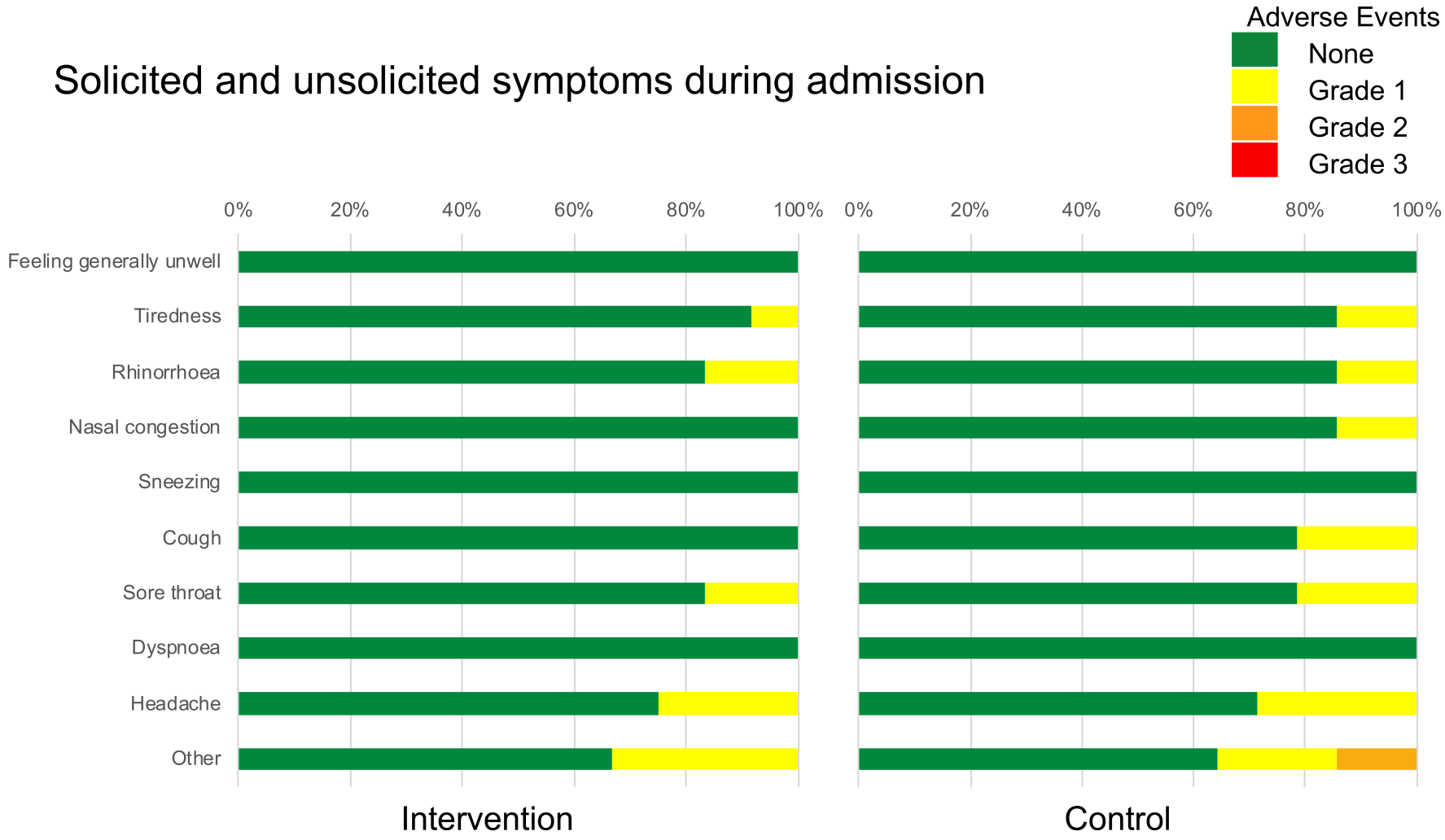
Solicited and unsolicited symptoms during admission
Adverse Events
None
Grade 1
Grade 2
Grade 3
0%
20%
40%
60%
80%
100%
Feeling generally unwell
Tiredness
Rhinorrhoea
Nasal congestion
Sneezing
Cough
Sore throat
Dyspnoea
Headache
Other
Intervention
Control

Figure S7: Adverse events reported during the admission period of the controlled human infection model experiment.

The percentage of challenge participants who reported solicited or any other symptoms during admission is shown, comparing the intervention and control groups. The indicated severity is the maximal severity of each symptom reported by individual participants at any point during the 4.5-day admission period. All symptoms self-resolved or resolved with simple analgesia.

Figure S8.

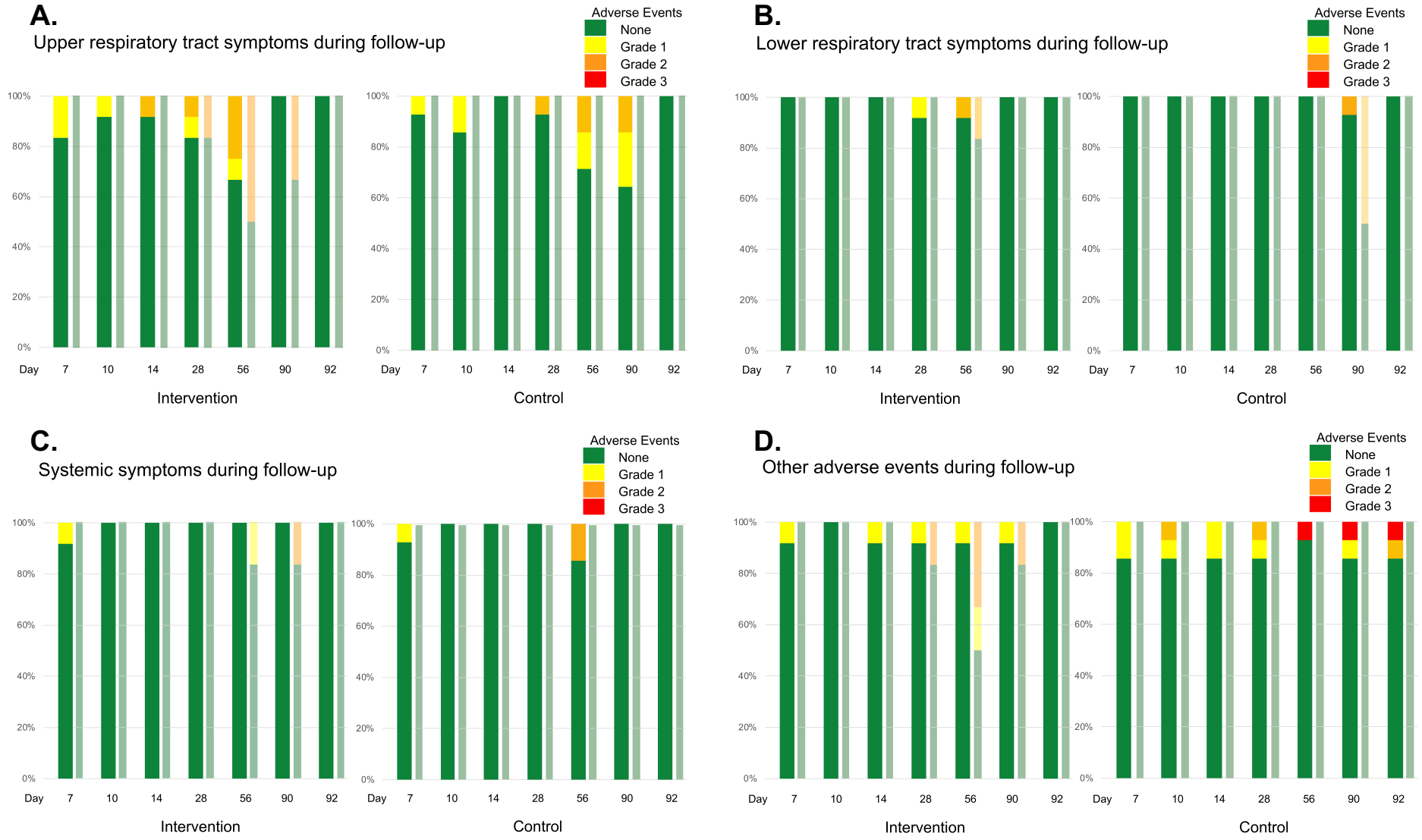
A.
Upper respiratory tract symptoms during follow-up
B.
Lower respiratory tract symptoms during follow-up
C.
Systemic symptoms during follow-up
D.
Other adverse events during follow-up
Adverse Events
None
Grade 1
Grade 2
Grade 3
100%
80%
60%
40%
20%
0%
Day 7 10 14 28 56 90 92
Intervention
Control

Figure S8: Adverse events reported during the follow-up period of the controlled human infection model experiment.

The percentage of participants in each group who, during the follow-up period of the study (post-residential to pre-clearance) reported: (**A**) upper respiratory tract symptoms (including coryza, sore throat, ear pain and epistaxis), (**B**) lower respiratory tract symptoms (including cough and exacerbation of asthma), (**C**) systemic symptoms (any of: malaise, feeling generally unwell, aching, lymphadenopathy) and/or (**D**) 'other' adverse events. The indicated severity is the maximal severity of each symptom reported by individual participants at any point during the follow-up period. Challenge volunteers are shown in the thicker columns and contact volunteers in the thinner columns for each visit day. Symptoms continuing over more than one visit are shown in both.

Figure S9.


Clinical observations
Adverse Events
None
Grade 1
Grade 2
Grade 3
0%
20%
40%
60%
80%
100%
Heart rate (high)
Systolic blood pressure (high)
Systolic blood pressure (low)
Diastolic blood pressure (high)
Diastolic blood pressure (low)
Respiratory rate (high)
Temperature (high)
Oxygen saturations (low)
Intervention
Control

Figure S9: Clinically observed adverse events during the admission and follow-up periods of the controlled human infection model experiment.

The percentage of challenge participants in each group with abnormal clinical observations during the admission period or at follow up visits, graded according to pre-determined adverse event ranges**.** The maximal severity of each observation recorded for individual participants is shown, with comparison between the intervention and control groups. Three individuals in the intervention group had Grade 2 systolic hypertension during the admission period, two of these reported significant stress unrelated to the study at that time. The participants with Grade 1 pyrexia and low saturations were all otherwise clinically well at the time, and all self-resolved.

Figure S10.

A. Laboratory results

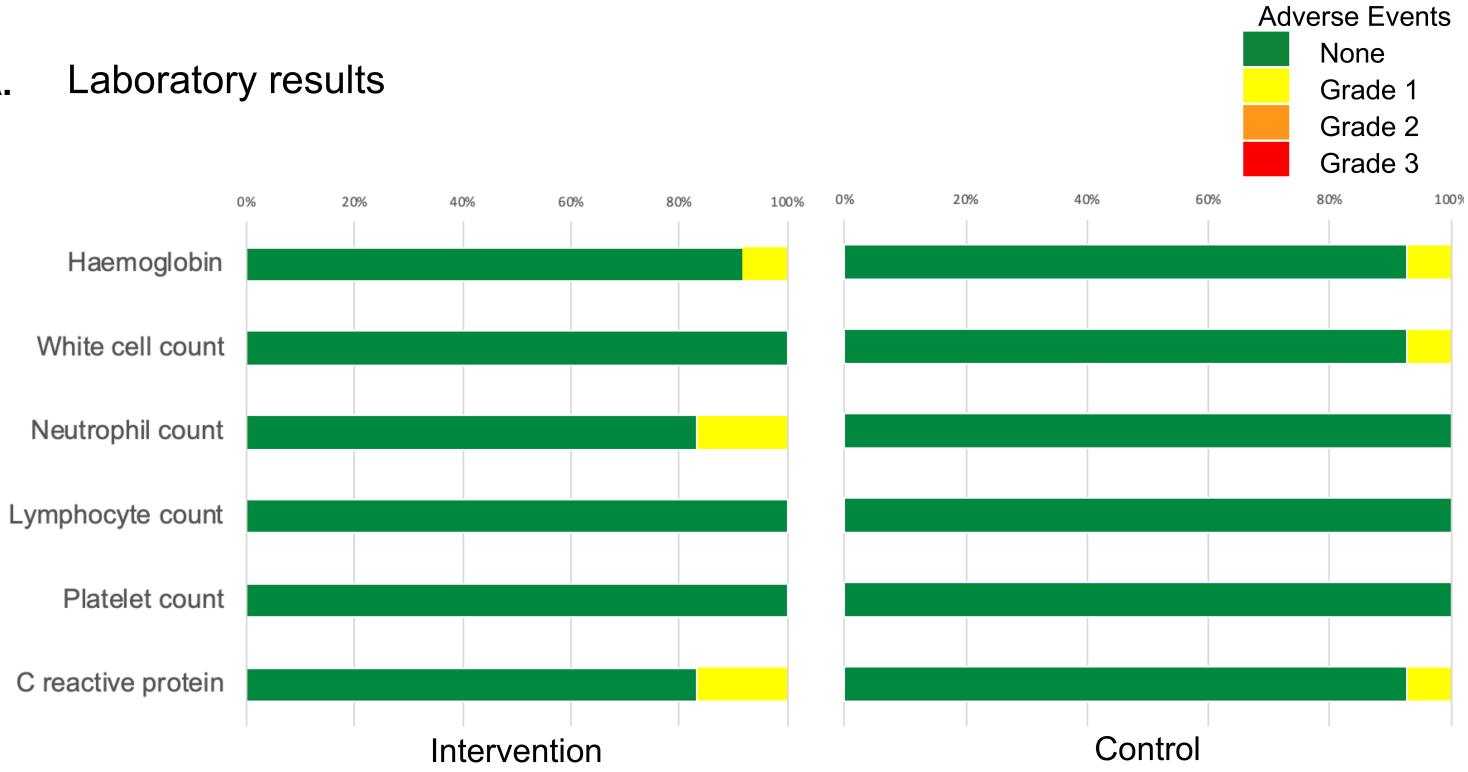

B.

Parameter	units	None	Grade 1	Grade 2	Grade 3
Haemoglobin (M)	g/dL	126 - 170	115 - 125	100 - 114	< 100
Haemoglobin (F)	g/dL	114 - 150	105 - 113	90 - 104	< 90
White cell count	x 10^9/L	3.5 - 11.5	11.6 - 15 or 2.5 - 3.49	15.1 - 20 or 1.5 - 2.49	> 20 or < 1.49
Neutrophil	x 10^9/L	1.5 - 7.5	1.0 - 1.49	0.5 - 0.99	< 0.5
Lymphocyte	x 10^9/L	1.0 - 4.0	0.75 - 0.99	0.5 - 0.74	< 0.5
Platelet	x 10^9/L	136 - 450	125 - 135	100 - 124	< 100
C-reactive protein	mg/L	1.0 - 10.0	10.1 - 20.0	20.1 - 50.0	> 50

Figure S10: Laboratory parameter adverse events during the admission and follow-up periods of the controlled human infection model experiment.

(**A**) The percentage of challenge participants in each group with abnormal laboratory results during the admission period or at follow-up visits, graded according to pre-determined adverse event ranges (**B**). The maximal severity of each laboratory parameter is shown, with comparison between the intervention and control groups. Two participants in the intervention group had a rise in CRP on Day 14. One of these participants was clinically well but had run a marathon on both Day 12 and 13. The other had concurrent upper respiratory tract symptoms with Grade 1 neutropenia, which resolved by the next follow up visit. One participant in the intervention group had a Grade 1 neutropenia on Day 7 associated with mild upper respiratory tract symptoms. All other laboratory parameter adverse events were in clinically well participants. One participant in the control group had a CRP within the Grade 1 range throughout the study including prior to inoculation. This was related to an underlying condition rather than the study. Other than CRP in this participant, all laboratory parameters spontaneously returned to the normal range.

Figure S11.

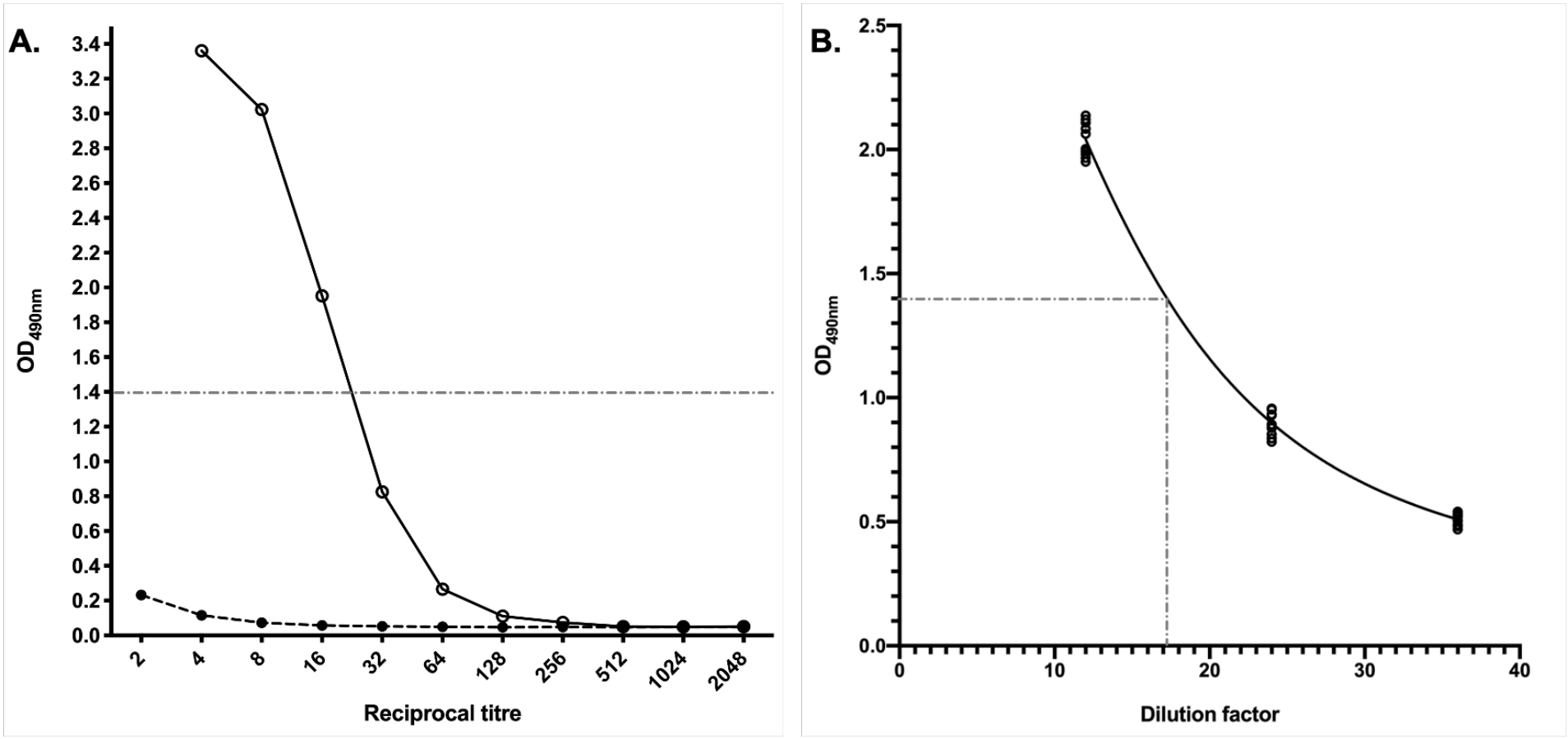
A.
OD490nm
3.4
3.2
3.0
2.8
2.6
2.4
2.2
2.0
1.8
1.6
1.4
1.2
1.0
0.8
0.6
0.4
0.2
0.0
2
4
8
16
32
64
128
256
512
1024
2048
Reciprocal titre
B.
OD490nm
2.5
2.0
1.5
1.0
0.5
0.0
0
10
20
30
40
Dilution factor

Figure S11.

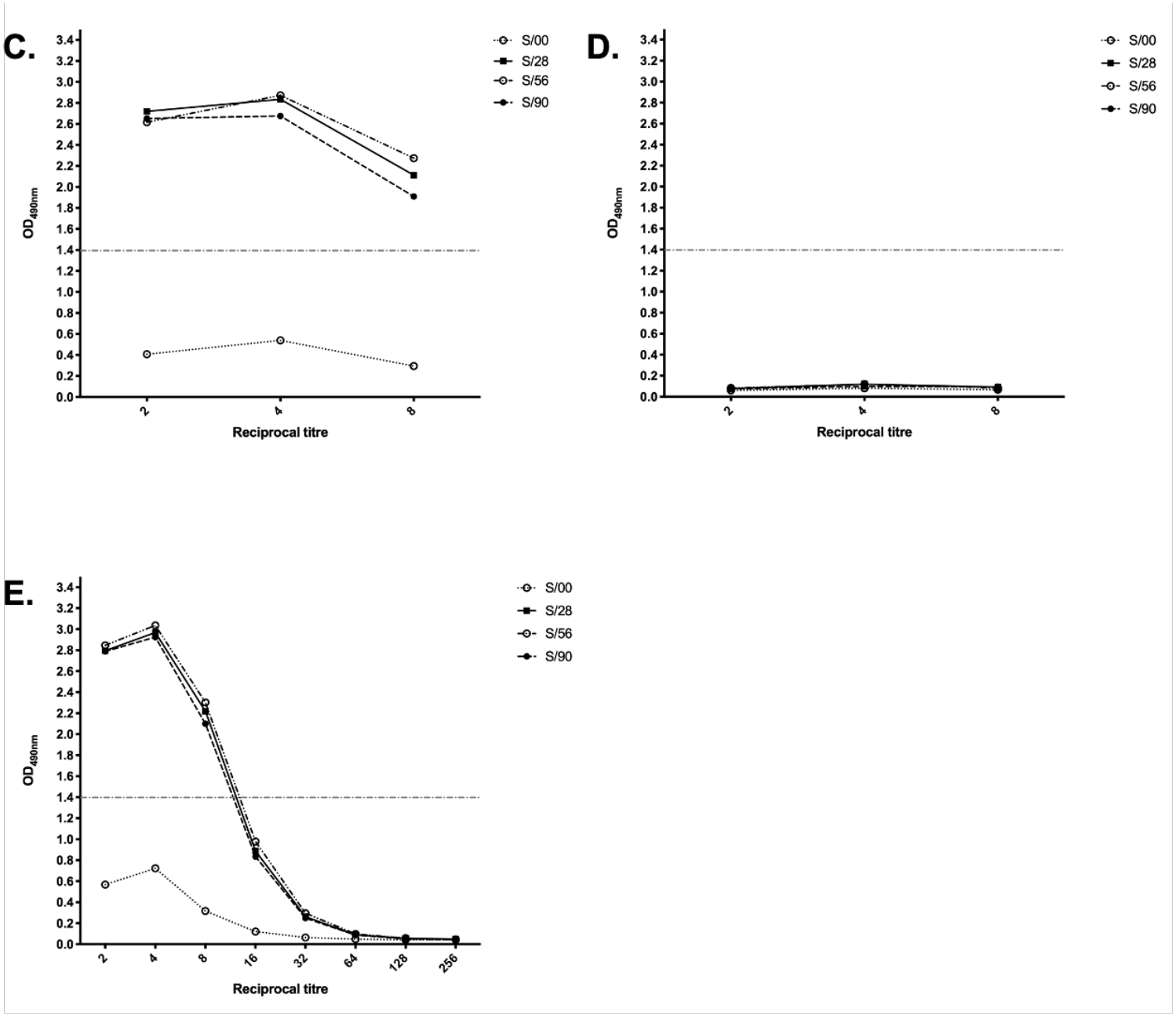
C.
D.
E.
S/00
S/28
S/56
S/90
OD490nm
Reciprocal titre
2
4
8
16
32
64
128
256

Figure S11: Determination of endpoint titre for anti-NadA IgG in human serum samples.

(**A**) Serum samples NA8746 (●) and NA9136 (○) were extracted from whole blood taken from the same human male before and 28 days after vaccination with Bexsero, respectively. Sera were serially diluted 2-fold in PBS across the range shown. Duplicate aliquots of each serum dilution were incubated in sNadA-coated wells of an ELISA plate, and captured anti-sNadA IgG was detected as an increase in OD_{490nm} using biotinylated, anti-human IgG monoclonal antibody, streptavidin-HRP and OPD substrate. Points represent Mean of duplicate measurements. An OD_{490nm} = 1.4 (indicated) represents a strong positive signal in this ELISA and sits on the linear portion of this representative reference curve. (**B**) Serum NA9136 was diluted x12, x24 and x36 (n = 10) and the anti-sNadA IgG titer of each serial dilution was measured in duplicate using the anti-sNadA ELISA. Each point represents the Mean of duplicate measurements. Data were fitted to a 4PL nonlinear regression in Graphpad Prism. The reciprocal titer of serum NA9136 corresponsing to a measurement of OD_{490nm} = 1.4 was interpolated from the reference curve (= 17.245). Serum from Participant 15 (**C**) and Participant 5 (**D**) (as numbered in Figure 3B) was extracted from whole blood taken prior to inoculation with GM-Nlac (S/00) and at 28, 56 and 90 days post-inoculation (S/28, S/56 and S/90, respectively). Sera were diluted 2-fold in PBS across the narrow range of concentrations shown. Duplicate aliquots of each serum dilution were incubated in sNadA-coated wells of an ELISA plate, and captured anti-sNadA IgG was detected as described in (**A**). Where a signal of $OD_{490nm} \geq 1.4$ was detected, all serum samples from that participant were diluted 2-fold in PBS across the broader range of dilutions shown (**E**)**.** Duplicate aliquots of each serum dilution were incubated in sNadA-coated wells of an ELISA plate, and captured anti-sNadA IgG was detected as described in (**A**). The reciprocal anti-

sNadA IgG endpoint titre of each serum sample was determined as the reciprocal of the last dilution tested that generated an $OD_{490nm} \geq 1.4$. Reciprocal anti-sNadA IgG titres of participant 15's serum samples are therefore: (i) S/00 = < 2 (i.e. undetectable), (ii) S/28 = 8, (iii) S/56 = 8 and (iv) S/90 = 8.

Figure S12.

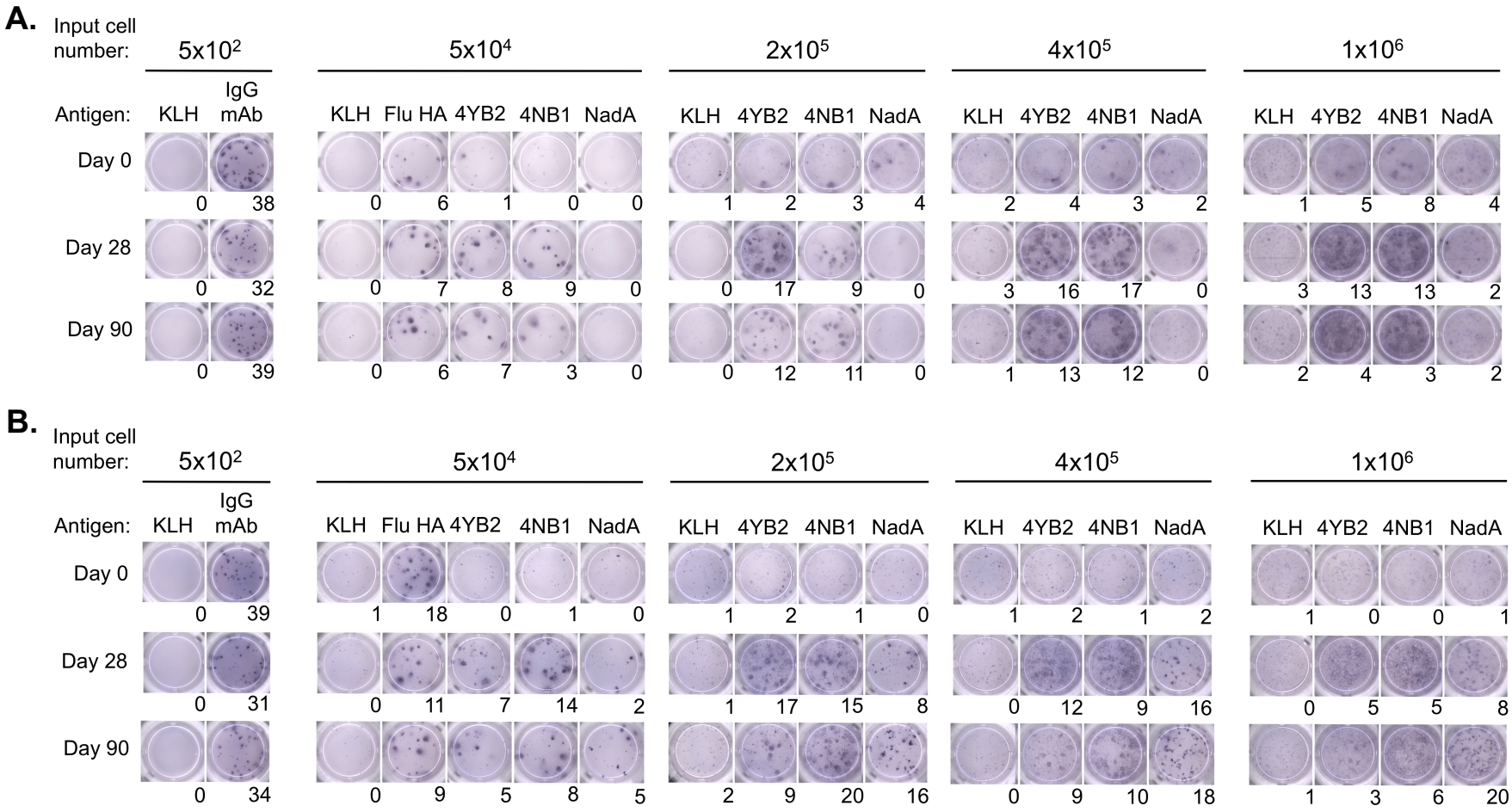
A.
Input cell number:
5x10^2
5x10^4
2x10^5
4x10^5
1x10^6
Antigen:
KLH
IgG mAb
Flu HA
4YB2
4NB1
NadA
Day 0
Day 28
Day 90
0 38
0 6 1 0 0
1 2 3 4
2 4 3 2
1 5 8 4
0 32
0 7 8 9 0
0 17 9 0
3 16 17 0
3 13 13 2
0 39
0 6 7 3 0
0 12 11 0
1 13 12 0
2 4 3 2
B.
Input cell number:
5x10^2
5x10^4
2x10^5
4x10^5
1x10^6
Antigen:
KLH
IgG mAb
Flu HA
4YB2
4NB1
NadA
Day 0
Day 28
Day 90
0 39
1 18 0 1 0
1 2 1 0
1 2 1 2
1 0 0 1
0 31
0 11 7 14 2
1 17 15 8
0 12 9 16
0 5 5 8
0 34
0 9 5 8 5
2 9 20 16
0 9 10 18
1 3 6 20

Figure S12: Representative outputs from IgG-secreting memory B cell ELISpot assay on participants colonized with GM-Nlac.

PBMC isolated at Day 0, Day 28 and Day 90 from Participants 3 (**A**) and 19 (**B**) (as numbered in Figure 3B) were polyclonally stimulated for 5-days, allowing memory B cells to differentiate into antibody-secreting cells. Cells were then added at the concentrations shown to duplicate wells containing membranes coated with the following antigens: keyhole limpet haemocyanin (KLH), rat anti-human IgG monoclonal antibody (mAb) clone M1310G05 (IgG mAb), influenza haemagluttinin (FluHA), deoxycholate-extracted outer membrane vesicle preparation (dOMV) derived from strain 4YB2 (4YB2), dOMV derived from strain 4NB1 (4NB1) or the soluble domain of the meningococcal adhesin, NadA (NadA). Note that only a single, representative well for each condition is shown in these examples. Following overnight incubation, antigen-specific antibody-secreting cells (or IgG-secreting cells captured by the anti-IgG mAb) were lysed in hypotonic buffer and human IgG was detected using an alkaline-phosphatase-conjugated, anti-human IgG polyclonal antibody (pAb) and BCIP as substrate. The number of spot-forming units (SFU) per membrane, as counted by the AID ELISpot reader, is shown underneath each image. The assumption was that one SFU equates to a single antibody-secreting cell.

Figure S13.

Participant #	Day 00			Day 28		
	α	*β*	[IgA] (µg/ml)	*α*	*β*	[IgA] (µg/ml)
1			–			318.8
2		✓	107.7			135.4
3		✓	167.7		✓	165.0
4		✓	–		✓	256.2
5	✓		246.8			234.3
6	✓	✓	559.6		✓	178.2
7		✓	193.7	✓	✓	74.2
8			324.8			130.6
9		✓	263.4	✓		228.8
10			245.2			240.5
11			183.7			206.9
12			343.5			138.5
13	✓		267.4	✓	✓	124.4
14			206.2			166.9
15	✓	✓	517.4	✓	✓	–
16			170.4			151.3
17			90.3		✓	262.6
18			98.6			241.6
19	✓	✓	368.7	✓	✓	143.9
20			201.3			193.5
21		✓	123.7			165.5
22	✓		209.2	✓		151.8
23			–			–
24	✓	✓	234.9	✓	✓	174.2
25			373.7			N/A
26			307.6			N/A

Figure S13: Results of salivary IgA ELISAs.

Saliva samples isolated at Day 0 and Day 28 from all participants (as numbered in Figure 3B) were diluted 3x and assayed for anti-sNadA IgA in single wells coated with either coating buffer alone, or coating buffer plus sNadA. Wells in which the resulting OD_{490nm} equalled or exceeded the threshold value (= Mean + 3SD of appropriately-coated wells) (i.e. sNadA-coated wells (α): 0.07; uncoated wells (β): 0.068) are denoted with a tick symbol. Saliva samples considered to be 'positive' for anti-sNadA IgA (i.e. contain a reciprocal titer of anti-sNadA IgA > 3 in the absence of signal in uncoated wells) are shown in grey. The total IgA concentration (in μg ml^{-1}) of each saliva sample was interpolated by reference to a standard curve generated using human IgA isolated from colostrum. Saliva samples wherein there was insufficient remaining volume to perform the total IgA measurement are denoted with '-'.

Table S1: Bacterial strains used in this study.

Species	Strain	Designation	Genotype	Derived:	Reference
Neisseria lactamica	Y92-1009	ND: P1.ND,ND: F4-8: ST-3493	WT		[25]
	ΔpilE		Y92-1009 *ΔpilE:aadA1*	Y92-1009	This work
	JRL0001		Y92-1009 *ΔlacZ*	Y92-1009	This work
	JRL0002		Y92-1009 *ΔlacZ* NHCIS1::*lacZ*	JRL0001	This work
	JRL1001		Y92-1009 *ΔlacZ* NHCIS1::[*lst*400]*lacZ*	JRL0001	This work
	JRL1002		Y92-1009 *ΔlacZ* NHCIS1::[*lst*250]*lacZ*	JRL0001	This work
	JRL1003		Y92-1009 *ΔlacZ* NHCIS1::[*lst*200]*lacZ*	JRL0001	This work
	JRL1004		Y92-1009 *ΔlacZ* NHCIS1::[*lst*150]*lacZ*	JRL0001	This work
	JRL1005		Y92-1009 *ΔlacZ* NHCIS1::[*lst*100]*lacZ*	JRL0001	This work
	JRL1006		Y92-1009 *ΔlacZ* NHCIS1::[*lst*50]*lacZ*	JRL0001	This work
	JRL1007		Y92-1009 *ΔlacZ* NHCIS1::[*lst*]*lacZ*	JRL0001	This work
	4YB2	GMO (Control)	Y92-1009 *ΔlacZ* NHCIS1::(X)-*lacZ*	JRL0001	This work
	4NB1	GMO (Intervention)	Y92-1009 *ΔlacZ* NHCIS1::*nadA-lacZ*	JRL0001	This work
Neisseria meningitidis	MC58	B: P1.7,16-2: F1-5: ST-74	WT		[63]
	ΔsiaD		MC58 *ΔsiaD:aphA3*	MC58	This work
	ΔnadA		MC58 *ΔnadA:aphA3*	MC58	This work
	N54.1	P1.21,16: F3-7: ST-8510	WT		[23]

Table S2: Plasmids used in this study.

Plasmid	Construct	Derivative of:	Reference
pUC19	pMB1 amp^R		[64]
pSC101	ΔpMB1::*ori/repA (*pSC101) amp^R	pUC19	This work
pJL0001	*ΔnlaIII*::CLOVER(2)-*aphA3*	pUC19	This work
pJL0002	*ΔnlaIII*::CLOVER(1a)-*aphA3*	pJL0001	This work
pJL0003	*ΔnlaIII*::CLOVER(1b)-*aphA3*	pJL0001	This work
pJL0004	*ΔnlaIII*::CLOVER(0)-*aphA3*	pJL0002	This work
pJL0005	*ΔnlaIII*::*aphA3*	pJL0001	This work
pJL0006	*ΔlacZ:*DUS	pUC19	This work
pJL0007	NHCIS1::[porB]*lacZ*	pUC19	This work
pJL0009	NHCIS1::[lst]*lacZ*	pJL0007	This work
pJL0010	NHCIS1::[lst400]*lacZ*	pJL0009	This work
pJL0011	NHCIS1::[lst250]*lacZ*	pJL0010	This work
pJL0012	NHCIS1::[lst200]*lacZ*	pJL0010	This work
pJL0013	NHCIS1::[lst150]*lacZ*	pJL0010	This work
pJL0014	NHCIS1::[lst100]*lacZ*	pJL0010	This work
pJL0015	NHCIS1::[lst50]*lacZ*	pJL0010	This work
pJL0016	NHCIS1::[porA/porB200](X)-[lst]*lacZ*	pJL0012	This work
pJL0017	NHCIS1::[porA/porB200]*nadA*-[lst]*lacZ*	pJL0016	This work
pJL0018	*ΔsiaD::aphA3*	pSC101	This work
pJL0019	*ΔnadA::aphA3*	pSC101	This work
pZP0001	*ΔpilE::aadA1*	pSC101	This work

Table S3: Primers used in this study.

Name	Sequence (5' ➔ 3')	Product	Template
pSC101_FOR	GTTTCCTGTGTGAAATTGCATAAGAACCTCAGATCCTTCCGTATTTAG	pSC101 *ori/repA*	pSC101
pSC101_REV	GATCAAAGGATCTTCGATTTGCCCGAGCTTGCGAG		
5PRIMEEND*ΔnlaIII*_FOR	GGATCCTCTAGAGTCGCCTTACAAGCAGAATGTCG	5PRIMEEND*ΔnlaIII*	gDNA (Y92-1009)
5PRIMEEND*ΔnlaIII*_REV	GACAGTTGCCGAATATTCTCTCGCCAATGGAGAATC		
3PRIMEEND*ΔnlaIII*_FOR	GATGAATTATTCTAGTATCTAGAGATGCAATCCGCC	3PRIMEEND*ΔnlaIII*	gDNA (Y92-1009)
3PRIMEEND*ΔnlaIII*_REV	GCATGCCTGCAGGTCTCTAGATCGACCAATTTGCCCAAGCC		
*ΔnlaIII*VECTOR_FOR	GGGCAAATTGGTCGATCTAGAGACCTGCAGGCATGCAAGCTTG	*ΔnlaIII*VECTOR	pUC19
*ΔnlaIII*VECTOR_REV	CATTCTGCTTGTAAGGCGACTCTAGAGGATCCCCGGG		
*nlaIII*LOCUS_FOR	CGGGTGATTAGCTCAGTTGG	*nlaIII*LOCUS	gDNA (Y92-1009)
*nlaIII*LOCUS_REV	GGTTTTCATTGTGCCGATAACGG		
CLOVERcatg1_FOR	ACCCGGATCATATGAAACAACACGAC	PCR-pJL0002	pJL0001
CLOVERcatg1_REV	AGCGCGAGAAGCAGGCGA		
CLOVERcatg2_FOR	AACGCGACCATATGGTTCTGC	PCR-pJL0003	pJL0001
CLOVERcatg2_REV	TTTCATTCGGATCTTTGGACAG	PCR-pJL0004	pJL0002
*ΔpilE:aadA1*VECTOR_FOR	GACCTGCAGGCATGCAAGCTTG	*ΔpilE*VECTOR	pSC101
*ΔpilE:aadA1*VECTOR_REV	GACTCTAGAGGATCCCCGGGTAC		
*pilE*_FOR	TGAAAGCAATCCAAAAAGGTTTCACC	*ΔpilE:aadA1*	pZP0001
*pilE*_REV	TTATTTGGCGCGGCAGGAAG		
*ΔnlaIII:aphA3*INSERT_FOR	GAATGGAGTTTAAAGGAAATCATATGGCCAAAATGCGCATTAGTCCG	*ΔnlaIII:aphA3*INSERT	pJL0001
*ΔnlaIII:aphA3*INSERT_REV	CAATTTCAGACGGCATAGATCTAGAATAATTCATCCAACAGGATATAATATTTG		
*ΔnlaIII:aphA3*VECTOR_FOR	GATGAATTATTCTAGATCTATGCCGTCTGAAATTGCGGCCGCGCGGCCAAATATACATCGGAC	*ΔnlaIII:aphA3*VECTOR	pJL0001
*ΔnlaIII:aphA3*VECTOR_REV	GCGCATTTTGGCCATATGATTTCCTTTAAACTCCATTC		
ΔnlaIII:aphA3-600_FOR	GCATTGGCGTATGGCAATTG	*ΔnlaIII:aphA3*-600	pJL0005
ΔnlaIII:aphA3-600_REV	ACAAAGCAGGTTCGAGCGAC		
ΔnlaIII:aphA3-300_FOR	CAGTCGATATCGACCGGACGACCGCCTTTATG	*ΔnlaIII:aphA3*-300	pJL0005
ΔnlaIII:aphA3-300_REV	GAAGTTCGCCCGCTTTAAGAATAC		
ΔnlaIII:aphA3-300DUS_FOR	TTCAGACGGCATACCGGACGACCGCCTTTATG	*ΔnlaIII:aphA3*-300DUS	
ΔnlaIII:aphA3-150_FOR	CAGTCGATATCGCAAAAACAGAACTATTTTTAAGATTAG	*ΔnlaIII:aphA3*-150	pJL0005
ΔnlaIII:aphA3-150_REV	AAAATACTTTATCAGACAGCG		
ΔnlaIII:aphA3-150DUS_FOR	TTCAGACGGCATCAAAAACAGAACTATTTTTAAGATTAG	*ΔnlaIII:aphA3*-150DUS	
ΔnlaIII:aphA3-75_FOR	CAGTCGATATCGTGCCGGGGAATATAAAGATTTG	*ΔnlaIII:aphA3*-75	pJL0005
ΔnlaIII:aphA3-75_REV	TGGAGCCGATATAATTCATCCG		
ΔnlaIII:aphA3-75DUS_FOR	TTCAGACGGCATTGCCGGGGAATATAAAGATTTG	*ΔnlaIII:aphA3*-75DUS	
5PRIMEEND*ΔlacZ*_FOR	CAGACAGCATATCGGGCGATG	5PRIMEEND*ΔlacZ*	gDNA

5PRIMEEND*ΔlacZ* REV	CAATTTCAGACGGCATAGATCCTCCTAATTTGAAACATCGCTC		(Y92-1009)
3PRIMEEND*ΔlacZ* FOR	ATCTATGCCGTCTGAAATTGGGGATATATGCTAACCGCAG	3PRIMEEND*ΔlacZ*	gDNA (Y92-1009)
3PRIMEEND*ΔlacZ* REV	GTCTCTAGACATACATCCGCTCATCGC		
*ΔlacZ*VECTOR FOR	GAGCGGATGTATGTCTAGAGACCTGCAGGCATGCAAG	*ΔlacZ*VECTOR	pUC19
*ΔlacZ*VECTOR REV	CGCCCGATATGCTGTCTGGACTCTAGAGGATCCCCGG		
*lacZ*LOCUS FOR	GGGTACAGTCAATCGGTTTCTTTG	*lacZ*LOCUS	gDNA (Y92-1009)
*lacZ*LOCUS REV	GAAAGGGGGCGTGTGTTC		
5PRIMEENDNHCIS1 FOR	CTCTAGAGTCCTGATACCGAGCTTTTCCCATG	5PRIMEENDNHCIS1	gDNA (Y92-1009)
5PRIMEENDNHCIS1 REV	AAAACAAACTTGTCGACTTCAGACGGCGTTGCACAGTTTTACTCCATG		
3PRIMEENDNHCIS1 FOR	GTTTTTAGATGCCGTCTGAATGCTGAAGTAGAAAACCAGC	3PRIMEENDNHCIS1	gDNA (Y92-1009)
3PRIMEENDNHCIS1 REV	GTCTCTAGACTGAAAGAAGCTATCACCTTCATAAATAAG		
NHCIS1VECTOR FOR	GCTTCTTTCAGTCTAGAGACCTGCAGGCATGCAAG	pUC19NHCIS1	pUC19
NHCIS1VECTOR REV	GGGAAAAGCTCGGTATCAGGACTCTAGAGGATCCCCGG		
*porB*promoter FOR	CAACGCCGTCTGAAGTCGACAGTTTGTTTTTTCGGGCGGG	*porB* promoter	gDNA (Y92-1009)
*porB*promoter REV	ATTCGCTAATAACATATGATTCCTTTTTTGGTTAAGAAATTTAAGCG		
Nlac*lacZ* FOR	AACCAAAAAAGGAATCATATGTTATTAGCGAATTATTATCAAGATCC	*lacZ*	gDNA (Y92-1009)
Nlac*lacZ* REV	GATACCAATCTTTGCAGAAAGCTTATAACCGGATACTTATATCGAAATTG		
*porB*terminator FOR	GTATCCGGTTATAAGCTTTCTGCAAAGATTGGTATC	*porB* terminator	gDNA (Y92-1009)
*porB*terminator REV	CTACTTCAGCATTCAGACGGCATCTAAAAACAG		
NHCIS1LOCUS FOR	CAAAGGTAATCAGGTAACGGCTCAT	NHCIS1LOCUS	gDNA (Y92-1009)
NHCIS1LOCUS REV	CAACAGGGTAAATTCCGGAGGTC		
*lst*promoter FOR	GCAACGCCGTCTGAAGTCGACTCGGCAACTGTCGGAATATCTG	*lst* promoter	pJL0005
*lst*promoter REV	ATTCGCTAATAACATATGTGTATTCCTTTAAACTCC		
NHCIS1-*lacZ*VECTOR FOR	GGAGTTTAAAGGAATACACATATGTTATTAGCGAATTATTATC	NHCIS1-*lacZ*VECTOR	pJL0007
NHCIS1-*lacZ*VECTOR REV	CAGTTGCCGAGTCGACTTCAGACGGCGTTGCACAGTTTTACTCCATG		
NHCIS1-lst400-*lacZ* FOR	GATATTTGTTCTGAAAATCGGCAACTGTCGGAATATCTGC	PCR-pJL0010	pJL0009
NHCIS1-lst400-*lacZ* REV	GAAATCAAGCCGAATGTCGACTTCAGACGGCGTTG		
porAupstream FOR	CAACGCCGTCTGAAGTCGACATTCGGCTTGATTTCGATACACCC	*porA* UAS	gDNA (MC58)
porAupstream REV	GATATTCCGACAGTTGCCGATTTTCAGAACAAATATCTGATAAATGCCGCAAC		
NHCIS1-lst250-*lacZ* FOR	CATCGTACGTCGACGAGCTAAGGCGAGGCAACGCC	PCR-pJL0011	pJL0010
NHCIS1-lst200-*lacZ* FOR	CATCGTACGTCGACGTGCCGCGTGTGTTTTTTTATGGCG	PCR-pJL0012	pJL0010
NHCIS1-lst150-*lacZ* FOR	CATCGTACGTCGACGGCAGCAGCGCATCGGC	PCR-pJL0013	pJL0010
NHCIS1-lst100-*lacZ* FOR	CATCGTACGTCGACAAACACAACGTTTTTGAAAAAATAAGCTATTG	PCR-pJL0014	pJL0010
NHCIS1-lst50-*lacZ* FOR	CATCGTACGTCGACTCATTTTTAAAATAAAGGTTGCGGCATTTATC	PCR-pJL0015	pJL0010
NHCIS1-lst200(X)-*lacZ*FOR	ATCTATTATATAACGCGGCCGCATATTCGGCAACTGTCGGAATATCTG	PCR-pJL0016	pJL0012
NHCIS1-lst200(X)-*lacZ*REV	CGCCCGAAAAACCATTTTTCAGAACAAATATCTGATAAATG		
NHCIS1-*nadA*-*lacZ*FOR	AACTACGAATGGTAAGCGGCCGCATATTCGGCAACTG	PCR-pJL0017	pJL0016
NHCIS1-*nadA*-*lacZ*REV	GTGTTTCATGCTCATCTCGAGTTCCTTTTGTAAATTTG		

5PRIMEEND*ΔnadA* FOR	GTGCCACCTTCTAGACCGACAAAAAGGCCGTCTGAAC	5PRIMEEND*ΔnadA*	gDNA (MC58)
5PRIMEEND*ΔnadA* REV	GCCGAATATGACGTCGGCGTTGGTGGTTTCATCC		
3PRIMEEND*ΔnadA* FOR	GAATTATTCTAGGCGGCCGCGGGAGAAAATATAACGACATTTGC	3PRIMEEND*ΔnadA*	gDNA (MC58)
3PRIMEEND*ΔnadA* REV	GCCTTTTGCTCTAGACGGCCGGATAGAAAATAAAAAC		
ΔnadAaphA3 FOR	GAAACCACCAACGCCGACGTCATATTCGGCAACTGTCG	*ΔnadAaphA3*	pJL0005
ΔnadAaphA3 REV	GTTATATTTTCTCCCGCGGCCGCCTAGAATAATTC		
MC58*ΔnadA*VECTOR FOR	TTTTCTATCCGGCCGTCTAGAGCAAAAGGCCAGC	*ΔnadA:aphA3*VECTOR	pJL0005
MC58*ΔnadA*VECTOR REV	CGGCCTTTTTGTCGGTCTAGAAGGTGGCACTTTTC		
5PRIMEEND*ΔsiaD* FOR	GAAAAGTGCCACCTTCTAGACAGAGGATTGGCTATTACATATAG	5PRIMEEND*ΔsiaD*	gDNA (MC58)
5PRIMEEND*ΔsiaD* REV	CAGTTGCCGAATATGACGTCAAGTATATTAGGGGCTCAATTAG		
3PRIMEEND*ΔsiaD* FOR	GAATTATTCTAGGCGGCCGCAACAAATCCTAAAGGAATTATAGGC	3PRIMEEND*ΔsiaD*	gDNA (MC58)
3PRIMEEND*ΔsiaD* REV	GCTGGCCTTTTGCTCTAGAATATAAAGCGCGTAAGGCTATAG		
ΔsiaDaphA3 FOR	GAGCCCCTAATATACTTGACGTCATATTCGGCAACTGTCGGAATATC	*ΔsiaDaphA3*	pJL0005
ΔsiaDaphA3 REV	TAATTCCTTTAGGATTTGTTGCGGCCGCCTAGAATAATTC		
trunc.pUC19*ΔsiaD* FOR	TAGCCTTACGCGCTTTATATTCTAGAGCAAAAGGCCAGCAAAAG	*ΔsiaD:aphA3*VECTOR	pJL0005
trunc.pUC19*ΔsiaD* REV	ATGTAATAGCCAATCCTCTGTCTAGAAGGTGGCACTTTTCGG		
Band1FOR	NNNNCCTACGGGNGGCWGCAG	Band 1	gDNA (GM-Nlac)
Band1REV	GACTACHVGGGTATCTAATCC		
Band3dFOR	CACTCGGGGCGTATGTTCAATTTG	Band 3	gDNA (GM-Nlac)
Band3dREV	GCACATTGATTTGTTTCGTAAAAGCGATTTC		